THE ROLE OF INTRASPECIES AND INTERSPECIES COMMUNICATION OF *PSEUDOMONAS AERUGINOSA* PA14 TOWARDS PHENAZINE PRODUCTION AND VIRULENCE

A Dissertation

Presented to the Faculty of the Graduate School

of Cornell University

In Partial Fulfillment of the Requirements for the Degree of

Doctor of Philosophy

by

Arvind Venkataraman

January 2012

THE ROLE OF INTRASPECIES AND INTERSPECIES COMMUNICATION OF *PSEUDOMONAS AERUGINOSA* PA14 TOWARDS PHENAZINE PRODUCTION AND VIRULENCE

Arvind Venkataraman Ph. D.

Cornell University 2012

Pseudomonas aeruginosa is an opportunistic pathogen and a model organism for studying quorum sensing (QS) - bacterial communication via secreted signaling factors (acyl homoserine lactones). *P. aeruginosa* also produces electrochemically-active compounds that are called phenazines, which help it to respire with an electrode in bioelectrochemical systems (BESs). Phenazine production by this microbe is strongly controlled by QS amongst other environmental stimuli. In the BES microbiota, we proposed that intraspecies and interspecies communication(s) could influence phenazine production by *P. aeruginosa* subsequently affecting current generation.

Intraspecies communication: First, we showed that QS modulates the current production by *P. aeruginosa* in BESs by controlling phenazine production. The current and phenazine production by a wildtype strain (WT) and a mutant were investigated under conditions that favor or inhibit QS. As hypothesized, anaerobic current production by the mutant was 5.8-fold higher with extraneously supplied QS signaling lactones than without.

Interspecies communication: Next, we studied *P. aeruginosa* in association with a fermenter (*Enterobacter aerogenes*) and found that the current generation by this co-culture was 14-fold higher than either of these two bacteria alone. This phenomenon was due to metabolite-based mutualism in which a fermentation product of *E. aerogenes* stimulated specific phenazine production (i.e., pyocyanin) by *P. aeruginosa*. *E. aerogenes* switched from fermentation to electrode respiration with pyocyanin. We further demonstrated that common fermentation products of several microorganisms, which co-habit infections with *P. aeruginosa*, significantly increase the virulence of *P. aeruginosa* compared to the common blood sugar - glucose. Finally, we demonstrated that in a defined mixed-culture BES, bacterial synergism between *P. aeruginosa* and *E. aerogenes* results in phenazine-based mediated electron transfer (MET) becoming equally important to direct electron transfer by *Geobacter sulfurreducens*. A mechanistic mathematical model revealed that in the synergism, *E. aerogenes* possessed faster kinetics of phenazine reduction, thereby, resulting in improved MET compared to a pure culture of *P. aeruginosa*. Overall, we showed that intermicrobial cooperation considerably affects the phenazine production and virulence of *P. aeruginosa* with implications in microbial communities outside BESs.

BIOGRAPHICAL SKETCH

Arvind Venkataraman grew up in Calcutta (present day Kolkata), West Bengal, India. After graduating from the Indian Institute of Technology, Bombay, India with a degree in Environmental Science and Engineering in 2007, he began graduate work at Washington University in St. Louis under the direction of Dr. Largus T. Angenent. There he met his fiancée Cara Marie Fosdick, who is currently a psychiatry resident at the University of Michigan Hospital, Ann Arbor. The lab moved to Cornell in August 2008, where Arvind continued his pursuit of a Ph.D. in Biological and Environmental Engineering. Next, Arvind will be starting a post-doctoral position at Michigan State University with Dr. Thomas Schmidt. He and Cara will be getting married in India in February 2012.

This thesis is dedicated to my parents and my fiancée Cara. My parents sacrificed all their dreams and comforts without a second thought only with the single minded goal that I could work towards my Ph.D. During stressful times of the Ph.D., my fiancée Cara was a pillar of strength and kept me on track by reminding me of how much I actually liked my Ph.D., and that I should see it through to the end.

ACKNOWLEDGMENTS

First, I would like to thank my committee members: Dr. Stephen C. Winans and Dr. Ashim Datta, for taking time to critically review my work and constantly provide feedback. I will always remember the one-on-one scientific discussion(s) with Dr. Stephen C. Winans. During these, I learnt to dig deeper in my research and I always left the meeting(s) with the feeling that "I do not know anything", which was an excellent starting point for re-evaluating my results and claims. I am grateful to Dr. Datta for his very helpful pointers on mathematical modeling and making certain that I was not working on mathematical modeling just because he was on my committee. I thank all the Angenent Lab members, past and present. By name, I would like to mention Dr. Miriam Agler Rosenbaum, who taught me everything I know about bioelectrochemical systems and for her patience and efforts towards shaping my attitude towards research. Special thanks go to Zhongjian Li and Michaela Anne TerAvest with whom there was a constant exchange of ideas and for the camaraderie in the lab, which kept me sane during research. Last but not least, I will forever be grateful to my advisor Dr. Largus T. Angenent. He took me in and taught me everything regarding scientific research, including being detail oriented, goal-driven, and working constantly to improve and develop oneself each and every day. He invested a lot of time and effort towards my scientific and most importantly, personal development in the past few years. His insistence on never being complacent and freedom in allowing me to pursue my creativity in research is invaluable. Thanks to everyone.

This entire thesis was supported by NSF Career Grant #0939883 to Largus T. Angenent.

TABLE OF CONTENTS

LIST OF FIGURES

LIST OF TABLES

1 CHAPTER 1. Introduction: Central hypothesis and summary of experiments conducted.

The opportunistic pathogen *Pseudomonas aeruginosa* is capable of quorum sensing, which enables intraspecies and likely interspecies communication and controls the production of antibiotic compounds, which are called phenazines and certain extracellular virulence factors by this microbe. Recently, it has emerged that phenazines are also electrochemically active, thereby, enabling *P. aeruginosa* to respire with the electrode in devices known as bioelectrochemical systems (BESs). Since the electric current in BESs can be directly correlated to phenazine concentration, these devices are an excellent real-time *in-situ* tool to monitor phenazine production by *P. aeruginosa* under different conditions. Given the "social" and "electrochemical" nature of this microbe, we hypothesized that both intraspecies and interspecies communication mechanisms of *P. aeruginosa* would help determine phenazine production by this microbe, subsequently affecting electron transfer to the electrode in the complex microbial ecology of BESs. Further, we postulated that these principles would also apply towards the virulence of *P. aeruginosa* in certain microbial communities. To investigate this hypothesis we formulated the following sub hypotheses and conducted experiments using pure cultures and defined mixed cultures:

Intraspecies communication:

Quorum sensing controls electric current generation by *Pseudomonas aeruginosa*

- We screened the electrochemical activity of nine mutants and the wildtype of *P. aeruginosa* under different experimental conditions to relate quorum sensing and current production and justify our use of BESs as a research tool. CHAPTER 3.

Interspecies communication:

Metabolite-based mutualism between *P. aeruginosa* and *Enterobacter aerogenes* improves current production in bioelectrochemical systems

- We chose *Enterobacter aerogenes* on the basis of its abundance in a BES operated in our lab, and investigated the synergistic electrochemical activity of a defined mixed culture consisting of *P. aeruginosa* and *E. aerogenes*.
- We conducted pure culture experiments with both these organisms to determine the mechanism of the synergism between these two microbes. CHAPTER 4.

Common fermentation products increase the production of virulence factors by *P. aeruginosa*

- We measured the production of extracellular virulence factors and biofilm formation by *P. aeruginosa* under various conditions and conducted proteomics with this microbe to obtain a mechanistic explanation of the observed phenomena.
- We quantified the changes in population of *P. aeruginosa* in a defined mixed culture in a bioreactor to determine whether the interactions between *P. aeruginosa* and the fermenters could influence the growth of *P. aeruginosa* in polymicrobial communities. CHAPTER 5.

Mediator-based and direct contact-based exocellular electron transfer are equally important in synergistic bacterial communities of bioelectrochemical systems.

- We operated BESs with various combinations of defined mixed cultures consisting of *P. aeruginosa*, *E. aerogenes*, and *G. sulfurreducens* (an organism which transfers electrons to the electrode directly by outer membrane cytochromes) to determine the relative contribution of direct (cytochrome/conductive pili based) electron transfer and bacterial partnership driven mediated (phenazine based) electron transfer towards current production in a BES.
- We formulated a simple mathematical model to determine the rate-limiting step with respect to electron transfer to the electrode via phenazines by a mixed culture of *P. aeruginosa* and *E. aerogenes*. CHAPTER 6.

2 CHAPTER 2. Literature Review

This chapter has not been published.

This review focuses on introducing bioelectrochemical systems (BESs) and discusses the ecology and mechanisms involved in microbial exocellular electron transfer to the electrode. The ecology has been explained with specific focus on one model electrode-respiring bacterium *Pseudomonas aeruginosa* and its interaction(s) with other microorganism(s), this being the focus of the thesis. *P. aeruginosa* possesses two unique traits, which makes it an invaluable organism for understanding the ecology of BESs: i) the social nature of *P. aeruginosa*, owing to its ability for intraspecies and interspecies communication; and ii) production of compounds that are called phenazines, which help this organism to respire with the electrode and also act as antibiotics along with several other extracellular virulence factors, thereby, introducing a pressure on selection of microbial consortia. In addition, the mathematical modeling of BESs has been reviewed in detail as mathematical models can serve as precious tools to: i) answer questions with respect to the ecology and function of key organisms in a BES (this has been performed in Chapter 6); and ii) aid experimental design for hypothesis validation.

2.1 Bioelectrochemical systems

Bioelectrochemical systems (BESs) are devices in which a biological system (either enzymes or microbes) can be linked to an (insoluble) electrode for different applications. The most extensively researched type of BESs are microbial fuel cells (MFCs) for which microorganisms act as catalysts for generating electricity from the chemical energy of organic compounds (Potter, 1915). A MFC consists of two electrodes, which are the anode and cathode, and located in their respective compartments. Usually, at the MFC anode, the electron donor is an organic compound that also fulfils the role of a carbon source. Bacteria oxidize this electron donor and transfer the

electrons in their metabolic pathway to the electrode via different mechanisms. To maximize the flux of these electrons to the electrode (i.e., for obtaining the maximum possible electric current) alternative electron acceptors, such as O_2, Fe^{3+}, NO^{3-}, need to be minimized at the anode. The anode and cathode are separated by a membrane (anion exchange or cation exchange), which isolates the two environments while still permitting ion flow for charge balance. At the cathode of MFCs (Figure 2.1a), oxygen is reduced to H_2O either abiotically by using appropriate catalysts (e.g., Pt catalyst on carbon) or biologically by bacteria as demonstrated by Bergel et al. (2005). The use of bacteria on the cathode as catalysts is economically beneficial since typically expensive noble metals have to be used as catalysts, owing to the high overpotential (difference between the applied potential in practice to achieve the reaction and theoretical potential as predicted from the Nernst equation) associated with oxygen reduction (Logan et al., 2006). In the second kind of BESs, - microbial electrolysis cells (MECs) – the anodic process is often the same as a MFC, but in addition valuable products, such as H_2 (Kim and Logan, 2011; Logan et al., 2008), CH_4 (Clauwaert and Verstraete, 2009), and H_2O_2 (Rozendal et al., 2009), are generated at the cathode by applying an appropriate voltage between the anode and cathode (Figure 2.1b). The applied voltage serves to overcome the thermodynamic limitations associated with product generation. Since both MFCs and MECs almost always utilize reducing power generated by microbial oxidation of organic substrates at the anode, MFCs and MECs have been hailed as a sustainable technology for wastewater treatment (Rozendal et al., 2008) greenhouse gas reduction (Fornero et al., 2010; Nevin et al., 2011), and chemical production (Rabaey and Rozendal, 2010). The cathode can also serve as an electron donor for bioremediation processes, such as uranium removal (Gregory and Lovley, 2005), trichloroethene removal (Aulenta et al.,

2008), and perchlorate reduction (Thrash and Coates, 2008), and for denitrifying bacteria (Clauwaert et al., 2007).

The third kind of BESs – Microbial 3-electrode cells (M3Cs) are valuable research tools since in these devices, a well-defined electrochemical environment is maintained by poising the working electrode at a constant potential with respect to a reference electrode with the help of a third electrode – the counter electrode (Figure 2.1c). Electrochemical reactions of interest happen at the working electrode, which is analogous to the anode of MFCs depending upon the applied potential. This permits focused investigation into the electrochemical activity of pure and defined mixed cultures (Bond and Lovley, 2003; Marsili et al., 2008a; Marsili et al., 2008b; Venkataraman et al., 2011; Venkataraman et al., 2010), biofilm formation; and application as versatile biocomputing platforms (Li et al., 2011).

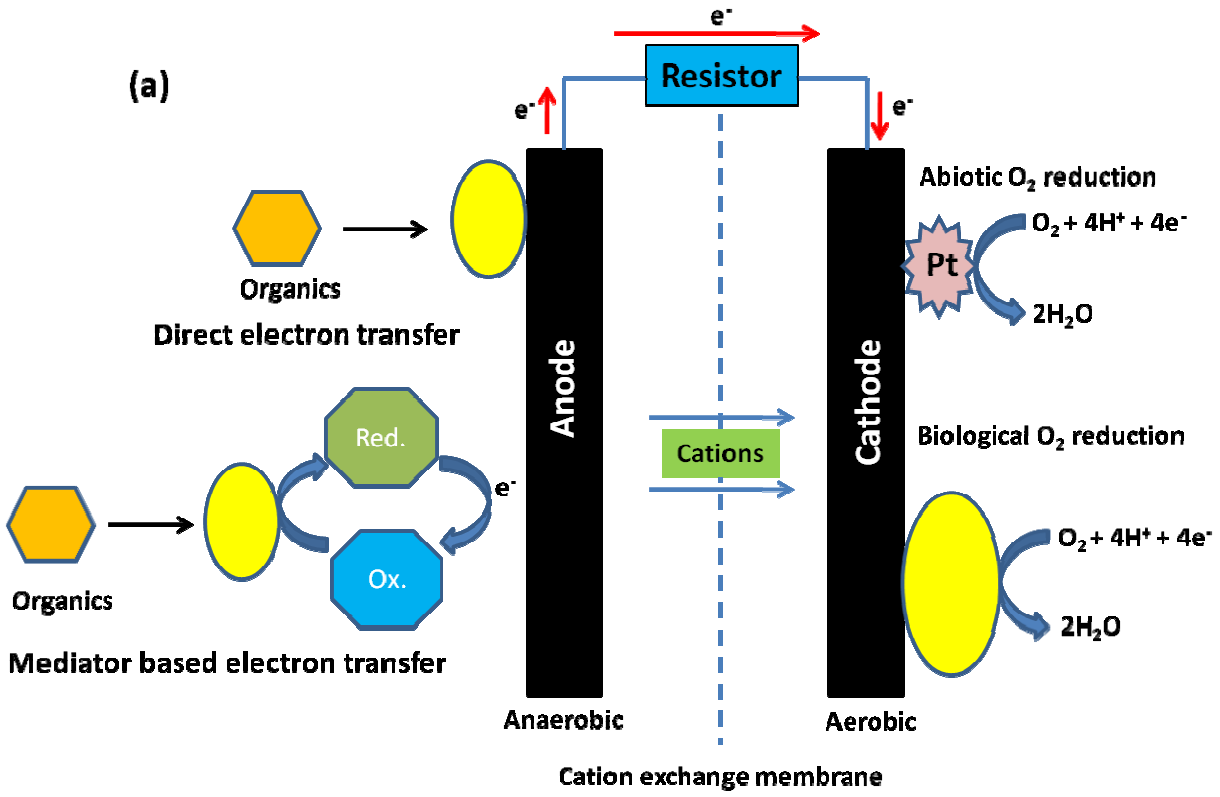

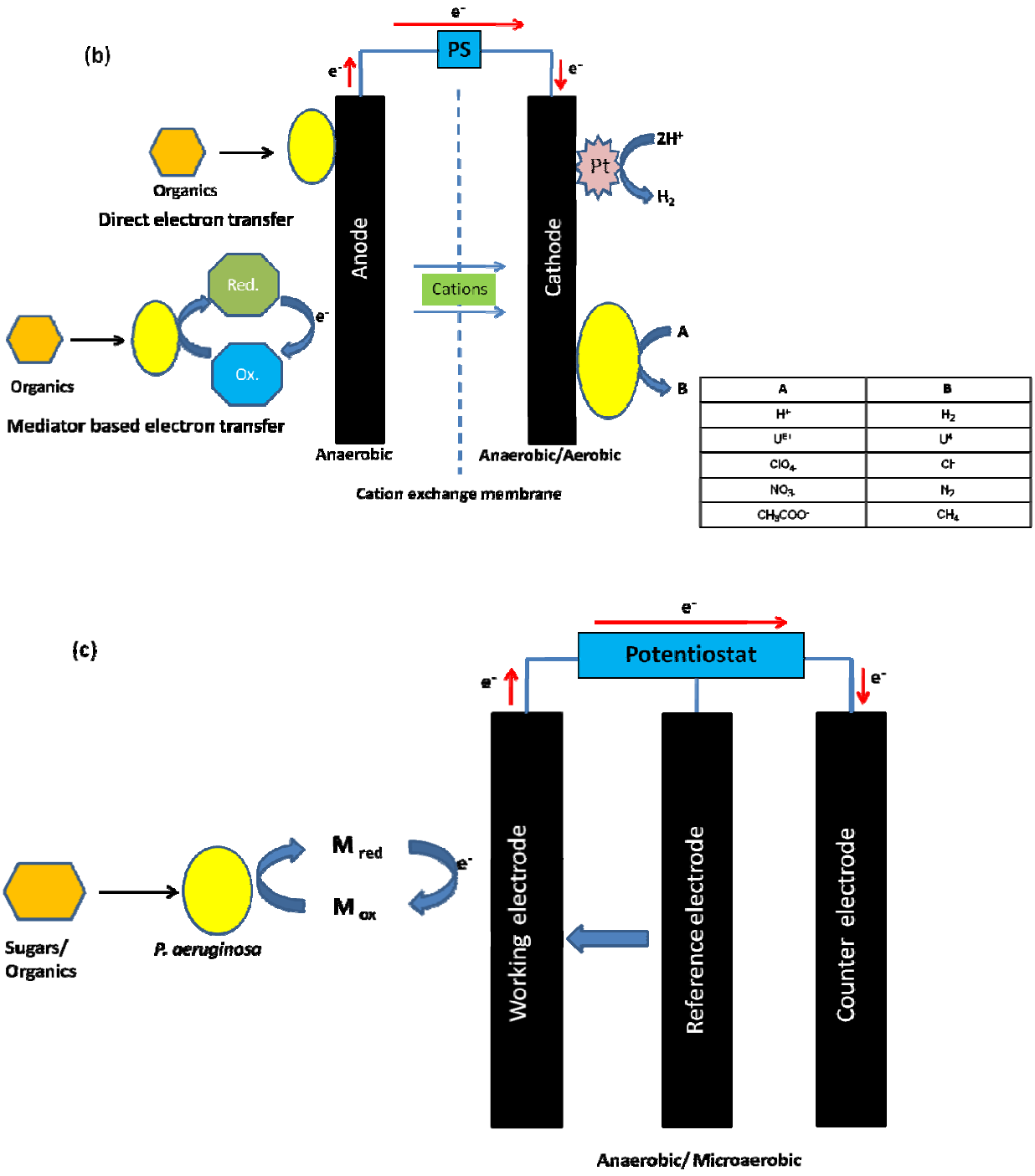

Figure 2.1. Schematic of different bioelectrochemical systems: (a) MFC; typically, the anode is biological and anaerobic, while the cathode can be abiotic or biological, this figure shows a cation exchange membrane permitting passage of cations, such as Na^+, K^+, H^+, NH_4^+ from the anode to cathode and the anode and cathode are connected through a resistor (R); (b) MEC; the anode and cathode are connected through a power supply (PS) and the cathode potential is poised at a potential depending upon the reaction kinetics, various reactions can happen at the cathode as shown in the figure; and (c) M3C operated with *P. aeruginosa*.

2.2 Microbial bioenergetics in BESs

A wide range of organic compounds are oxidized at the anode of BESs by a diverse bacterial community. One of the main characteristics of BES ecology is the existence of multiple pathways that can be used by microorganisms for harvesting energy through, for example, respiration with the electrode either directly or via mediated compounds, fermentation, and methanogenesis via the fermentation products of other organisms.

2.2.1 Respiration in BESs

When bacteria use the electrode as the electron acceptor, it is recognized as respiration in BESs. This respiration can happen via two mechanisms: i) direct electron transfer (DET); and ii) mediator-based electron transfer (MET).

2.2.1.1 DET

DET involves the microorganism (e.g., *G. sulfurreducens*, *Shewanella oneidensis*) establishing physical contact with the electrode as a biofilm since the terminal electron transfer step occurs via tightly bound outer cell membrane components (Bond and Lovley, 2003). Since the entire biofilm is electrically conductive (Malvankar et al., 2011), this eliminates the diffusion limitations that are typically more problematic with MET (i.e., the mediator has to diffuse from the microbe to the electrode and back). The respiratory chain of DET-capable microbes is directly linked to the electrode via outer membrane cytochromes and conductive pili. This minimizes any biological energy losses in electron transfer to the electrode and represents the most efficient mechanism of electrode based respiration with respect to conversion of substrate to electric current (i.e., coulombic efficiency) (Schröder, 2007). In addition, the majority of DET-capable cells grow as biofilms, which minimizes loss of electroactive components and bacteria in continuous flow systems. On the other hand, this implies that the electrode area can

be a limiting factor for DET. However, the biggest limitation of DET capable organisms lies in their substrate specificity. Most DET capable organisms cannot use complex substrates, such as, glucose, and rely on fermenters in the BES microbiota to provide low molecular weight organic acids (e.g., acetate, lactate) as substrate (Nevin and Lovley, 2002). Finally, some DET capable organisms such as *G. sulfurreducens* require strict anaerobic conditions for growth as a pure culture.

2.2.1.2 MET

MET involves the microorganism (e.g., *P. aeruginosa*) producing extracellular electrochemically-active compounds, which shuttle electrons between the microbe and the electrode (Rabaey et al., 2005), thereby circumventing physical contact with the electrode. Therefore, MET capable microbes can establish a "connection" with the electrode over longer distances than DET and enabling the microorganism to transfer electrons to the electrode at high rates with small quantities of mediators (Rabaey et al., 2005; Rabaey et al., 2004a). In addition, these organisms typically exhibit a wider substrate diversity than DET-capable microbes, enabling the biotransformation of multiple substrates to electric current. However, the circuitous link of the respiratory chain of MET-capable microbes to the electrode via these secondary metabolites: i) presents higher biological losses since the production of the metabolites can be energetically expensive, which translates to lower coulombic efficiency; and ii) increases the number of steps involved in electron-electrode transfer, which increases the probability of bottlenecks in the extracellular electron transfer process (e.g., in diffusion/electrochemical oxidation/microbial reduction). Further, since these redox mediators can be easily flushed out in continuous flow systems, this represents a loss in the energetic efficiency of such BESs.

2.2.2 Fermentation in BESs

In a typical oxygen-limited BES environment, not all bacteria can use the electrode as an electron acceptor, and thus fermentation is an integral part of the BES metabolism. The ATP yield in fermentation is between 2-4 ATP/glucose depending upon the product (acetogenesis results in 4 ATPs and homolactic fermentation results in 2 ATPs). Therefore, to compensate for the low ATP yield (compared to 38 in respiration), fermenters exhibit a high substrate turnover rate, which makes them highly competitive with respirers for the consumption of organic sources. Since DET-capable microbes typically cannot consume complex carbon sources, fermentation in the BES provides the carbon source for these DET microbes in the form of short-chain organic acids. However, in the BES microbiota, some fermenters can also switch to electrode-based respiratory metabolism via exogenous mediators produced by other microbes (Pham et al., 2008; Rabaey et al., 2005; Rabaey et al., 2004b; Venkataraman et al., 2011; Wang et al., 2008).

2.2.3 Community interactions in BESs

Microorganisms in any ecosystem exist in complex communities involving competitive, cooperative; and neutral interactions. It is needless to say that community interactions are important in a BES and that understanding these interlinks between microorganisms is necessary for optimum system performance. Molecular tools, such as 16S rRNA gene sequencing surveys, have been applied to the anodic community of MFCs in several cases (Back et al., 2004; De Schamphelaire et al., 2010; Ishii et al., 2008a; Ishii et al., 2008b; Jeong et al., 2008; Jong et al., 2006; Kim et al., 2006; Lee et al., 2003; Parameswaran et al., 2010; Patil et al., 2009; Phung et al., 2004; Shimoyama et al., 2009; Venkataraman et al., 2011; White et al., 2009; Xing et al., 2009) and this has revealed a very diverse community. The electrochemical activity of several

bacterial species is being discovered every year. Interactions between multiple community members are being realized as governing the electricity generation and understanding these interactions is essential for BES performance improvement. With respect to BESs, the proposed interactions thus far, have focused on: i) syntrophy between fermenters and DET capable microbes; and ii) the ability of certain fermenters to respire with the electrode by using mediators produced by other members of the community. Pham et al. (2008) demonstrated that the gram positive *Brevibacillus* sp. could use the phenazines produced by *P. aeruginosa* and that the rhamnolipids (a secondary metabolite) produced by *P. aeruginosa* increased the availability of phenazines for *Brevibacillus* sp. Symbiotic relationships have not been explored, thus far. The focus of this thesis is about understanding the interactions of *P. aeruginosa* with other chosen microbial members of the BES community and this necessitates a definition of the interactions commonly observed in ecological communities irrespective of BESs (Table 2.1).

Table 2-1. Definition of common terms pertaining to ecological interactions

Term	Definition
Synergism	Two agents working together to achieve a result that neither one can achieve independently.
Symbiosis	A term used to describe interactions between biological species. It is recognized as a major driving force for evolution and can be further subdivided into several classes as shown below (Dethlefsen et al., 2007):
	Mutualism – Both organisms benefit from this relationship. This relationship might be facultative (not necessary for either organism) or obligate (necessary for either organism).
	Commensalism – One organism is benefited whereas the other remains unaffected.
	Parasitism – One organism benefits whereas the other is harmed.
	On the basis of physical interaction symbiosis is also classified as: 1. Ectosymbiosis – Symbiont lives on the surface of the host. 2. Endosymbiosis – Symbiont lives within the host.
Syntrophy	The metabolic products of one organism are the carbon source for another organism.

2.2.4 Quorum sensing (QS) and phenazine production by *P. aeruginosa*

P. aeruginosa is a model organism for studying quorum sensing - interbacterial communication using secreted signaling factors. At high cell densities, bacteria can "sense" the presence of other bacteria often of the same species, and correspondingly regulate several metabolic pathways depending upon the environmental conditions. For *P. aeruginosa* quorum sensing aids the formation of biofilms, which are an integral part of its pathogenicity because they confer higher antibiotic resistance and resilience than the planktonic phase. The core QS system in *P. aeruginosa* is formed by the autoinducer synthases (LasI and RhlI) and transcriptional regulatory proteins (LasR and RhlR). *lasI* produces the acyl homoserine lactone (AHL), 3-oxo-dodecadonyl homoserine lactone (3O-C12-HSL), which binds with *lasR*. This in turn, initiates the production of the second AHL, n-butyryl homoserine lactone (C4-HSL) by *rhlI* and subsequent activation of *rhlR*. Recent studies have found that the *Pseudomonas* quinolone signal (PQS) acts as a third quorum sensing molecule specific to *P. aeruginosa* (Kim et al., 2005). Together, the *las* and *rhl* systems control about 15% of the *Pseudomonas* genome (Whiteley et al., 1999). Several two-component regulatory systems, such as the GacS/GacA system also control QS in this organism.

P. aeruginosa is also an electrochemically-active organism in BESs, due to the production of phenazines (pyocyanin, phenazine-1-carboxamide, 1-hydroxyphenazine and phenazine-1-carboxylic acid), which are excellent redox shuttles (Pham et al., 2008; Rabaey et al., 2005). The reduced form of these phenazines (generated by the bacteria) are oxidized at the anode of a MFC and then re-reduced by the bacteria (possibly by NADH in the cytoplasm or by glutathione) (O'Malley et al., 2004), ensuring cycling between the organism and the electrode. Thus, these phenazines act as an electron acceptor for *P. aeruginosa*, enabling indirect respiration with the electrode. It was recently shown that phenazines promote survival under anaerobic conditions by

allowing energy conservation (Wang et al., 2010b). The various phenazines and their electrochemical potentials are shown in Table 2.2.

Table 2-2. Structure and potentials of phenazines produced by *P. aeruginosa.*

Redox couple	Redox reaction	E^0 @ pH = 6.5
Pyocyanin	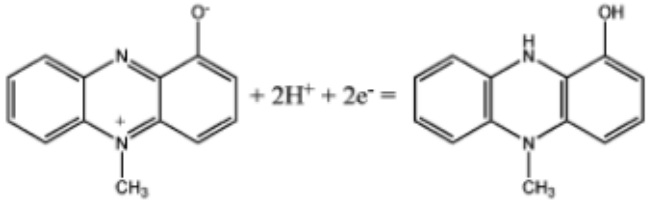	+ 28.5
phenazine-1-carboxylic acid	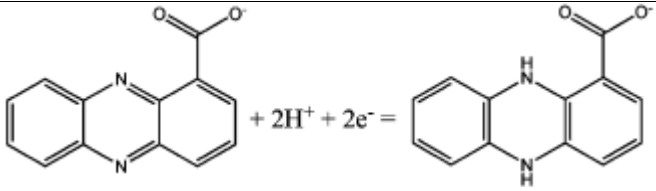	-108 mV
phenazine-1-carboxamide	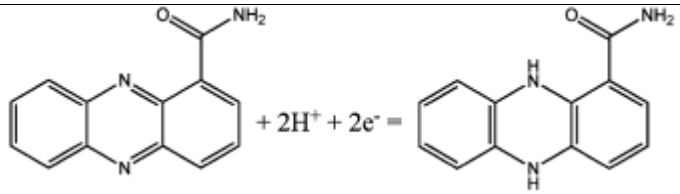	- 133 mV
1-hydroxyphenazine	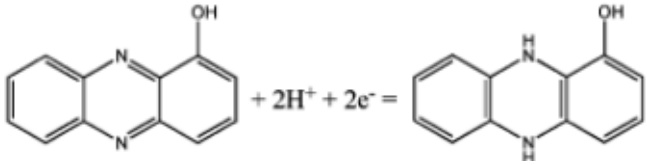	-178 mV

The *phzABCDEFG* operon is responsible for phenazine production in this organism (Wang et al., 2010b). This operon is controlled by the *pqsABCDE* operon, which is positively regulated by LasR. Therefore, QS plays a pivotal role in phenazine production in *P. aeruginosa*. The *phzA-G* operon metabolizes chorismate to phenazine-1-carboxylic acid, which in turn is transformed to pyocyanin, 1-hydroxyphenazine, and phenazine-1-carboxamide by the genes *phzM*, *phzS*, and *phzH*, respectively (Dietrich et al., 2006). With respect to mixed communities, phenazines play an important role as antibiotics because, for example, pyocyanin can reduce O_2 to O_2^-, generating

H_2O_2. Due to their high reactivity, these compounds can oxidize almost any organic compound in the cell, and therefore are highly toxic to bacterial cells. *P. aeruginosa* can withstand this oxidative stress by: i) possessing elevated levels of superoxide dismutase/catalase enzymes, which oxidize O_2^- to O_2 (Hassett et al., 1992); and ii) by being less permeable to extracellular pyocyanin (Hassan and Fridovich, 1980).

2.3 Mathematical modeling of bioelectrochemical systems

Mathematical models are valuable tools to probe the underlying mechanisms of current generation in BESs. One aspect of BES research is to understand the fundamental mechanisms and limitations involved in electron transfer to the electrode. Due to the wide variety of proposed hypotheses in this aspect and the necessity of prolonged experiments to prove/disprove each hypothesis, mathematical models can facilitate efficient experimental design. Mathematical models can work the other way around also, for example, after detailed experiments one can reduce the results to mathematical relationships, simulate the system *in-silico* and confirm the initial hypothesis. The design of more efficient BESs for electricity/product formation is another area which can benefit from mathematical modeling. The model can outline the rate-limiting factors and indicate the areas that need to be focused on for increased system performance, thereby, helping to streamline efforts (Picioreanu et al., 2007).

Mathematically, BESs are composed of biological, electrochemical, and mass transport processes. These three components are not independent and are bound together in an intricate fashion and this interaction results in the observed system performance. Due to the complexity and lack of knowledge in several areas specifically with respect to BESs, mathematical modeling demands a clearly defined goal and purpose. The general objectives of mathematical models for BESs are to understand performance parameters, such as, electrical potential, current, and

concentrations are affected by operating conditions, such as, influent concentration, biofilm composition/density, pH, microbial competition, and cooperation etc.

The basic idea of any BES model is to convert the concentrations of certain key components into electrical potential and/or currents. This can be accomplished via different approaches. The biofilm may be considered separately from the electrode (Picioreanu et al., 2007; Picioreanu et al., 2008; Picioreanu et al., 2010) or it might be assumed to be a conductive matrix as an extension of the electrode itself (Marcus et al., 2007). The first mathematical model that described a BES was developed by Zhang and Halme (1995). Their BES consisted of planktonic bacteria and an extraneously added redox mediator. The electrochemically-active component was the reduced form of the mediator and its concentration was related to the current production simply by equating the current to the rate of oxidation of the reduced form (first order kinetics). The model does not involve any mass transfer limitations or spatial concentration gradients (as a biofilm is not considered). Although the model is adequate for the authors' experimental system, it lacks versatility.

Picioreanu et al. (2007) were the first to build a detailed mathematical model based on extensive growth kinetics, biofilm structure, spatial concentration gradients, and electrode reactions based on the Butler-Volmer equation. Their model is significantly more complex and detailed than Zhang and Halme (1995). Their system also involves exogenously supplied redox mediators as the electrochemically active component but does not consider endogenous production of the mediators by bacteria as explained by Pham et al. (2009). The general structure of the model leaves room for introducing direct electron transfer as well. All the growth kinetic parameters are calculated from Heijnen (1999). The model was operated under different considerations, such as competition between planktonic and biofilm cells, exclusively planktonic cells, higher mediator

diffusivity, endogenous metabolism, different external resistances and mass transfer limitations, competition in the biofilm between methanogenic bacteria and electroactive bacteria, and varying mediator redox potential. The model output was concurrent with the expected results in all the cases; the authors could obtain realistic polarization curves, and thus this model is an excellent generalization. The authors also used experimental data from Bond and Lovley (2003) to validate their model by suitably changing parameters and conclusively showed that the electricity production by *G. sulfurreducens* could not be based upon redox mediators. This reiterates the use of mathematical models for proving/disproving experimentally observed results. The authors further integrated this model with the anaerobic digestion model-ADM1 (Batstone et al., 2002). This extended the BES model (Picioreanu et al., 2008) to incorporate glucose metabolism into acetate and methane, providing a realistic picture of methanogenesis and competition for substrate in the system. The electroactive bacteria still use acetate as the carbon source to reduce the mediator. The kinetic parameters for glucose metabolism (i.e. acidogenesis, acetogenesis and methanogenesis) are obtained from Batstone et al. (2002). The model successfully predicted current density and organic concentrations. The biofilm is allowed to evolve and develop depending upon the concentrations based on an individual based model (Xavier et al., 2005). This feature provides detailed species-based biofilm composition as an output depending upon the carbon source and the external resistance.

Kato-Marcus et al. (2007) developed a one-dimensional model based on the conductivity of the biofilm using the Nernst-Monod equation. Thus, direct electron transfer is considered as the main electron-electrode transfer mechanism. The authors characterized the biofilm as being composed of electrochemically active and inert biomass and provided it a conductivity value ranging from $10^{-5} – 10^{-3}$ mS/cm^2. This is an input parameter and not experimentally determined.

However, it does provide a simplistic way of dealing with biofilm activity. Unlike Picioreanu et al. (2008), the species-based biofilm composition is ignored and a biomass-based lumped conductivity parameter approach is adopted. The authors determined the optimum biofilm detachment rate (an input parameter), which indicated that a high shear, high turbulence rate may be beneficial for BES operation. However, the authors do not provide any other species composition apart from the biomass. They do not consider any ohmic losses in the system. In summary, the lumped conductivity approach does provide a simpler and concise way of dealing with the biofilm.

Zeng et al. (2010) assumed a constant electrode capacitance in their model. The authors did not consider biofilm kinetics. Spatial concentration gradients were neglected. However, this model considers ion transport across the membrane and due to a cation exchange membrane (there are more cations in the anode and therefore cations travel from the anode to the cathode) cathode kinetics involve the transport of ions across the membrane. This model is again a lumped parameter approach and provides a very concise way of expressing relationships and ease of model implementation. The authors successfully exhibited that the model could be used for acetate oxidation as well as complex carbohydrate (glucose and glutamic acid) oxidation. The authors assume that ohmic losses due to electrical connections in the system are negligible and the resistance is exclusively due to membrane and solution resistance. The lack of biofilm kinetics results in this model becoming suitable for selected applications only. Some reviews (Rodriguez and Premier, 2010) have also outlined other approaches that have been employed to model BESs.

The modeling approaches, thus far, have considered mediator-based electron transfer and direct-contact based electron transfer separately. Studies, which incorporate both are lacking. Such

models can help determine the conditions for which both or one of these mechanisms are active. Mediated electron transfer mechanisms are based on diffusion and direct electron transfer mechanisms are based on Ohm's law. Although, direct electron transfer mechanisms are the most energy efficient with respect to bioenergetics of microorganisms, these also necessitate direct physical contact with the electrode. With mediators, microorganisms can respire with the electrode even in the planktonic phase, though, they might be diffusion limited. Therefore, models determining the most efficient mechanism of electron transfer will have to be based on bioenergetics as microbial growth is proportional to the energy difference between the electron donor and acceptor. Such studies can reveal the pathway taken by microorganisms under different energy niches. The fact that electrode potential is determined by microbial activity and *vice versa* complicates the mathematical modeling of BESs. Some scientists (Rodriguez and Premier, 2010) have suggested that the maximum microbial growth rate occurs when a combination of both electron transfer mechanisms occurs.

Pinto et al. (2010) clearly demonstrated that coupled ordinary differential equations were sufficient to describe the microbial populations over the operating time and determine the optimum operating parameters in a MFC. The authors studied the competition between electrode-respiring bacteria and methanogens for a common substrate and its effect on MFC operation. The problem is similar to the one studied by Picioreanu et al. (2008). However, Pinto et al. (2010) use their own experimental data to determine the parameters and validate the model.

The above mentioned models clearly outline the various strategies that can be used to mathematically model BESs. This is extremely desirable as the various strategies can indicate what parameters are paramount and, which ones can be left out of the model description. However, all the models are currently applied to very specific and different systems and this does

not create a common ground for researchers to model BESs. The lumped parameter approach does portray an unsophisticated picture of the system and the overall ease of implementation make it a powerful approach for some applications. Models by Picioreanu et al. (2008-2010) are detailed and are useful for understanding the biofilm composition and evolution over time in concurrence with electrical parameters, such as potential and current. In addition, these models are very useful in answering scientific questions regarding biofilm evolution and stratification in a mixed culture over time. Nevertheless, these systems require a large number of parameters and intensive computational time. Therefore, a middle path is required when developing a generic approach for modeling BESs. Lastly, no model, thus far, takes into account the inter-microbial interactions occurring in a BES. Only substrate-based competition has been modeled in multi-species models. Therefore, a two-pronged *in-vitro* and *in-silico* approach involving ecological relationships in BES microbiota will yield valuable results for further development of BESs.

3 CHAPTER 3. Quorum sensing regulates electric current generation of *Pseudomonas aeruginosa* PA14 in bioelectrochemical systems.

Partially adapted from: Venkataraman, Rosenbaum, Arends, Halitschke, and Angenent Electrochemistry communications, January 2010. 12(3):459-462.

Note that some sections of this chapter were not published. These have been accordingly marked in the thesis.

Abstract

Here, we show that quorum sensing (QS) modulates current generation by the anode-respiring bacterium *P. aeruginosa* by controlling the production of the electron-mediating phenazines. The current generation by a wildtype (WT) strain of *P. aeruginosa* PA14, two QS signal-negative mutants Δ*lasI* and Δ*rhlI*, and a GacS/GacA protein-regulatory mutant *retS*::TN was investigated under different environmental conditions. The QS signal-negative mutants exhibited significant increases in current production (Δ*lasI*: 5.8-fold; Δ*rhlI*: 17.6-fold) when the growth medium was exogenously supplemented with the appropriate QS inducing lactone compared to growth medium devoid of the lactones. The *retS*::TN mutant generated significantly higher current (45-fold) than the WT under anaerobic conditions. Interestingly, anaerobic current generation by the WT was 28-fold higher with exogenously supplied lactones. Compared to anaerobic conditions, the WT with some oxygen (microaerobic conditions) exhibited enhanced phenazine production (39-fold) and current levels (48-fold). Iron-rich medium and microaerobic conditions had a negative impact on current generation by *retS*::TN. All these results are directly linked to QS activity in *P. aeruginosa*, thus, demonstrating the importance of this bacterial communication

system for current generation in BESs. We also show that BESs represent a new tool for real-time investigation of phenazine-related QS activity.

3.1 Introduction

Bioelectrochemical systems (BESs) are gaining importance as innovative biotechnological devices for the renewable generation of electricity from wastewater in microbial fuel cells (MFCs), generation of chemical products in microbial electrolysis cells, and sequestration of CO_2. In previous studies, *Pseudomonas* sp. in the anodic microbial community of an MFC was related to current generation (Pham et al., 2008; Rabaey et al., 2005). Phenazines produced by *Pseudomonas aeruginosa* (pyocyanin, 1-hydroxyphenazine, phenazine-1-carboxamide, and phenazine-1-carboxylate) act as redox shuttles to facilitate respiration of *P. aeruginosa* with the electrode (Rabaey et al., 2005). It has been recently shown that these endogenous phenazines are responsible for survival of *P. aeruginosa* PA14 under anaerobic conditions(Wang et al., 2010b).

Besides its importance in BESs, *P. aeruginosa* is also a model organism for understanding quorum sensing (QS). QS is the bacterial mode of communication via secreted signaling factors (Fuqua et al., 1994). The core components of the QS system in *P. aeruginosa* are the *las* and *rhl* systems, respectively, consisting of autoinducer synthases (LasI and RhlI) and transcriptional regulatory proteins (LasR and RhlR; Figure 3.1). LasI controls the production of 3-oxo-dodecanoyl homoserine lactone (3O-C12-HSL) and RhlI controls the production of N-butyryl homoserine lactone (C4-HSL), which initiate the QS cascade (Figure 3.1)(Kim et al., 2005). The *las* and *rhl* systems also affect the expression of the *phzABCDEFG* operon, which is required for phenazine synthesis (Whiteley et al., 1999). Additionally, QS in *P. aeruginosa* is also controlled by several two-component regulatory systems, such as GacS/GacA (Gooderham and Hancock, 2009) (Figure 3.1).

Therefore, based on the regulation of the phenazine biosynthesis pathway by QS and the fact that *P. aeruginosa* respires with the electrode via phenazines, we hypothesized that QS controlled current production in this microbe. To answer this hypothesis, we screened three mutants and the wildtype (WT) strain of *P. aeruginosa* PA14 for their electrochemical behavior. Two of these mutants lacked the genes coding for production of the QS signaling lactones (Δ*lasI*: 3O-C12-HSL and Δ*rhlI*: C4-HSL) and the third mutant had a transposon insertion in genes involved in GacS/GacA regulation which indirectly represses QS (*retS*::TN). Our experimental results substantiate this hypothesis of a direct link between electricity generation of *P. aeruginosa* PA14 and QS. We also investigated the current production by the protein-regulatory mutant *retS*::TN in further detail because of its superior performance compared to the WT.

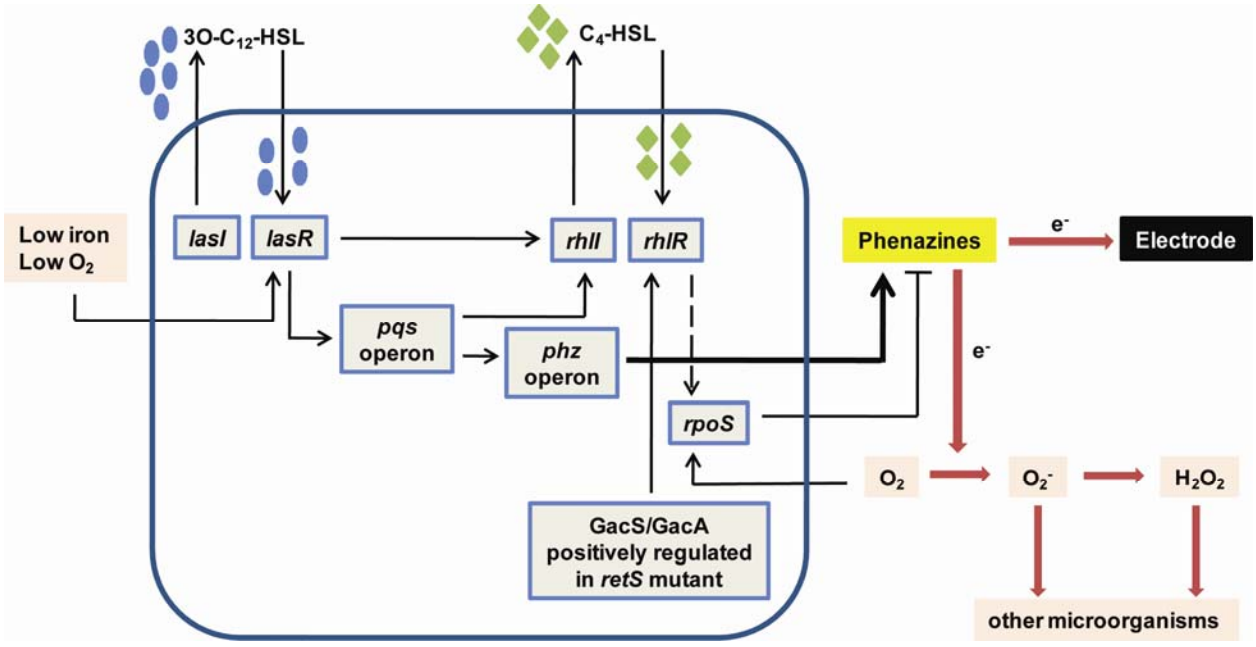

Figure 3.1. Cartoon of the interaction between the quorum-sensing cascade of *P. aeruginosa* PA14 with environmental factors, including the electrode.

3.2 Materials and Methods

3.2.1 Bacterial strains and medium

P. aeruginosa PA14 wildtype and the *retS*::TN mutant were obtained from the PA14 Transposon Insertion Mutant Library (Liberati et al., 2006). The Δ*lasI* and Δ*rhlI* mutants were kindly provided by Deobrah A. Hogan (Dartmouth Medical School). Experiments were performed in minimal AB medium(Clark and Maaløe, 1967) (30 mM glucose) at 37^{o}C.

3.2.2 Electrochemical experiments

The electrochemical cells consisted of a glass vessel with a tight rubber stopper and a three-electrode setup: working electrode (anode) – 12 cm^2 carbon paper (P50, AvCarb, www.fuelcellstore.com); counter electrode – graphite rod (Poco graphite, Decatur, TX); and reference electrode – Ag/AgCl sat. KCl (all potentials given vs. this reference). The vessel was autoclaved, filled with sterile anoxic medium (150 mL), assembled in an anaerobic hood (Coy Labs, Grass Lake, MI), and sealed. For anaerobic experiments, the headspace was maintained under sterile nitrogen gas. For microaerobic experiments, oxygen was allowed to diffuse through a 0.2-µm filter into the headspace. The electrochemical measurements (BioLogic VSP; Bio-Logic USA, Knoxville, TN) were structured in a repetitive loop, starting with cyclic voltammetry from -0.5 V to +0.5 V @ 2mV s^{-1} and followed by chronoamperometry for 24 h at 0.3 V for up to 21 days. After 24 h of measurement in blank medium, the cell was inoculated with 100 µL of an overnight culture of *P. aeruginosa* in Luria-Broth (LB) medium. All experiments except the screening of mutants were performed in triplicate. 3O-C_{12}-HSL and C4-HSL (Cayman Chemical Company, Ann Arbor, MI) were dissolved in dimethyl sulfoxide prior to addition to the medium. Iron was supplied as ferric chloride.

3.2.3 Phenazine analysis

Pyocyanin (Cayman Chemical Company, Ann Arbor, MI) and 1-hydroxyphenazine (Chemos GmbH, Regenstauf, Germany) were extracted, detected, and quantified with a LC/MS (Thermo Scientific, Waltham, MA) with a protocol adapted from Dekimpe *et al.* (2009) with an additional selective reaction monitoring (SRM) to enhance sensitivity using external standard calibration curves. The concentrations of pyocyanin and 1-hydroxyphenazine were summed together and the value reported as the total phenazine concentration.

3.2.4 Data analysis

Statistical analysis (pairwise ANOVA comparisons) was performed using SYSTAT 12 (Systat Software Inc., Chicago, IL).

3.3 Results and Discussion

3.3.1 Δ*lasI* and Δ*rhlI* mutants (not published)

Owing to the incapability of these signal-negative mutants to produce the QS inducing lactones (Δ*lasI*: 3O-C12-HSL and Δ*rhlI*: C4-HSL), the QS cascade is interrupted in these mutants upstream of the phenazine production pathway (Figure 3.1). Further, since *lasI* and *rhlI* are in direct control of phenazine production, this implies that these mutants would produce significantly less phenazines compared to the WT (in which the QS cascade is intact). Consequently, we expected that both these mutants would exhibit a drastic decrease in current production compared to the WT. Indeed, we observed that under microaerobic conditions the Δ*lasI* mutant produced 14.4-fold lesser current densities than the WT (0.45 μA cm^{-2} by Δ*lasI* vs. 6.5 μA cm^{-2} by the WT) and the Δ*rhlI* mutant produced 17.10-fold lesser current densities than the WT (0.38 μA cm^{-2} by Δ*rhlI* vs. 6.5 μA cm^{-2} by the WT; Figure 3.2). Next, we proposed that

exogenous addition of the respective QS-inducing lactones in the growth medium for both these mutants would restore complete functionality of the QS cascade in these mutants, resulting in enhanced phenazine production compared to growth medium devoid of the lactones. Indeed, the current production by Δ*lasI* increased by 5.8-fold when the medium was supplemented with exogenous 5 μM 3O-C12-HSL and the current production by Δ*rhlI* increased by 17.6-fold upon supplementing the medium with 5 μM C4-HSL (Figure 3.2). This confirms our hypothesis that QS is a direct regulator of electric current generation in *P. aeruginosa*.

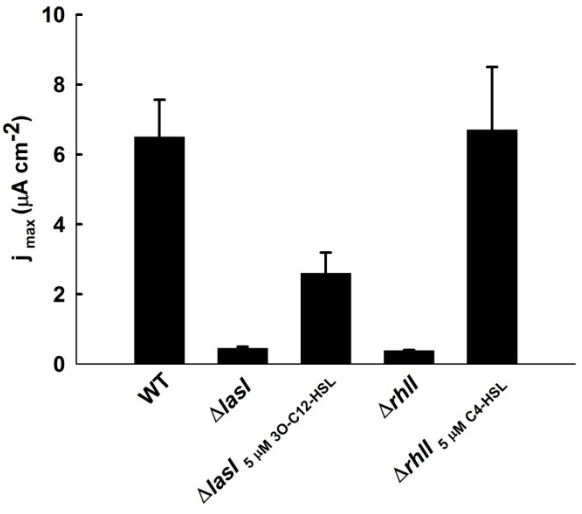

Figure 3.2. Mean maximum current densities in μA cm^{-2} by the WT, Δ*lasI*, and Δ*rhlI* mutants under different experimental conditions. Note that these experiments were carried out under microaerobic conditions.

3.3.2 *retS*::TN mutant

The absence of RetS in this mutant results in increased autophosphorylation of GacS (Goodman et al., 2009), which subsequently increases the transcription of the small RNAs: RsmY and RsmZ. These small RNAs sequester the mRNA-binding protein RsmA. This protein (when not sequestered in WT) has a negative effect on the core QS *rhlIrhlR* system. Therefore, the sequestered RsmA in the *retS*::TN mutant allows for increased phenazine synthesis by the

mutant compared to the WT. This implies that the *retS*::TN mutant should produce higher current than the WT. Indeed, under anaerobic BES conditions, the *retS*::TN mutant produced a 45-fold higher current than the WT (6.08 μA cm^{-2} vs. 0.136 μA cm^{-2}; Figure 3.3a). Correlating with this higher current, we found higher phenazine production by the *retS*::TN mutant (8.94 μg mL^{-1} vs. 0.32 μg mL^{-1}; Figure 3.3b). Since the lack of regulation of the GacS/GacA system in the absence of RetS upregulates QS in the *retS*::TN mutant compared to the WT, this further validates our hypothesis linking QS and current generation in *P. aeruginosa*.

To further study the relationship between QS and current generation, experiments were performed to downregulate and upregulate phenazine production in the *retS*::TN mutant and in the WT, respectively, by introducing suitable environmental factors (i.e., iron-rich medium and 3O-C12-HSL, respectively). Previous researchers found that iron deficiency results in enhanced production of extracellular virulence factors (i.e., phenazines) (Kim et al., 2003) because the expression of *lasR* is enhanced by iron limitation (Figure 3.1). Therefore, to downregulate phenazine production under anaerobic conditions we increased the iron concentration in *retS*::TN mutant experiments (from 1 μM to 100 μM $FeCl_3$). As predicted, the current and phenazine levels with 100 μM iron were significantly lower than with 1 μM iron (Figure 3.3). To upregulate phenazine production in WT experiments under anaerobic conditions, we added 3O-C12-HSL, which is an initial inducer of QS in *P. aeruginosa* (Dietrich et al., 2006). Despite the fact that the WT is capable of producing indigenous lactones, we hypothesized that under the bioenergetically challenging anaerobic conditions, the presence of exogenous 3O-C12-HSL in the growth medium would facilitate phenazine production. As predicted, the WT showed increasing current generation and phenazine production with exogenous 3O-C12-HSL (Figure 3.3).

We performed our experiments under anaerobic conditions that are common in BESs, while most QS studies are performed with oxygen. To understand the effect of oxygen on phenazine production, we performed experiments under microaerobic conditions. Current and phenazine levels for the WT under microaerobic conditions were significantly higher than under anaerobic conditions (Figure 3.3), which can be attributed to a faster growth rate of *P. aeruginosa* with O_2 (Sabra et al., 2002). We also performed WT experiments under microaerobic conditions with and without exogenous addition of 3O-C12-HSL, but no significant difference was observed (Figure 3.3). Most likely, the enhanced growth under microaerobic conditions epistatically overshadowed the effect of exogenously supplemented 3O-C12-HSL.

The enhanced electrochemical activity of WT under microaerobic vs. anaerobic conditions is an important finding for BES research. It has already been reported that oxygen enhances the electrochemical activity of *Shewanella oneidensis* MR-I (Ringeisen et al., 2007). The presence of oxygen is also responsible for the antibiotic activity of the phenazine pyocyanin, which is attributed to its ability to reduce oxygen to superoxide (O_2^-), leading to the formation of hydrogen peroxide. Both these oxidants are toxic to most microorganisms (Figure 3.1) (Hassett et al., 1992). *P. aeruginosa* overcomes this toxicity by expressing elevated levels of the enzyme superoxide dismutase(Suh et al., 1999). In the anodic microbial ecology of a mixed-culture BES with oxygen intrusion, this may have broad implications because phenazines can introduce a pressure on microbial survival and selection. Therefore, phenazines will have a dual role as a redox-shuttle and as an antibiotic in BESs under microaerobic conditions.

Conversely, the *retS*::TN mutant exhibited significantly lower current and phenazine levels under microaerobic conditions compared to anaerobic conditions (Figure 3.3). Oxidative stress controls phenazine production in *P. aeruginosa* via the stationary phase sigma factor RpoS (Figure 3.1),

which also protects the bacterium against various other stresses(Hassett et al., 1992). Suh *et al.* (1999)(Suh et al., 1999) further verified this with a *P. aeruginosa rpoS* mutant characterized by low *rpoS* expression; which, accordingly, produced elevated concentrations of phenazines compared to the WT in the presence of oxygen (Venturi, 2003). The negative feedback effect of oxygen on phenazine production via RpoS could explain why we observed a significantly lower current and phenazine level for the *retS*::TN mutant than the WT under microaerobic conditions (Figure 3.2). We hypothesize that RpoS is more dominant in the *retS* mutant due to the positive reinforcement of the GacS/GacA system, which can be indirectly linked to the production of RpoS (transcriptional regulation via the *rhl* system) (Venturi, 2003). However, further studies are necessary to conclude that the *retS*::TN mutant is more susceptible to oxidative stress than the WT.

Phenazine concentration is an excellent indicator of the status of QS in *P. aeruginosa* and has been used by several studies to monitor QS in this microbe. In our system, the final phenazine concentration correlates very well with the maximum current densities (Figure 3.3). It is important to note that the phenazine production has to be measured after a laborious extraction procedure and LC-MS analysis, whereas the current can be monitored *in-situ* real time. Thus, BESs represent a new tool for real-time investigation of phenazine-related QS activity because of the direct link between current generation and phenazine production (Figure 3.3).

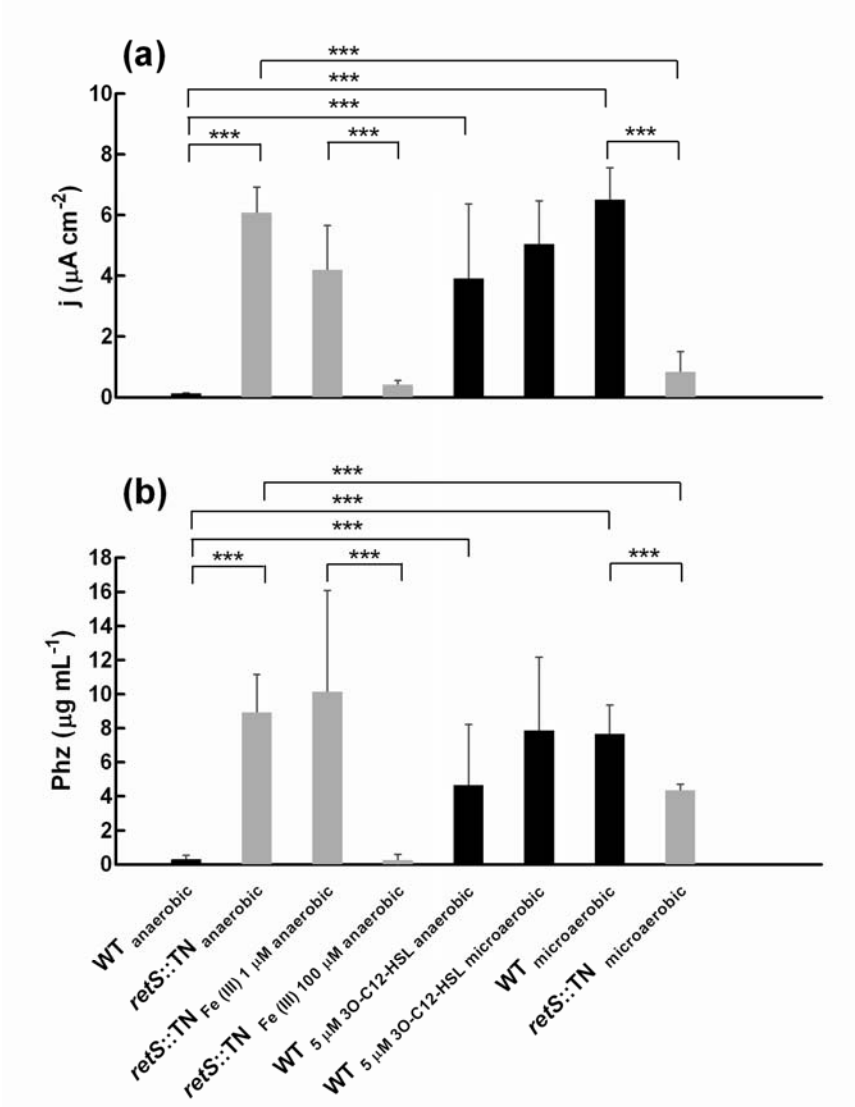

Figure 3.3. Relationship between current and phenazine concentration: (a) mean maximum current density in μA cm^{-2} by the WT and *retS*::TN mutant under different experimental conditions; and (b) mean phenazine concentration (sum of pyocyanin and 1-hydroxyphenazine) in μg mL^{-1} by the WT and *retS*::TN under different experimental conditions (pairs with p-value < 0.05 are marked *).**

3.4 Conclusions

Here, we showed that QS and current generation in BESs for *P. aeruginosa* are closely linked via phenazine production. The presence of environmental factors positively or negatively affected certain parts of QS. Subsequently, this resulted in the modulation of phenazine production,

thereby, controlling the current generation by this microorganism. *P. aeruginosa* is an important organism in the anodic community of BESs and it can influence community selection via the antibiotic action of pyocyanin, especially in the presence of oxygen. Additionally. through the real-time electrochemical detection of changes in the phenazine levels, BESs represent a new laboratory tool to study QS-related responses in *P. aeruginosa*.

3.5 Acknowledgements

This work was supported through NSF career grant # 645021 to L.T.A.. We thank Dr. Andrew Goodman at Washington University in St. Louis and Dr. Stephen Winans at Cornell University for strain acquisition and fruitful discussions.

4 CHAPTER 4. Metabolite-based mutualism between *Pseudomonas aeruginosa* PA14 and *Enterobacter aerogenes* enhances current generation in bioelectrochemical systems.

Adapted from: Venkataraman, Rosenbaum, Perkins, Werner, and Angenent. Energy and Environmental Science. September 2011. 4(4). 4550-4559.

Abstract

Understanding the ecological relationships of the microbiota in bioelectrochemical systems (BESs) is necessary to gain deeper insight into their performance. Here, we show that the fermentation product 2,3-butanediol stimulates mutually beneficial interactions between *Pseudomonas aeruginosa* PA14 and *Enterobacter aerogenes* in a BES with glucose as the initial substrate under microaerobic conditions. The experiments were conducted in potentiostatically-poised 3-electrode reactors. Under these conditions: i) the current density by a co-culture of *P. aeruginosa* and *E. aerogenes* increased at least 14-fold compared to the current density by either of these two bacteria alone; and ii) *E. aerogenes* fermented glucose principally to 2,3-butanediol, which was subsequently consumed by *P. aeruginosa*. To determine the benefits to each microorganism in this symbiosis, we conducted experiments with pure cultures. The current production by a pure culture of *P. aeruginosa* with 2,3-butanediol was increased 2-fold compared with glucose as the carbon source. This was due to enhanced phenazine production by *P. aeruginosa*. Further, pyocyanin comprised the majority (92%) of the phenazines produced by *P. aeruginosa* with 2,3-butanediol, but only 29% with glucose. The current production by a pure culture of *E. aerogenes* increased ~19-fold when the growth medium was supplemented with 35 μg mL^{-1} of pyocyanin as the electron mediator. We also observed that *E. aerogenes* generated

maximum current densities with pyocyanin compared to the other three phenazines, indicating that *E. aerogenes* respires most effectively with pyocyanin – the phenazine whose production is stimulated by this microbe's product (2,3 butanediol). Concomitantly, a decrease in fermentation products and enhanced growth with increasing concentrations of pyocyanin implies a shift towards electrode-based respiration by *E. aerogenes* rather than fermentation. Therefore, the synergism in current generation by the co-culture can be attributed to the combination of enhanced pyocyanin production by *P. aeruginosa* with 2,3-butanediol and the ability of *E. aerogenes* to efficiently respire. This study is the first to demonstrate metabolite based "inter-species communication" in BESs, resulting in enhanced electrochemical activity. It also explains how an inconsequential fermenter can become an important electrode-respiring bacterium within an ecological network at the anode.

4.1 Introduction

Bioelectrochemical systems (BESs) are gaining importance to generate electricity and valuable products (e.g. H_2, CH_4, H_2O_2) from wastewater (Cheng et al., 2009; Logan et al., 2008; Rozendal et al., 2009), to desalinate sea water (Cao et al., 2009a), to sequestrate CO_2 (Cao et al., 2009b; Wang et al., 2010a), and to use as biosensors and biocomputing devices (Chang et al., 2005). Typically, BESs consist of an anode (where bacteria catalyze the oxidation of wastewater/acetate), and a cathode (where O_2 is reduced or products are generated). Bacteria can transfer electrons to the anode of a BES via two mechanisms: i) direct electron transfer – the microorganism establishes physical contact with the electrode to transfer electrons through outer membrane cytochromes, and ii) mediated electron transfer – the microorganism produces redox-active compounds, which are oxidized at the anode and reduced by the bacteria (i.e. electron mediators) (Bretschger et al., 2010). As a first step towards better understanding of the inter-

species interactions at the BES anode, genome-enabled tools, such as 16S rRNA gene sequencing surveys, have been applied to characterize the diverse anodic community (Back et al., 2004; Ishii et al., 2008b; Parameswaran et al., 2010; White et al., 2009). However, the various interactions between community members have been studied mainly with respect to syntrophy wherein metabolites produced by one species are the substrates for other species (Freguia et al., 2008; Rosenbaum et al., 2009; Rosenbaum et al., 2010). While undefined mixed culture-based studies with BESs are suitable for environmental applications, defined mixed culture-based studies are necessary to better understand the complex ecological networks at the BES anode.

For BES research, *P. aeruginosa* has been a model organism for mediated electron transfer. *P. aeruginosa* produces four phenazines, which are electrochemically active compounds (pyocyanin [PYO], 1-hydroxy phenazine [1-OH-PHZ], phenazine-1-carboxylic acid [PCA], and phenazine-1-carboxamide [PCN]) (Pham et al., 2008; Rabaey et al., 2005; Rabaey et al., 2004a). *P. aeruginosa* is also a model organism for studying: i) quorum sensing – the bacterial mode of communication by secreted signaling factors; and ii) biofilm formation (Dietrich et al., 2006). Previously, we have established that quorum sensing controls the electrochemical activity of this microorganism by regulating phenazine production (Venkataraman et al., 2010). Lopes *et al*. (2010) recently established that *P. aeruginosa* in biofilms could exert a selective pressure on the microbial community via its metabolites, but the authors were unable to determine the specific signals/metabolites. The authors found that *Escherichia coli* grown with the supernatant of *P. aeruginosa* exhibited lower biomass and respiratory activity (Lopes et al., 2010). Owing to the "social" nature of *P. aeruginosa*, multiple co-culture studies involving *P. aeruginosa* in association with fermenters in BESs have been reported in the literature. Pham *et al.* (2008)

demonstrated that Gram-positive *Brevibacillus* sp. could use the phenazines produced by *P. aeruginosa* for electron transfer to the electrode. Further, the rhamnolipids (a secondary metabolite) produced by *P. aeruginosa* increased the availability of phenazines for *Brevibacillus* sp., thereby asserting the ecological role of this microorganism in BESs. The synergism (two agents working together to achieve a result that cannot be attained independently) between *P. aeruginosa* and *Enterococcus faecium* in a BES was demonstrated although the authors did not investigate the mechanisms of the symbiosis (Read et al., 2010).

Enterobacter aerogenes is being investigated for bioenergy applications due to its hydrogen production capability (Nakashimada et al., 2002; Ren et al., 2009). *Enterobacter* sp. has also captured the attention of BES researchers (Rezaei et al., 2009; Tanisho et al., 1989; Zhuang et al., 2010). For instance, previous studies have found that hydrogen is used as a mediator by *E. aerogenes* for current generation (Tanisho et al., 1989; Zhuang et al., 2010). Further, Zhuang *et al.* (2010) claim that *E. aerogenes* evolves over time to directly transfer electrons to the electrode via unspecified mechanisms, although the given evidence (cyclic voltammograms of the biofilm) was not substantial. *Enterobacter cloacae* was shown to degrade cellulose and generate an electric current without the addition of any exogeneous mediators (Rezaei et al., 2009; Zhuang et al., 2010).

E. aerogenes is a facultative aerobe capable of aerobic respiration and anaerobic fermentation while *P. aeruginosa* is an obligate respirer (Madigan et al., 2002). *Pseudomonas* sp. and *Enterobacter* sp. were found at the anode of a microbial fuel cell treating nitrobenzene (Li et al., 2010). The co-existence of *P. aeruginosa* and *E. aerogenes* in marine sediment has been well documented (Angell et al., 2006). The authors found these two microorganisms as a synergistic culture in environmental isolates in Hawaii. A blue colored pigment (later identified as

pyocyanin) was produced only when both organisms were present with *P. aeruginosa* as the producer and *Enterobacter* as the inducer. The authors found that metabolite exchange between the two organisms was necessary for the induction and synergism, but the mechanism was not elucidated. Pyocyanin also exhibits anti-microbial activity by generating superoxide radicals and/or hydrogen peroxide or nitric oxide radicals, which in turn can cause oxidative stress and damage to DNA (Hassett et al., 1992). The existence of synergism between these two species in the natural environment indicates that pyocyanin is not toxic to *E. aerogenes*. These two species were also present in a microbial community responsible for causing corrosion in water distribution systems, thus, highlighting the presence of these two microorganisms in areas with oxidation-reduction gradients (Emde et al., 1992).

When we studied the bacterial community composition of a biofilm at the anode of a BES after a three-month operating period, we found that the relative presence of bacterial sequences closely related to *P. aeruginosa* PA14 (Figure 4.1) were similar between the inoculum and the anode biofilm. However, sequences related to *E. aerogenes* were most abundant at the anode (Figure 4.1), while they had been below detection limit in the inoculum (i.e. anaerobic granules). Under oxygen-limited conditions; such as found in our BES, *E. aerogenes* exhibits fermentation and inconsequential electrochemical activity. This poses the question: why did *E. aerogenes* emerge as a dominant member of the BES community? We hypothesized that *P. aeruginosa* and *E. aerogenes* exhibited mutualism, which is a form of symbiosis in which both agents benefit from the relationship. Our experiments with pure and defined cultures, substantiated this hypothesis and, in addition, also ascertained that the synergism between *P. aeruginosa* and *E. aerogenes* was regulated by the fermentation product – 2,3-butanediol.

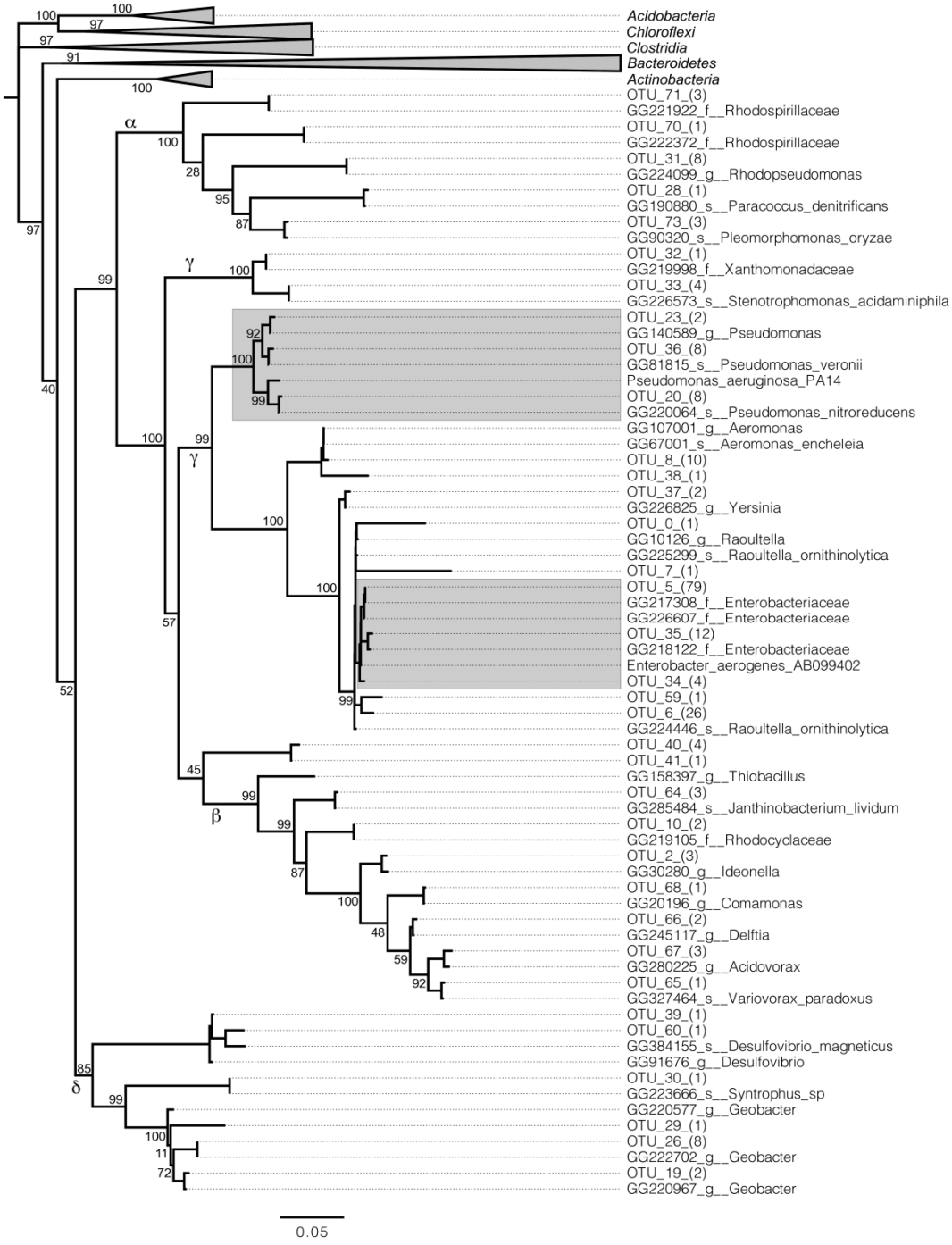

Figure 4.1. Maximum-likelihood phylogenetic tree (FastTree) of OTUs from this study belonging to the phylum Proteobacteria, with most similar Greengenes sequences included. Abundance of each OTU is indicated in parentheses (N sequences); taxonomy following reference sequences is the deepest taxonomic assignment available in the Greengenes taxonomy ("s = species, g = genus, f = family"). Greek letters indicate the class of the proteobacteria. Percent support values are listed for higher-order nodes. Highlighted regions include OTUs similar to *Pseudomonas* sp. and *Enterobacter* sp..

4.2 Materials and Methods

4.2.1 Bacterial strains and medium

We obtained *P. aeruginosa* PA14 wildtype from the PA14 Transposon Insertion Mutant Library (Liberati et al., 2006) and *E. aerogenes* from NRRL (strain B-115). Experiments were performed in minimal AB medium (Clark and Maaløe, 1967) supplemented with 30 mM of one carbon source (2,3-butanediol/glucose/ethanol) at 37^{o}C.

4.2.2 16S rRNA gene sequencing

A 16S rRNA gene survey characterized the anodic mixed culture of an upflow microbial fuel cell (UMFC) operated for three months (He et al., 2006). Bulk DNA from the inoculum and anode biofilm was extracted using bead beating and phenol:chloroform extraction; 16S rRNA genes were amplified with a 30-cycle PCR protocol using bacterial primers 8F and 1391R. The 20-μl reaction utilized AmpliTaq-Gold (Promega Corp, Madison, WI), 0.4 pmol μl^{-1} forward and reverse primers, 0.5 mM $MgCl_2$, 0.2 mM dNTPs, 0.8 mg ml^{-1} BSA, 5 mg ml^{-1} acetamide, and 1 μl of template. Amplicons were gel purified (Qiagen, Valencia, CA), cloned into TOPO TA pCR4.0, and transformed into *E. coli* TOP10 cells (Invitrogen, Carlsbad, CA). Clones were sequenced using vector-specific primers and an internal 16S rRNA gene primer 907R with an ABI 377 DNA sequencer (BigDye terminator ready reaction mixture, PE Applied Biosystems, Inc., Carlsbad, CA) at the Genome Sequencing Center, Washington University School of Medicine, St. Louis, MO (Ley et al., 2006). We sequenced 254 16S rRNA genes (1.3 kb) from the inoculum (anaerobic granular sludge, with GenBank accession numbers EF515481 - EF515734) and 302 genes from the UMFC anode biofilm (EF515179 - EF515480). 16S rRNA

gene sequences were edited and assembled into consensus sequences using PHRED and PHRAP aided by Xplorseq (Frank, 2008), and bases with a PHRAP quality score <20 were trimmed.

16S rRNA gene sequences were aligned to the Greengenes core alignment (DeSantis et al., 2006) using PyNAST (Caporaso et al., 2010). Aligned sequences were clustered into operational taxonomic units (OTUs) at 97% similarity using the furthest neighbor algorithm in mothur 1.15 (Schloss et al., 2009). A close reference sequence for each OTU was picked from the Greengenes prokMSA, and the combined alignment of OTU representative sequences and reference sequences was filtered using the Greengenes Lane mask (DeSantis et al., 2006) and an approximately-maximum-likelihood tree was built from the filtered alignment using FastTree (Price et al., 2010). Two additional 16S rRNA gene reference sequences were obtained from NCBI, aligned as described above, and included in the tree: *P. aeruginosa* PA14 (GI 116048575:733095-734620) and *E. aerogenes* (AB099402).

4.2.3 Electrochemical experiments

The electrochemical cells consisted of a glass reactor with a three-electrode setup: working electrode (anode) – 150 cm^2 carbon cloth (PANEX ® 30 - PW06, Zoltek Corp, St Louis, MO) mounted to a graphite rod (Poco graphite, Decatur, TX) with carbon cement (CCC Carbon Adhesive, EMS, Hatfield, PA); counter electrode – graphite rod (Poco graphite); and reference electrode – Ag/AgCl sat. KCl (all potentials given vs. this reference). The vessel was autoclaved and filled with sterile medium (350 mL). For anaerobic experiments, the reactors were continuously sparged with N_2 via a 0.22-µm filter. For microaerobic experiments, oxygen was allowed to diffuse through a 0.22-µm filter into the headspace. The electrochemical measurements with a potentiostat (BioLogic VSP; Bio-Logic USA, Knoxville, TN) were structured in a repetitive loop, starting with cyclic voltammetry from -0.5 V to +0.5 V @ 2 mV s^-

[1] and followed by chronoamperometry for 24 h at 0.3 V vs. Ag/AgCl sat. KCl for up to 7 days. After a 24-h measurement in blank medium, the reactor was inoculated with 100 μL of an overnight culture of *P. aeruginosa* and/or *E. aerogenes* in Luria-Bertani broth (LB) medium. For abiotic experiments, H_2 was sparged through a diffuser continuosly. Triplicates were conducted for each experiment and the average values along with standard deviations were reported throughout the text. The current and pyocyanin concentration vs. time profile for one experiment is shown in the supplementary information (Figure 8.1 in Appendix 1).

4.2.4 Metabolite and phenazine measurement

Metabolites were detected and measured with a HPLC (Shimadzu, Columbia, MD), using a Aminex HPX-87H column (BioRad, Hercules, CA). 5 mM sulfuric acid was used as the eluent at a flow rate of 0.6 ml min^{-1} at 60 ^{o}C. Pyocyanin (Cayman Chemical Company, Ann Arbor, MI), 1-hydroxy phenazine (Chemos GmbH, Regenstauf, Germany), phenazine-1-carboxylic acid, and phenazine-1-carboxamide (Princeton Building Blocks, Monmouth Junction, NJ) were extracted and detected and quantified via a LC/MS (Thermo Scientific, Waltham, MA) with a protocol adapted from Dekimpe *et al.* (2009) with an additional selective reaction monitoring (SRM) to enhance sensitivity using external standard calibration curves.

4.3 Results and discussion

4.3.1 Community analysis of a UMFC anode biofilm

The first step in understanding and forming hypotheses with respect to interactions between community members of a BES anode is to identify bacterial species that enrich at the electrode during operation. We inoculated an upflow microbial fuel cell (UMFC) with a mixed culture of bacteria and archaea (granular sludge) from an anaerobic bioreactor treating brewery wastewater.

Our UMFC was operated in continuous mode at a loading rate of 1.0 g COD L^{-1} day^{-1} with a synthetic wastewater consisting of sucrose and an inital flow rate of 0.36 mL min^{-1}. After a 3-month operating period, a thick biofilm on the anode was visible to the naked eye (whitish in color). Subsequently, we sequenced more than 300 16S rRNA genes, and found that 12 different phyla were representative of the 98.7% of the UMFC anode sequences that were classifiable in a phylum (Figure 4.2). Rarefaction curves and Chao diversity estimates (generated with DOTUR (Schloss and Handelsman, 2005)) showed that the inoculum was more diverse than the UMFC biomass. We attribute a lower diversity in the UMFC to the lower complexity of the artificial wastewater solution (sucrose) that was fed to the UMFC biomass compared to the real brewery wastewater that was fed to the granular sludge (inoculum). The ability of bacteria to transfer electrons to the anode in a BES has been shown to be phylogenetically widespread; known electrode-respiring bacteria include species in the phyla Proteobacteria, which increased in our study from 27.2% to 69.5% for the inoculum and the UMFC culture, respectively (Figure 4.2) (Bond and Lovley, 2005; Rabaey et al., 2004c; Shimoyama et al., 2009). The enrichment of Proteobacteria in the UMFC was supported by an increased representation of the subgroups Alphaproteobacteria and Gammaproteobacteria, while the subgroup Delta-proteobacteria decreased compared to the inoculum. However, the known electrode-respiring bacterium *Geobacter* sp. within the Deltaproteobacteria increased in abundance from 1.6% to 3.3% (3 OTUs; 11 UMFC sequences). We identified 53% of the UMFC sequences as Gammaproteobacteria (160 sequences out of 302). *P. aeruginosa* remained at similar levels between the inoculum and the UMFC (3 OTUs; 18 UMFC sequences). Among the Gammaproteobacterial sequences in the UMFC anode biomass, however, the largest representation (95 sequences) was found for the 3 OTUs that are closely related to *E. aerogenes*

(Figure 4.1). This genus had been below the level of detection in our sequencing survey of the inoculum.

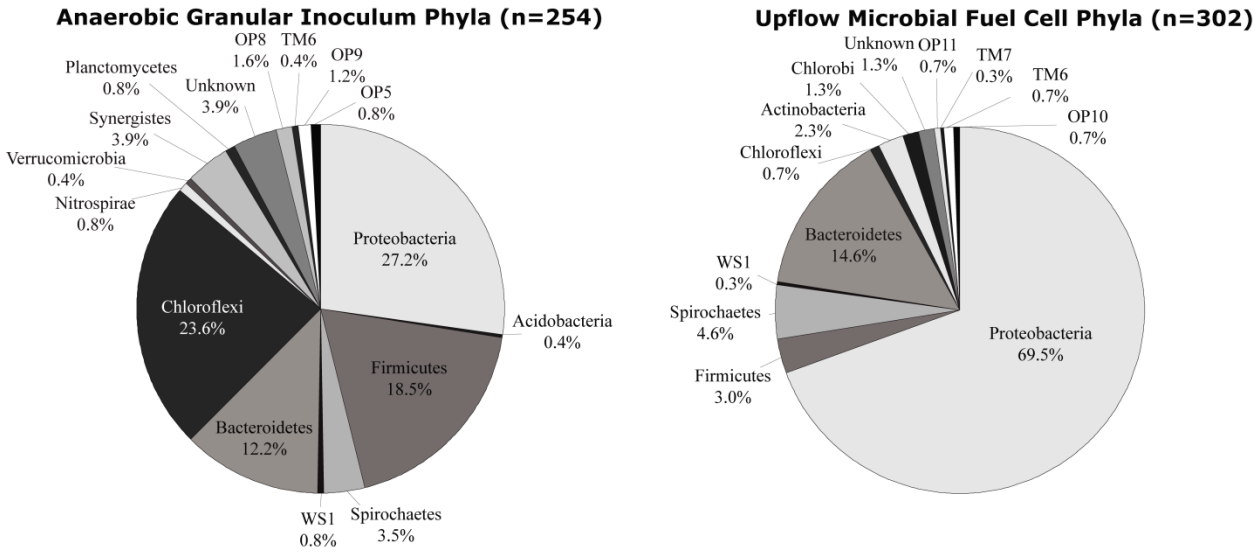

Figure 4.2. Distribution of observed phyla from the anaerobic granular inoculum and the UMFC.

4.3.2 BES experiments with *P. aeruginosa* and *E. aerogenes*

E. aerogenes is known to primarily ferment under microaerobic or anaerobic conditions with H_2 as a product. H_2 can subsequently be electrochemically oxidized with metal catalysts at the anode. However, electrochemical oxidation of H_2 is not directly energetically beneficial to *E. aerogenes*. In addition, there is no conclusive proof of direct electron transfer by *E. aerogenes* (Tanisho et al., 1989; Zhuang et al., 2010). Therefore, the success of *Enterobacter* sp. under the environmental conditions of an UMFC anode was unexpected, and we raised the question whether respiration with the anode in association with *P. aeruginosa* can be an important physiological process of *E. aerogenes*. To investigate this we performed bioelectrochemical experiments in triplicate under microaerobic and anaerobic conditions with: i) a co-culture of *P. aeruginosa* and *E. aerogenes*; ii) a pure culture of *P. aeruginosa*; and iii) a pure culture of *E.*

aerogenes. The co-culture of both bacteria generated at least 14-fold higher current densities than the pure cultures under microaerobic conditions (46.53 ± 6.4 μA cm^{-2} with the co-culture vs. 3.25 ± 0.14 μA cm^{-2} with *P. aeruginosa* and 2.53 ± 1.3 μA cm^{-2} with *E. aerogenes*; Figure 4.3); thereby conclusively exhibiting synergism between the two microorganisms. Under anaerobic conditions, the co-culture also generated higher current densities than the pure cultures (0.45 ± 0.07 μA cm^{-2} with the co-culture vs. 0.14 ± 0.02 μA cm^{-2} with *P. aeruginosa* and 0.2 ± 0.13 μA cm^{-2} with *E. aerogenes*; Figure 4.3). The current densities under microaerobic conditions were two orders of magnitude higher than under anaerobic conditions (Figure 4.3). This confirms our previous findings with *P. aeruginosa* that microaerobic conditions are more conducive to electric current generation by this electrode-respiring bacterium (Venkataraman et al., 2010). Importantly, the long-standing notion that BESs have to be operated under strict anaerobic conditions for optimum performance has been recently questioned (Biffinger et al., 2008; Ringeisen et al., 2007; Rosenbaum et al., 2009).

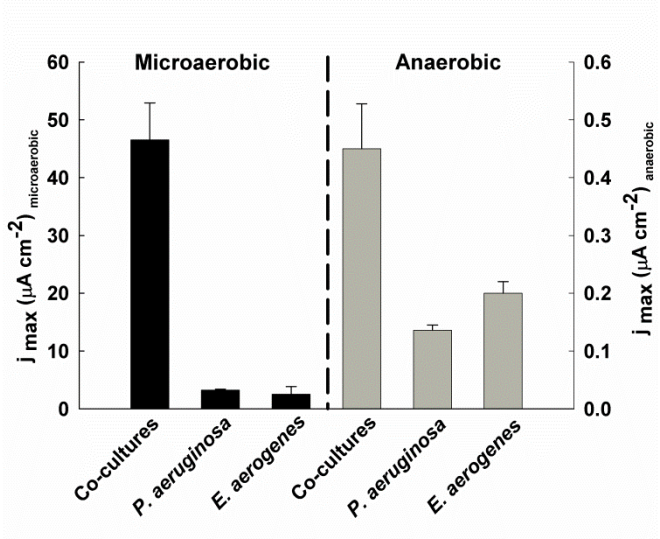

Figure 4.3. Maximum current densities (j_{max}) obtained with co-cultures and pure cultures of *P. aeruginosa* and *E. aerogenes* under microaerobic and anaerobic conditions.

E. aerogenes has a higher growth rate than *P. aeruginosa* (doubling time in AB media with glucose for *E. aerogenes* is 16 min vs. 50 min for *P. aeruginosa*). Therefore, it is likely that in BESs, *E. aerogenes* grows faster than *P. aeruginosa* and initially ferments glucose to metabolites that subsequently act as substrates for *P. aeruginosa*. Indeed, the metabolic analysis of the co-culture experiment for both microaerobic and anaerobic conditions over the operating period (Figure 4.4) revealed that: i) under microaerobic conditions, *E. aerogenes* had already depleted glucose by day 1, and *P. aeruginosa* consumed 2,3-butanediol (the major metabolite) during days 3-7; and ii) under anaerobic conditions glucose consumption by *E. aerogenes* was much slower and lactate and acetate were the main fermentation products. This is in accordance with previous studies asserting the importance of microaerobic conditions for 2,3-butanediol fermentation by *E. aerogenes* (Byun et al., 1994; Converti et al., 2003; Hsieh et al., 2007; Johansen et al., 1975; Perego et al., 2000). 2,3-butanediol is a pH-neutral metabolite, thereby, preventing lethal media acidification and also acts as an energy storage mechanism for *E. aerogenes* under conditions of glucose deprivation (Johansen et al., 1975). Because microaerobic conditions stimulated high current densities, all the subsequent experiments were performed under microaerobic conditions.

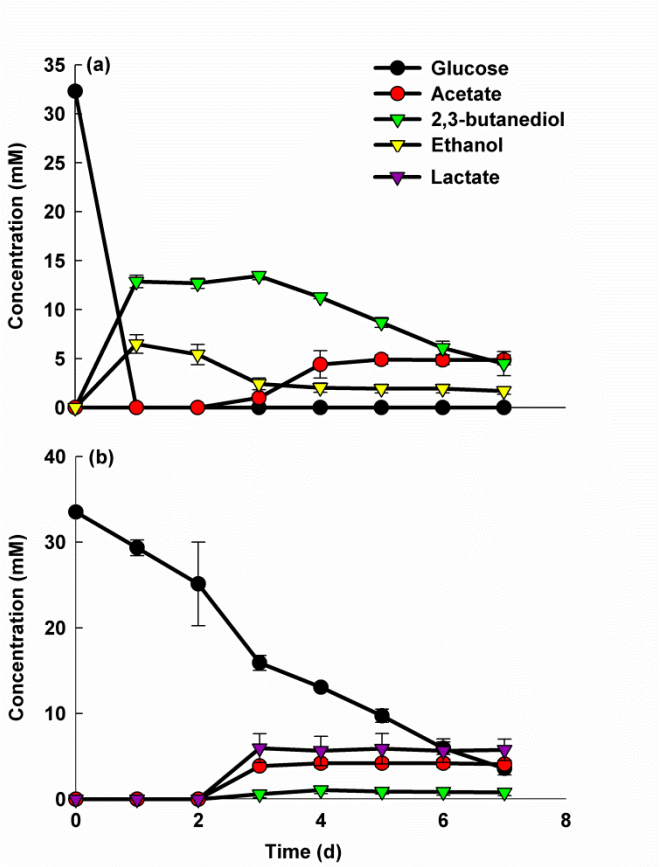

Figure 4.4. Metabolite profile over time with the co-culture under: (a) microaerobic and (b) anaerobic conditions.

4.3.3 Effect of 2,3-butanediol on *P. aeruginosa*

After establishing the synergism between the two species via increased current generation, our objective became to determine the mutually beneficial compound. Fermentation products link the two species in a food chain; thus, it is possible that such a product confers benefits to *P. aeruginosa*. Therefore, we assessed the electrochemical activity of *P. aeruginosa* in triplicate under microaerobic conditions with glucose (control), 2,3-butanediol, or ethanol (the latter two are fermentation products of *E. aerogenes* under microaerobic conditions) as the carbon source. The current densities were increased two-fold with 2,3-butanediol compared to glucose (control) and they were seven times higher with 2,3-butanediol compared to ethanol (5.23 ± 0.19 μA cm^{-2}

with 2,3-butanediol vs. 3.25 ± 0.14 μA cm^{-2} with glucose vs. 0.73 ± 0.07 μA cm^{-2} with ethanol; Figure 4.5), indicating that 2,3-butanediol was the most beneficial fermentation product for *P. aeruginosa*. In addition, the coulombic efficiencies were maximum with 2,3-butanediol (12.95 ± 0.39 % with 2,3-butanediol vs. 6.39 ± 0.79 % with glucose vs. 0.68 ± 0.48 % with ethanol; Figure 4.5).

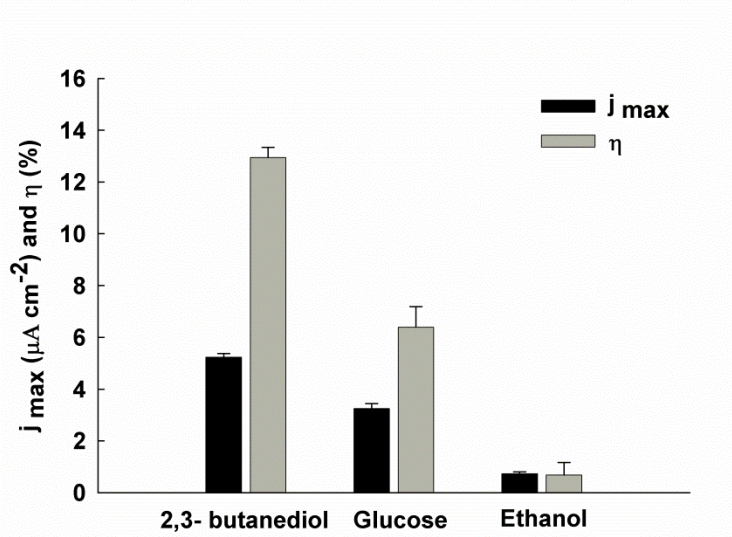

Figure 4.5. Maximum current densities (j_{max}) and coulombic efficiencies (η) obtained with *P. aeruginosa* grown in AB media with 30 mM 2,3-butanediol, 30 mM glucose, and 30 mM ethanol as carbon sources under microaerobic conditions.

The phenazines produced by *P. aeruginosa* possess different colors, for example, pyocyanin is blue, and 1-hydroxy phenazine is yellow under the environmental conditions of our BESs. Interestingly, the reactors with *P. aeruginosa* grown on 2,3-butanediol turned green in color whereas those grown on glucose turned yellow in color (Figure 4.6a). We have previously shown that phenazine concentrations correlate well with current densities in *P. aeruginosa* (Venkataraman et al., 2010). Because of the higher current generation and varying reactor colors, we hypothesized that 2,3-butanediol stimulated both higher phenazine production and a change in the phenazine spectrum of *P. aeruginosa*, respectively. Indeed, the phenazine analysis

indicated an increase in phenazine concentrations with 2,3-butanediol compared to glucose (sum of all phenazines: 20.8 ± 4.38 μg ml^{-1} with 2,3-butanediol vs. 6.4 ± 2.1 μg ml^{-1} with glucose; Figure 4.6b). In addition, 92% of the phenazines produced with 2,3-butanediol were pyocyanin, resulting in the green color (mixture of the blue color of pyocyanin and the yellow colors of 1-hydroxy phenazine and the other two phenazines). With glucose as the carbon source, 65% of the phenazines were 1-hydroxy phenazine with much lower concentrations of pyocyanin, thus, resulting in the yellow color (Figure 4.6b).

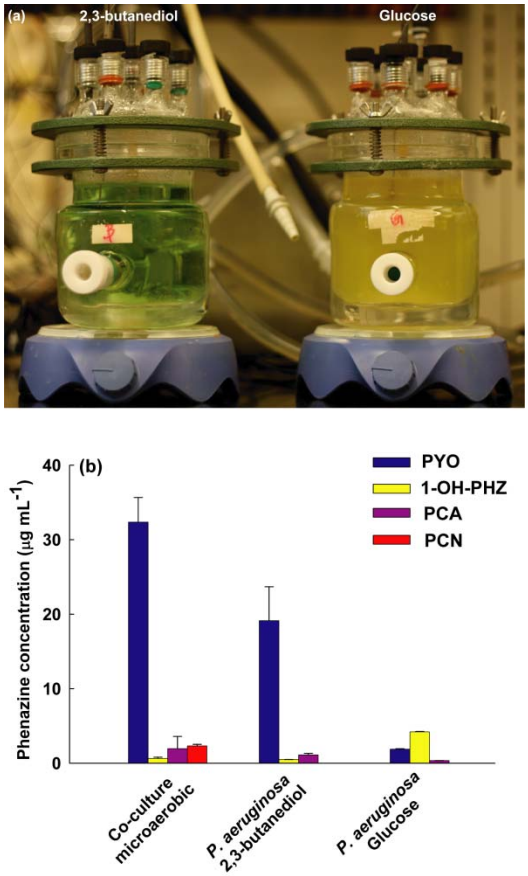

Figure 4.6. Phenazine production by *P. aeruginosa*: (a) BESs with *P. aeruginosa* grown on AB media with glucose and 2,3-butanediol; and (b) phenazine concentrations under different conditions (PYO – pyocyanin, 1-OH-PHZ – 1-hydroxy phenazine, PCA - phenazine-1-carboxylic acid, and PCN – phenazine-1-carboxamide) under microaerobic conditions.

Under anaerobic conditions, the relatively higher phenazine concentrations with the co-culture were also related to 2,3 butanediol, but were 3 orders of magnitude lower than microaerobic conditions (0.03 ± 0.014 μg ml^{-1} under anaerobic conditions vs. 37.25 ± 4.67 μg ml^{-1} under microaerobic conditions). The concentration of 2,3-butanediol in the co-culture under anaerobic conditions was $1/13^{th}$ compared to microaerobic conditions (1.06 ± 1.29 mM under anaerobic conditions vs. 13.45 ± 1.32 mM under microaerobic conditions).

The concentration of phenazines produced by *P. aeruginosa* in the co-culture with *E. aerogenes* (37.28 ± 4.67 μg ml^{-1}) was higher than produced by a pure culture of *P. aeruginosa* with 2,3-butanediol (20.8 ± 4.38 μg ml^{-1}). Although we cannot explain this difference definitively, it is possible that: i) a higher cell density of *P. aeruginosa* was achieved in the co-culture compared to the pure culture due to the availability of multiple substrates, resulting in a higher phenazine concentration; and ii) *P. aeruginosa* had to compete with *E. aerogenes* for phenazines as electron acceptors in the co-culture, resulting in enhanced phenazine production.

4.3.4 Benefit for *E. aerogenes* in a co-culture with *P. aeruginosa*

E. aerogenes exhibits respiration with O_2 as the electron acceptor under completely aerobic conditions and fermentation under microaerobic/anaerobic conditions. *E. aerogenes* is known not to use nitrate/sulfate or other electron acceptors for anaerobic respiration. Since respiration has often a higher energy gain than fermentation (38 ATPs with O_2 as the electron acceptor for respiration vs. a maximum of 4 ATP for acetogenesis), respiration is more energetically beneficial to *E. aerogenes* (Madigan et al., 2002). Therefore, we investigated if *E. aerogenes* could use the phenazines in their oxidized state as an electron acceptor for respiration and we determined the most effective phenazine. Electrochemical experiments were conducted in triplicate with *E. aerogenes* in AB media with glucose in the presence of each of the four

phenazines under microaerobic conditions. *E. aerogenes* generated the maximum current densities with pyocyanin (the major phenazine produced by *P. aeruginosa* with 2,3-butanediol as the carbon source) as the electron acceptor under the applied experimental conditions (18.52 ± 6.62 μA cm^{-2} with 5 μg ml^{-1} PYO, 2.67 ± 0.46 μA cm^{-2} with 5 μg ml^{-1} 1-OH-PHZ, 8.42 ± 1.52 μA cm^{-2} with 5 μg ml^{-1} PCA, and 1.78 ± 0.38 μA cm^{-2} with 5 μg ml^{-1} PCN; Figure 4.7).

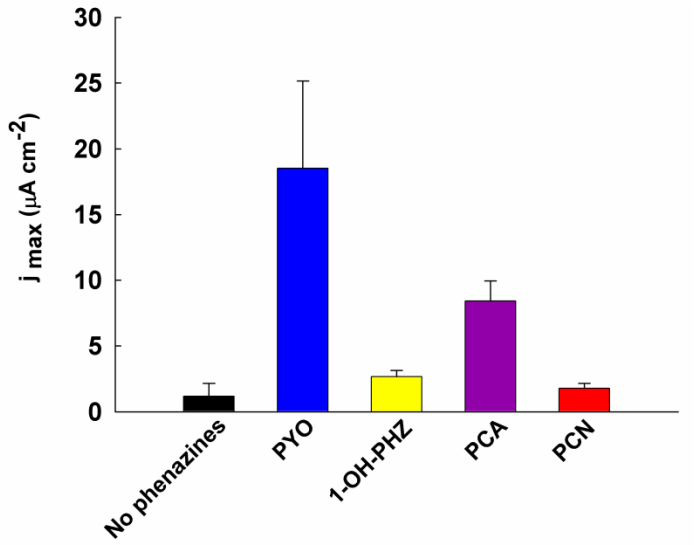

Figure 4.7. Maximum current densities (j_{max}) obtained with *E. aerogenes* grown in AB media supplemented with 5 μg ml^{-1} of different phenazines under microaerobic conditions.

When the growth medium was supplemented with 35 μg mL^{-1} pyocyanin (the concentration encountered by *E. aerogenes* in the co-culture; Figure 4.6b), the current density (49.11 ± 14 μA cm^{-2}) increased 19-fold compared to the absence of phenazines (2.53 ± 1.3 μA cm^{-2}), indicating that *E. aerogenes* was using the pyocyanin produced by *P. aeruginosa* for respiration with the electrode. This switch to respiration was also supported by a growth benefit for *E. aerogenes* with increasing pyocyanin concentrations as seen from the optical density at 600 nm (OD_{600} with 0 μg mL^{-1} pyocyanin = 0.62 ± 0.03 vs. OD_{600} with 35 μg mL^{-1} pyocyanin = 1.83 ± 0.09), verifying that *E. aerogenes* is not susceptible to the antibiotic effects of pyocyanin. Further, this

effect of enhanced growth of *E. aerogenes* due to respiration via pyocyanin might also be responsible for the abundance of this organism in our UMFC (95 sequences; Figure 4.1). If fermentation products, such as H_2, were responsible for reducing the phenazines then this would have: i) theoretically contributed to current generation; and ii) eliminated the energetic gain for *E aerogenes*. To eliminate this possibility, we conducted cyclic voltammetry and chronoamperometry in AB medium sparged with H_2 in the presence and absence of pyocyanin. Similar experiments were also performed with the supernatant of a *E. aerogenes* culture and pyocyanin to rule out the likelihood of any other metabolites exhibiting electrochemical activity with the phenazines. We found that: i) hydrogen did not exhibit any electrocatalytic activity on our electrode and could not reduce pyocyanin; and ii) the supernatant had no electrochemical activity (Figures 8.2-8.4 in Appendix 1). We also quantified the fermentation products of *E. aerogenes* (2,3-butanediol, ethanol, and acetate) when the growth medium was supplemented with 0 μg mL^{-1}, 1 μg mL^{-1}, 5 μg mL^{-1} , and 35 μg mL^{-1} pyocyanin (Figure 4.8). We observed a decreasing trend in the formation of these products with increasing pyocyanin concentration, and a 1323% increase in the number of coulombs transferred as electric current concomitant with a 3-fold increase in growth (between 0 μg mL^{-1} and 35 μg mL^{-1} pyocyanin). This indicates an increase in respiration and decrease in fermentation of *E. aerogenes* in a BES with pyocyanin, resulting in harnessing more energy by respiration with the electrode via the pyocyanin produced by *P. aeruginosa* than by fermentation. Such advantage in energy gain would result in a high growth rate that may explain the abundance of *E. aerogenes* in the UMFC (95 sequences; Figure 4.1).

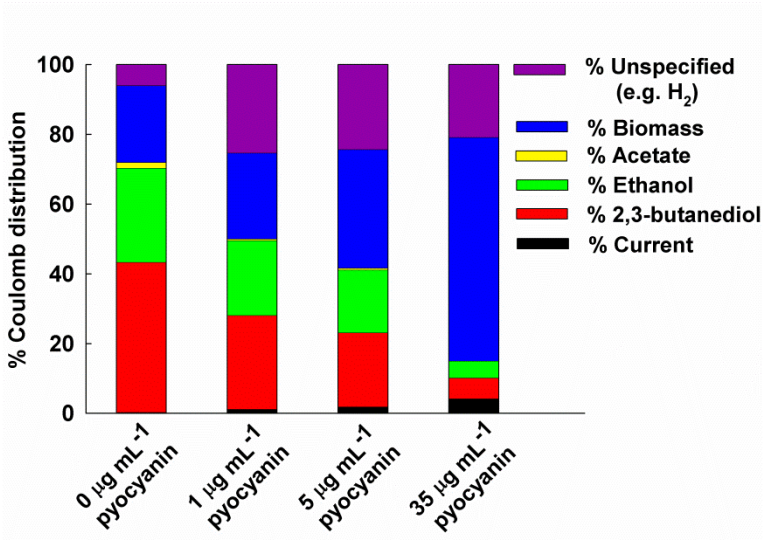

Figure 4.8. Coulombic distribution between various components with *E. aerogenes* grown under different concentrations of pyocyanin under microaerobic conditions. Note that the normalization was performed with respect to the total coulombs contained in the initial amount of glucose under each condition; biomass conversion to coulombs is based on (Heijnen, 1999).

4.3.5 Implications on BES microbiota

Multiple studies have characterized the anode microbiota and discovered unknown electrode-respiring bacteria (Back et al., 2004; De Schamphelaire et al., 2010; Ishii et al., 2008a; Ishii et al., 2008b; Jeong et al., 2008; Jong et al., 2006; Katayama et al., 2002; Kim et al., 2006; Lee et al., 2003; Marshall and May, 2009; Nguyet Thu et al., 2004; Parameswaran et al., 2010; Patil et al., 2009; Phung et al., 2004; Shimoyama et al., 2009; Vandecandelaere et al., 2008; White et al., 2009; Xing et al., 2009). This may suggest a unique microbial community in BESs, however, natural ecosystems characterized by the presence of reduction-oxidation gradients are analogous to anode environments. In BESs, these gradients are generated from the anode surface into the bulk reactor liquid, sludge, or biofilm. In nature, they exist in soil horizons, sediment-water interfaces, and marine sediments (Girguis et al., 2010). For example, the inverse correlation between oxygen concentration and depth in marine sediments supports a wide range of energy

yielding reactions, including both anaerobic and aerobic microbial processes. Benthic microbial fuel cells harvest energy from this natural gradient, thereby already challenging the notion of the "artificial" character of BES ecology. In regards to *P. aeruginosa*, the use of phenazines for long-range electron transfer to reduce Fe(III) in soil is already well established, and thus the electrochemical function of these compounds is not unique to BESs (Wang and Newman, 2008). *P. aeruginosa* and *E. aerogenes* have also been found to co-exist in: i) ocean floor sediments (Angell et al., 2006); ii) soil microbiota (O'Neill et al., 2009); and iii) microbiota causing corrosion in water distribution systems (Emde et al., 1992). It is, therefore, likely that the metabolite-based mutualism, which we describe here, evolved in nature. This also implies that our findings have implications beyond BES research to, for example, better understand carbon cycles in natural environments or corrosion prevention in engineered systems.

The functional anode in our UMFC, then, would have selected for this mutualistic partnership. This resulted in the enrichment of *E. aerogenes* at the anode compared to the inoculum, especially since redox gradients and *E. aerogenes* populations were not important in the environmental conditions of the inoculum. In part, this was possible due to microaerobic conditions at the UMFC anode because of dissolved oxygen in the substrate solution and oxygen diffusion from the catholyte to the anolyte through the membrane. The dual nature of phenazines as redox shuttles and antibiotics likely applied an additional selection pressure for the enrichment of *E. aerogenes*, because they are capable of tolerating this stress (Hassett et al., 1992; Hassett et al., 1999; Pal'chykovs'ka et al., 2008).

The respiration activity of *E. aerogenes* with pyocyanin under microaerobic conditions resulted in a higher growth rate (Figure 4.8), which would explain the dominant presence of *E. aerogenes* at the anode of our UMFC. We observed in the three-electrode BESs of this study that the bulk

of phenazine-based respiration was performed by *E. aerogenes* rather than *P. aeruginosa*; under analogous conditions compared to the co-culture (46.53 μA cm^{-2}), *E. aerogenes* obtained a maximum current density of 49.11 μA cm^{-2} with 35 μg ml^{-1} pyocyanin while this was only 5.23 μA cm^{-2} for *P. aeruginosa* with 30 mM 2,3-butanediol. Therefore, we predict that *P. aeruginosa* is more important within our described ecological network to support the production of pyocyanin rather than to respire. The resulting abundance of *E. aerogenes* (especially compared to *P. aeruginosa*) in the UMFC biofilm would be explained by this phenomenon, but of course we cannot be sure as *E aerogenes* is also able to ferment sugars without a symbiotic partner. In fact, a complete shift from fermentation to respiration for *E. aerogenes* would prevent the formation of 2,3-butanediol and nullify the symbiosis. Indeed, even at a pyocyanin concentration of 35 μg mL^{-1}, 10% of the glucose was still fermented to 2,3-butanediol and ethanol. Besides the likely important *E. aerogenes* respiration that we described here, *Geobacter* sp., which was also enriched within the UMFC anode biofilm compared to the inoculum, respired with the anode with acetate as the electron donor (possibly from *P. aeruginosa* [Figure 4.4]).

4.4 Conclusions

Here, we showed that *P. aeruginosa* and *E. aerogenes* are interlinked via a fermentation metabolite (i.e. inter-species communication) and that this relationship was not just restricted to syntrophy, but involved metabolite-based mutualism. This translated into synergism with respect to electric current generation in BESs. Both microorganisms benefited from the pH-neutral nature of 2,3-butanediol, thus, preventing lethal media acidification commonly encountered in fermentation. In addition, *P. aeruginosa* benefited by producing more phenazines (and shifting towards the production of pyocyanin) with 2,3-butanediol as the carbon source compared with glucose, resulting in higher respiration activity. *E. aerogenes* benefited by using pyocyanin as an

electron acceptor to respire with the electrode rather than to ferment, resulting in higher cell growth that may explain its abundance in the undefined mixed culture of an anode biofilm.

4.5 Acknowledgements

This work was supported through NSF CAREER grant # 0939883 to L.T.A.. We thank Dr. Andrew Goodman at Yale University for strain acquisition.

5 CHAPTER 5. Common fermentation products increase production of virulence factors by *Pseudomonas aeruginosa*

This chapter is not published.

Abstract

Interspecies microbial interactions shape microbiota and can increase pathogenesis of polymicrobial infections (Ramsey et al., 2011; Ratcliff and Denison, 2011). In the microbiota of the lungs of cystic fibrosis patients, in burn wounds, and on endotracheal tubes, *Pseudomonas aeruginosa* is ubiquitous (Hoffman et al., 2010; Perkins et al., 2010). *P. aeruginosa* is virulent, which reduces the fitness of other microbial community members, while it forms biofilms, which increases its persistence and antibiotic resistance. Guss *et al.* (2011) and Marris (2009) have postulated that for polymicrobial infections, cohabitants could stimulate *P. aeruginosa* to exhibit increased virulence. However, thus far, such interbacterial interactions have not been demonstrated. Here, we show *in vitro* that common fermentation products (*i.e.*, lactate, acetate, ethanol, and 2,3-butanediol) from cohabitants (Guss et al., 2011), significantly increase the virulence and biofilm formation by *P. aeruginosa* when used as substrates compared to the common blood sugar - glucose. 2,3-butanediol had the maximum stimulating effect compared to the other fermentation products. The global regulator *lasI*, which controls quorum sensing, biofilm formation, and virulence factor expression, was upregulated 3-fold in *P. aeruginosa* grown with 2,3-butanediol compared to glucose. Thus, the success of *P. aeruginosa* in an ecosystem is aided by metabolic cues from other community members. Consequently, we anticipate that our findings can serve as a foundation for the design of novel clinical treatment strategies for polymicrobial infections involving *P. aeruginosa*.

5.1 Introduction

The treatment of infections involving the opportunistic pathogen *P. aeruginosa* is clinically challenging due to the remarkable resilience exhibited by this bacterium *in vivo* (Hoffman et al., 2010). *P. aeruginosa* colonizes the airways of cystic fibrosis (CF) patients culminating in severe lung damage and death (Singh et al., 2002). In addition to the obligate respirer *P. aeruginosa*, fermenters, such as *Enterobacter aerogenes, Klebsiella pneumoniae*, *S. aureus*, *S. marcescens*, *Streptococcus* sp., and *Rothia* sp., are also present in this niche (Burns et al., 1998; Guss et al., 2011). Due to the oxygen limited conditions in lungs with CF (Guss et al., 2011; Hoffman et al.), fermentation products, either from bacterial metabolism or host-generated via neutrophil metabolism, are commonly found in the sputum of CF patients (Bensel et al., 2010; Palmer et al., 2007). Fermentation always involves a higher substrate turnover rate (~15-fold) than respiration to compensate for the lower ATP yield per mole substrate in fermentation compared to respiration (Madigan et al., 2002). This implies that in CF lungs, a syntrophic relationship exists of which *P. aeruginosa* uses the fermentation products from fermenters as the energy and carbon source. Palmer *et al.* (2007) also found that *P. aeruginosa* preferentially used lactate compared to glucose in a synthetic CF medium. Considering the prevalence of *P. aeruginosa* and the abundance of fermenters in CF lungs (Guss et al., 2011), we hypothesized that the success of *P. aeruginosa* in CF is significantly facilitated by the presence of fermenters. Specifically, we postulated that the fermentation products themselves induce increased virulence of *P. aeruginosa* in polymicrobial infections.

5.2 Materials and methods

5.2.1 Strains and growth conditions

We used *P. aeruginosa* PA14 (PA14 transposon insertion mutant library (Liberati et al., 2006)), *E. aerogenes* strain NRRL B-115, *K. pneumoniae* ATCC 9590 (Dr. Martin Wiedmann, Cornell University, NY), *S. aureus* Newman (Dr. Eric Skaar, Vanderbilt University, TN), and *S. marcescens* NRRL B-23389. Biofilm and virulence factor quantification was performed in minimal AB medium (Clark and Maaløe, 1967) supplemented with the appropriate carbon source (30 mM each). Motility experiments were performed in NB medium (Rashid and Kornberg, 2000) with varying agar concentrations and 30 mM carbon source. Dry cell weights were determined by weighing the cell pellet after overnight drying at 105^{o}C. OD_{600} was measured with a 96-well plate reader (BioTek). Statistical tests were performed using SYSTAT 12 (Systat).

5.2.2 Biofilm and motility experiments

P. aeruginosa was grown in bioreactors (Venkataraman et al., 2011) with a suspended glass cover slip as the solid substratum. Gram staining was performed with a gram staining kit (Difco). Biofilm protein was extracted from the cover slip in 0.1 N NaOH at 96^{o}C for 40 min. (Marsili et al., 2008a). Protein quantification was performed using the BCA assay (Thermo Scientific). Motility experiments were performed as previously described (Rashid and Kornberg, 2000).

5.2.3 Virulence factor, autoinducer measurement, and proteomics

Pyocyanin was quantified via a LC/MS protocol adapted from the study by Dekimpe and Deziel (2009). Elastase measurement was performed via elastin congo red hydrolysis activity (Suh et al., 1999) with elastase from porcine pancreas (Sigma) as reference. Pyoverdine was measured

fluorometrically by excitation at 400 nm and emission at 460 nm (Suh et al., 1999). 3O-C12-HSL was measured with *Escherichia coli* indicator strain MG4 with plasmid pkdT17 (kindly provided by Dr. Peter E. Greenberg, University of Washington, Seattle, WA) according to Pearson *et al*. (1994). Protein extraction and shotgun proteomics with isobaric tags for relative quantification was performed as previously described (Werner et al., 2009).

5.2.4 Plate quantification and metabolite analyses

Serial dilutions of daily bioreactor samples were plated on LB agar plates using an autoplater (Autoplate 4000, Spiral Biotech) and incubated for 18 h at 32 ^{o}C. Colonies of *S. marcescens* turned pink (prodigiosin production) and colonies of *P. aeruginosa* were green (pyocyanin production). Metabolites were detected and quantified with a HPLC (Waters)[22].

5.3 Results and discussion

To test the hypothesis of increased virulence of *P. aeruginosa* with the fermentation products compared to glucose, we evaluated the success of *P. aeruginosa* via quantification of: i) the virulence factor – elastase – a protease responsible for degrading bacterial cell walls (Kessler et al., 1998); and ii) biofilm formation by *P. aeruginosa* fed with four different fermentation products (*i.e.,* lactate, acetate, ethanol, and 2,3-butanediol) compared to glucose. We found that both elastase and biofilm protein density (protein present in biofilm-phase cells per unit area) were significantly higher with all fermentation products (Figure 5.1. a,b) compared to glucose. In addition, 2,3-butanediol had a maximum stimulating effect on *P. aeruginosa* compared to the other fermentation products. 2,3-butanediol is produced by several bacterial species, including *Staphylococcus* sp., *Serratia* sp., *Enterobacter* sp., and *Klebsiella* sp., (Ji et al., 2011) all of which are present in CF conditions (Burns et al., 1998). Finally, 2,3-butanediol is pH neutral, which is advantageous for microbiota, because it prevents lethal acidification unlike lactate and

acetate. Therefore, we studied the behavior of *P. aeruginosa* with 2,3-butanediol in more detail and compared this to glucose-fed cells. Biofilms grown on glass cover slips for two days were much denser with 2,3-butanediol compared to glucose (Figure 5.1c) and the total biofilm protein density with 2,3-butanediol-grown cells was 7.4-fold that of glucose-grown cells (Figure 5.1a,b; 188.69 ± 10.35 μg cm^{-2} with 2,3-butanediol vs. 25.57 ± 8.92 μg cm^{-2} with glucose). Since increased surface locomotion by type IV pili, which is referred to as twitching motility, negatively affects biofilm formation by limiting cell clustering and aggregation in *P. aeruginosa* (Singh et al., 2002), we compared swimming motility (bacterial locomotion in liquids; 0.3% agar), swarming motility (biosurfactant induced locomotion; 0.5% agar), and twitching motility (1.0% agar) of *P. aeruginosa* between 2,3-butanediol and glucose. While we detected no difference in twitching motility, we saw a remarkable reduction in swarming and swimming motility with 2,3-butanediol (Figure 5.1d), which may be responsible for facilitating biofilm formation by promoting increased cellular aggregation.

We further quantified the virulence of *P. aeruginosa* grown with 2,3-butanediol and glucose for 48 h by assaying the secondary metabolites pyocyanin and pyoverdine. Pyocyanin induces oxidative stress, which is lethal to some microbes (Hassett et al., 1992), and pyoverdine is a siderophore essential for pathogenesis of *P. aeruginosa* in iron-limiting situations (Kim et al., 2005). Oxygen concentrations differentially influence the production of these virulence factors by *P. aeruginosa* (Schuster and Greenberg, 2008), and therefore, we measured these products under two different oxygen tensions: i) microaerobic (passive O_2 diffusion into bioreactors via sterile 0.22-μm gas filters: dissolved oxygen < 0.3 mg L^{-1}); and ii) aerobic (vigorously shaken cultures in conical flasks). The concentration of pyocyanin was significantly higher with 2,3-butanediol compared to glucose under both microaerobic and aerobic conditions (Figure 5.1e).

Pyoverdine fluorescence was significantly higher with 2,3-butanediol compared to glucose under aerobic conditions, where enhanced growth compared to microaerobic conditions can lead to iron limitation. However, pyoverdine fluorescence was lower with 2,3-butanediol compared to glucose (Figure 5.1f) under microaerobic conditions (typically prevalent in CF lungs), where net growth is reduced compared to aerobic conditions (Table 9.1 in Appendix 2), and thus preventing iron limitation.

Next, we hypothesized that quorum sensing (QS), which controls biofilm formation and production of virulence factors in *P. aeruginosa* (Wagner et al., 2003; Whiteley et al., 1999), was upregulated with 2,3-butanediol. QS in *P. aeruginosa* is based upon acyl homoserine lactones produced sequentially by the two systems: *las* (3-oxo-dodecadonyl homoserine lactone - 3O-C12-HSL) and *rhl* (n-butyryl homoserine lactone - C4-HSL). Indeed, we confirmed via a bioassay (Pearson et al., 1994) that with 2,3-butanediol *P. aeruginosa* produced nearly 3-fold higher levels of the QS initiating lactone - 3O-C12-HSL - compared to glucose under both microaerobic and aerobic conditions (Figure 5.1g).

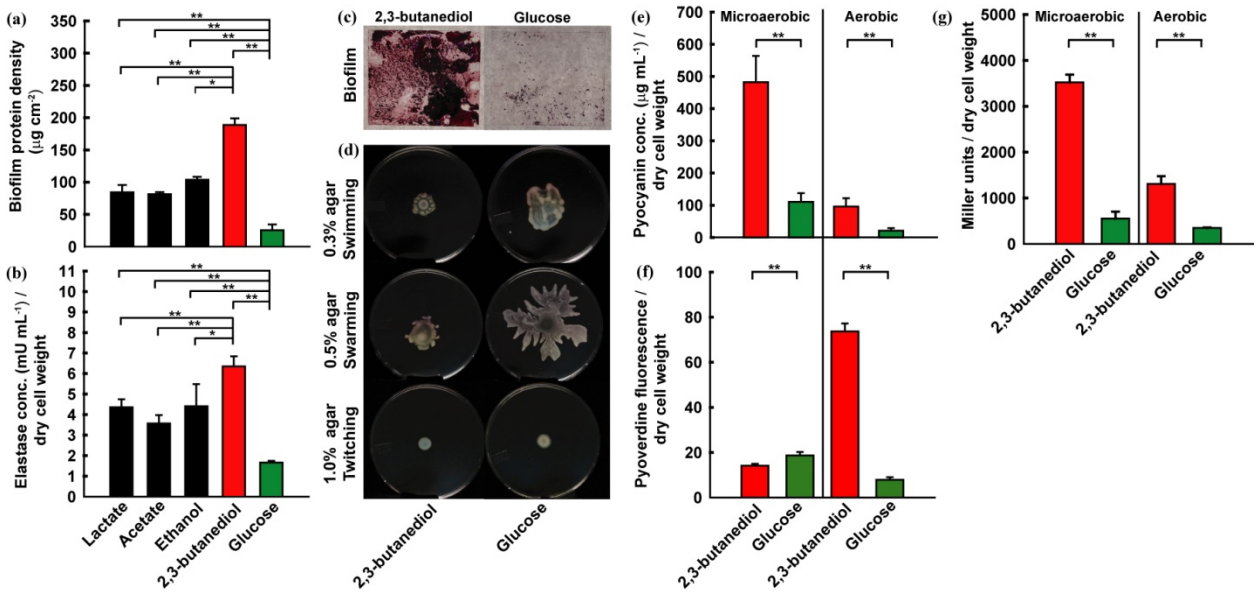

Figure 5.1. Biofilm formation, virulence factors, and quorum sensing with fermentation products and glucose: (a) biofilm protein density (as mass per unit area); (b) elastase concentrations (as milliunits per dry cell weight) with fermentation products and glucose; (c) biofilm images on glass cover slips; (d) motilities of *P. aeruginosa* with 2,3-butanediol and glucose; (e) pyocyanin concentration (as micrograms per milliliter); (f) pyoverdine fluorescence per dry cell weight; and (g) concentration of the quorum sensing initiating molecule - 3O-C12-HSL (expressed as β-galactosidase activity of *E. coli* indicator strain in Miller units) in supernatant of *P. aeruginosa* grown with 2,3-butanediol and glucose under microaerobic and aerobic conditions. Error bars indicate standard deviation among triplicates. A 2-way ANOVA was performed (* - p-value < 0.05; ** - p-val < 0.01).

To understand the biochemical mechanism behind this phenomenon of upregulation of virulence with 2,3-butanediol compared to glucose, we conducted comparative proteome analyses with pure cultures of *P. aeruginosa* grown aerobically with vigorous shaking, which prevented biofilm formation and resulted in growth of cells in the planktonic phase for both substrates. Cells were harvested for protein extraction in the late log phase and quantitative proteomics was performed on the six resulting samples (2 substrates x 3 replicates). We detected 268 statistically significantly changed proteins (2-way ANOVA, n = 3, p-value < 0.05) of which 109 were upregulated with 2,3-butanediol (ratio of protein signal in 2,3-butanediol to that in glucose; [B/G] > 2) and 102 were downregulated with 2,3-butanediol ([B/G] < 0.5). We classified these

detected proteins into functional categories and selected proteins are shown in Figure 5.2a (complete list in Appendix 2; Table 9.2). As expected, we found proteins involved in alcohol metabolism to be upregulated with 2,3-butanediol and proteins involved in hexose metabolism to be upregulated with glucose. Interestingly, Palmer *et al.* (2007) also reported that glucose metabolism was downregulated with *P. aeruginosa* in CF sputum. Concurrent with our observation that 2,3-butanediol increases biofilm formation by *P. aeruginosa*, the type IV pili core biogenesis protein PilE, and an alginate regulatory protein – PA14_69370 (alginate is an exopolysaccharide characteristic of *P. aeruginosa* biofilms (Nivens et al., 2001)) were upregulated 2.02 fold and 3.13 fold, respectively, with 2,3-butanediol, even though we prevented biofilm formation by vigorous shaking. In accordance with our experimental results (Figure 5.1e), two proteins in the phenazine synthesis pathway (PhzB and PhzF) were 3-fold higher with 2,3-butanediol than with glucose (Figure 5.2a,b). Proteins related to iron acquisition were downregulated with 2,3-butanediol, which is possibly due to the growth differences between 2,3-butanediol and glucose. Enhanced growth with glucose compared to 2,3-butanediol (Table 9.1 in Appendix 2) leads to iron limitation and over expression of the acquisition systems. Further, we detected increased levels of one protease (2.3 fold; PA14_21030) responsible for cleaving the QS inhibitor ClpA (Diggle et al., 2002) with 2,3-butanediol compared to glucose. Thus, the ClpA repression may be removed via proteolytic activity with *P. aeruginosa* grown with 2,3-butanediol leading to upregulation of QS. But also the QS inhibiting transcriptional regulator MvaT was upregulated with 2,3-butanediol (3.8 fold; Figure 5.2a,b). It is important to note that MvaT also strongly controls the production of the virulence factor - exotoxin A (Westfall et al., 2004). However, since the cells were harvested in the late log phase, it is likely that at this stage, the increased concentration of virulence factors with 2,3-butanediol had a negative feedback on

QS (signaling the cell to cease production of these factors to prevent cellular damage) via the expression of QS inhibiting pathways (*e.g.*, *mvaT*). Concurrent with our observation that QS was increased in *P. aeruginosa* grown with 2,3-butanediol (Figure 5.1g), we found a 2.2-fold increase with 2,3-butanediol in PhnB (Figure 5.2b), which is involved in the production of the third QS molecule - PQS (*Pseudomonas* quinolone signal). We also found several ABC-type transporters to be upregulated with 2,3-butanediol. The high concentration of virulence factors with 2,3-butanediol might also initiate increased stress response in *P. aeruginosa* fed with 2,3-butanediol, as indicated by the elevated levels of stress response proteins with 2,3-butanediol compared to glucose (Figure 5.2a). Although we were unable to determine the mechanism of QS upregulation with 2,3-butanediol, the proteome analysis validates our hypothesis of increased virulence of *P. aeruginosa* when grown on 2,3-butanediol compared to glucose.

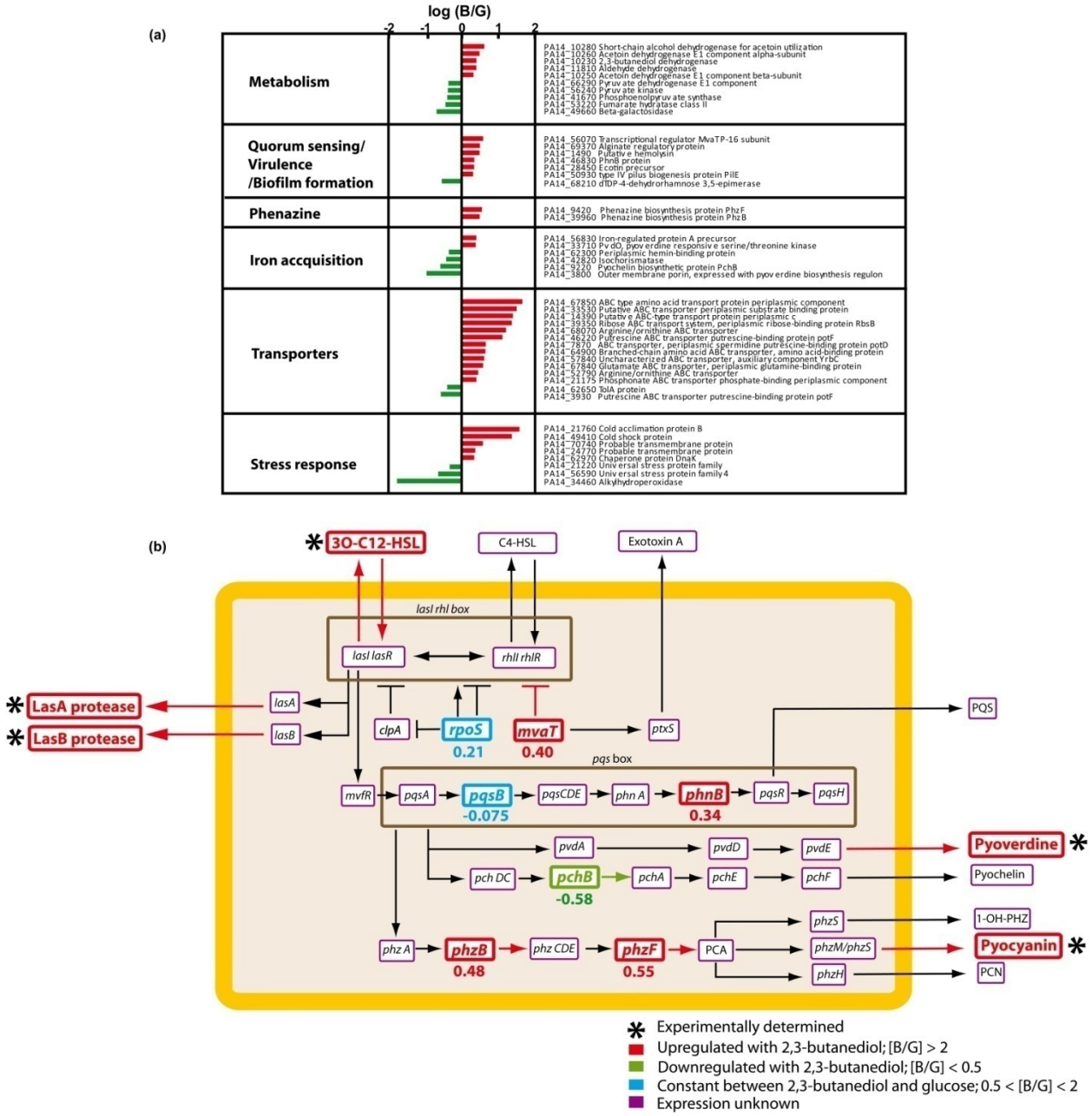

Figure 5.2. Shift in proteome with 2,3-butanediol: (a) logarithmic protein ratio between 2,3-butanediol and glucose; and (b) cellular genetic network depicting the relationship between quorum sensing and virulence factors for *P. aeruginosa* grown with 2,3-butanediol. The orange rectangle denotes the cell wall. Upregulated virulence factors (determined experimentally) and genes (detected through proteomics; [B/G] > 2) are shown in red. Downregulated genes (detected through proteomics; [B/G] < 0.5) are shown in green. Unchanged genes (detected through proteomics; 0.5 < [B/G] < 2) are shown in blue. Undetected genes are framed in purple. The numbers below the genes are the log ratio of the protein level in 2,3-butanediol to that in glucose.

To test if *P. aeruginosa* could become a dominant colonizer in microbiota by consuming fermentation products, we further investigated the antibiotic activity of the supernatants of a *P. aeruginosa* culture grown with 2,3-butanediol or glucose. First, we obtained growth curves with four microorganisms capable of 2,3-butanediol production – *E. aerogenes*, *K. pneumoniae*, *S. aureus*, and *S. marcescens* in: i) unsupplemented AB medium; ii) AB medium supplemented with the cell-free supernatant of *P. aeruginosa* grown with 2,3-butanediol; and iii) AB medium supplemented with the cell-free supernatant of *P. aeruginosa* grown with glucose. The supernatant of *P. aeruginosa* grown with 2,3-butanediol demonstrated the maximum inhibitory action towards growth of *S. aureus* and *S. marcescens* (Figure 5.3a). However, there was no statistically significant inhibition of *E. aerogenes* and *K. pneumoniae* and it is known that these two microbes can coexist with *P. aeruginosa* (Angell et al., 2006; Stewart et al., 1997; Venkataraman et al., 2011). *S. marcescens* produces all the four fermentation products – lactate, acetate, ethanol, and 2,3-butanediol from glucose, unlike the other microbes (*E. aerogenes*, *K. pneumoniae*, and *S. aureus*), where fermentation is principally focused towards a particular compound for example lactate by *S. aureues*. Therefore, we tracked the population of this microbe in a batch co-culture with *P. aeruginosa* over time (Figure 5.3b). To prevent substrate and pH based inhibition of *S. marcescens*, we added glucose and adjusted the pH daily. During days 1-6 of the bioreactor operation, *S. marcescens* dominated the co-culture, and glucose was fermented to lactate, acetate, ethanol, and 2,3-butanediol (Figure 5.3b,c). Subsequently, *P. aeruginosa* consumed these fermentation products, and became the more dominant organism in the reactor during days 8-14 of the experiment. After day 8, *S. marcescens* was inhibited (the colony forming units of *S. marcescens* decreased by 40.6%) by the virulence factors of *P. aeruginosa* (produced with the fermentation products) despite the presence of sufficient

concentrations of glucose (at least 30 mM). A control experiment with a *S. marcescens* pure culture (Figure 5.3b) indicated that *S. marcescens* growth in the *P. aeruginosa* co-culture experiment was inhibited even during the initial period. Therefore, fermentation products of other microbes aid in the emergence of *P. aeruginosa* as a dominant member of a microbiota. This agrees well with previous reports stating that the percentage of *P. aeruginosa* in CF lung microbiota increased from 20.8% to 76.9% between 0 and 36 years of age (FitzSimmons, 1993) and our finding that after 23 days of intubation, 95% of the sequences in an endotracheal tube belonged to *P. aeruginosa* while this microbe was below the detection limit initially (Perkins et al., 2010).

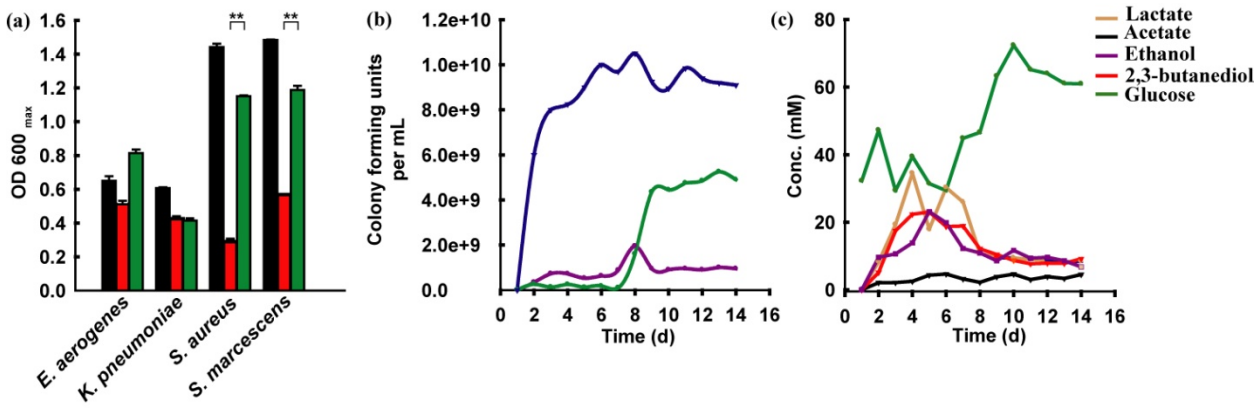

Figure 5.3. Antibiotic activity of *P. aeruginosa* grown with 2,3-butanediol and glucose: (a) maximum optical density at 600 nm attained by each microorganism in unsupplemented AB media (black), in AB media supplemented with cell-free supernatant of *P. aeruginosa* grown with 2,3-butanediol (red), and in AB media supplemented with cell-free supernatant of *P. aeruginosa* grown with glucose (green), the initial glucose concentration for all three media conditions was adjusted to 30 mM; (b) tracking the population of *S. marcescens* (dark pink) in a co-culture with *P. aeruginosa* (dark green) over time, and the population of a pure culture of *S. marcescens* (deep blue) under similar operating conditions; and (c) metabolite profile in the bioreactor operated with a co-culture of *S. marcescens* and *P. aeruginosa* (for (b) and (c): result of one trial is shown; the biological duplicate is shown in Figure 9.1 of Appendix 2). Error bars indicate standard deviation among triplicates. A 2-way ANOVA was performed (* - p-value < 0.05; ** - p-val < 0.01).

5.4 Conclusions and outlook

From a human health perspective, interbacterial metabolite transfer fuelling the pathogenesis of polymicrobial infections is an important clinical consideration. Our data suggests that in infections involving cohabitation of fermenters (*e.g.*, *S. aureus* or *S. marcescens*) and *P. aeruginosa*, and characterized by poor oxygen supply (*e.g.*, cystic fibrosis), fermenters could set the stage for colonisation by *P. aeruginosa*. While *P. aeruginosa* might not be detectable initially, the microcosm created by the fermenters will eventually promote colonization by *P. aeruginosa*. This is concurrent with previous reports that colonization of *P. aeruginosa* in CF occurs after fermenters, such as *S. aureus*, have infected the patient's airway (FitzSimmons, 1993; Palmer et al., 2007; Palmer et al., 2005). Therefore, the abundance of fermenters and fermentation products in a polymicrobial infection can be a warning sign for future invasion by *P. aeruginosa*. We envision that in initial stages of infection the destruction of this ecological relationship by either eliminating the fermenter or by targeting a key biochemical pathway responsible for this increased virulence in *P. aeruginosa* with fermentation products will lead to easier management of *P. aeruginosa* in polymicrobial infections. It is important to note that fermentation products, such as lactate, are also generated from the host via neutrophil metabolism (Bensel et al., 2010). This additional source of fermentation products must also be accounted for when devising treatment strategies based on this phenomenon of upregulated virulence in *P. aeruginosa* with fermentation products. The compounding of virulence exhibited by *P. aeruginosa* with fermentation products can occur in multiple ecological niches given the immense diversity of fermenters and fermentation products, and other ecological interactions with respect to community-aided success of *P. aeruginosa* must be unraveled. The over-expression of virulence factors by *P. aeruginosa* with fermentation products may be a survival

mechanism for this microbe. Our work suggests that *P. aeruginosa* has evolved to utilize the fermentation products of other microorganisms not just as a carbon source but also as a ”cue” (Ratcliff and Denison, 2011) to establish a strong presence in an ecosystem. Understanding these “cues” may be necessary to treat patients with cystic fibrosis.

5.5 Acknowledgements

This research was supported through NSF CAREER grant # 0939883 to Largus T. Angenent.

6 CHAPTER 6. Mediator-based and direct contact-based exocellular electron transfer are equally important within synergistic bacterial communities in bioelectrochemical systems.

This chapter is not published.

Abstract

Bioelectrochemical systems (BESs) link microbial metabolism with an electrode for versatile applications. In BESs, microorganisms respire with the anode via two mechanisms: i) direct electron transfer (DET); and ii) mediated electron transfer (MET). Since pure cultures of DET-capable microbes, such as *Geobacter sulfurreducens*, typically produce considerably more current than pure cultures of MET-capable microbes (e.g., *Pseudomonas aeruginosa*), DET is considered superior to MET with respect to microbial electrode-based respiration. However, this notion neglects the role of interspecies interactions in determining the importance of MET. Here, we show that in a potentiostatically-controlled 3-electrode BES with defined mixed cultures consisting of *Enterobacter aerogenes*, *P. aeruginosa*, and *G. sulfurreducens*, synergistic MET by *E. aerogenes* and *P. aeruginosa* was responsible for 56.93 ± 10.07 % of the total current production, while DET by *G. sulfurreducens* accounted for the rest. In contrast, we found that MET by *P. aeruginosa* alone (in the same defined mixed culture BES) contributed only 5.65 ± 1.67 % of the total current. A mathematical model was constructed to describe the synergism between *E. aerogenes* and *P. aeruginosa*. It showed that *P. aeruginosa* is kinetically limited with respect to reduction of the oxidized phenazine. However, in the synergistic community, *E. aerogenes* overcomes this constraint through faster kinetics of phenazine reduction; resulting in improved efficiency of MET compared to a pure culture of *P. aeruginosa*. In addition,

experiments revealed that the DET-based electrochemical activity of *G. sulfurreducens* was inhibited ~5.2-fold by the extracellular virulence factors of *P. aeruginosa*. These results underscore the significance of interspecies interactions by enhancing MET and inhibiting DET in a defined mixed culture BES. We anticipate that our findings will be relevant towards efforts for manipulating microbiota to maximize BES performance.

6.1 Introduction

Bioelectrochemical systems (BESs) are utilized as microbial fuel cells for generating electrical power from organic substrates (Fornero et al., 2008) or as microbial electrolysis cells for generating valuable products, such as hydrogen, hydrogen peroxide, methane, and caustic soda (Liang et al., 2011). Additional uses of this technology include biological denitrification, desalination (Clauwaert et al., 2007; Kim and Logan, 2011), CO_2 reduction (Cao et al., 2009b), biosensing, and biocomputing (Li et al., 2011). Regardless of the application, most often electrode-based respiration by the microbial community at the anode is included in its function. Thus, exocellular electron transfer (EET) at the anode is important to understand for future BES optimization and scaleup. In general, EET mechanisms fall into two categories: i) direct electron transfer (DET); and ii) mediated electron transfer (MET). For DET, the microbe (e.g., *G. sulfurreducens*) establishes physical contact with the electrode and the electrons from the metabolic pathway are transferred to outer membrane cytochromes (OMCs) or conductive pili on the cell surface, which subsequently relay the electrons to the electrode. For MET, the microbe either produces electrochemically-active compounds (e.g., phenazines by *P. aeruginosa*) or uses exogenously supplied compounds (e.g., methylene blue), which shuttle electrons between the microbe and the electrode. Since both DET and MET determine the overall performance of

mixed culture BESs with varying efficiencies, several studies have compared the two mechanisms (Table 6.1).

Table 6-1. Comparison of DET and MET (Bond and Lovley, 2005; Lovley, 2006; Malvankar et al., 2011; Nevin and Lovley, 2002; Schröder, 2007)

Mechanism	Schematic (IM – Inner membrane; OM – Outer membrane; M - Mediator)	Advantages	Disadvantages
Direct electron transfer	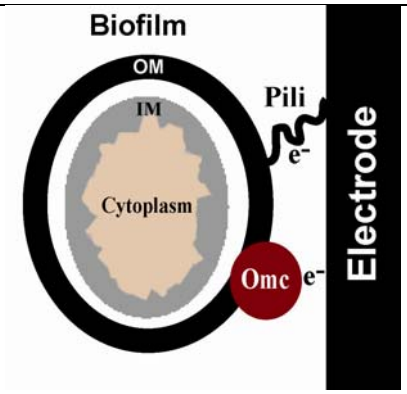	Conductive biofilm minimizes diffusion related losses and prevents loss of electroactive components in continuous flow systems. Direct link of respiratory chain to electrode improves bioenergetics.	Necessity of physical contact for EET implies that electrode area can be limiting. These microbes typically exhibit high specificity in substrate utilization.
Mediated electron transfer	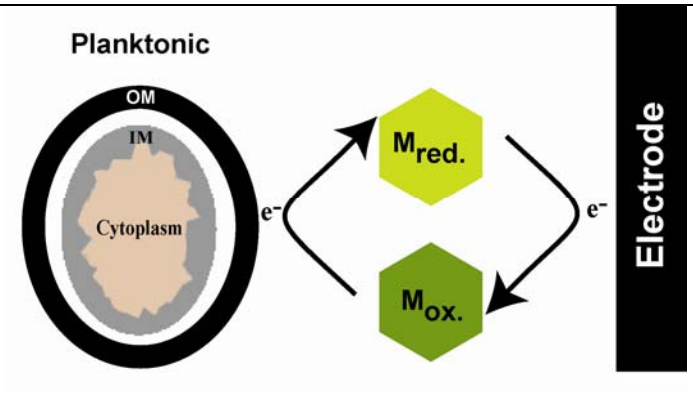	Long range electron transfer is possible via mediators. These microbes typically exhibit high diversity in substrate utilization.	Planktonic phase implies diffusion limitation and loss of mediators in continuous flow systems. Mediator production can be energetically expensive for the microbe.

Apart from bioenergetics and spatial location, Torres *et al.* (2009) elegantly demonstrated that the anode potential could also influence the mechanism of electrode respiration by influencing microbiota selection. According to the authors, DET by *G. sulfurreducens* dominated at anode potentials of -0.19 V, -0.05 V and +0.02 V vs. SHE, whereas at +0.37 V vs. SHE the microbiota was more diverse, and MET by Pseudomonads became more important. However, this study had two caveats: i) the 16S rRNA gene sequencing survey of the microbial community was performed on the biofilm attached to the electrodes, which assumes that only the biofilm is

responsible for current generation and would cause a bias towards DET capable microbes; and ii) the carbon source was acetate – a simple carboxylic acid, which is the preferred substrate for *G. sulfurreducens* and an unrealistic representation of the complex carbon sources encountered in full-scale BES applications.

Thus far, most experimental studies aimed at determining the relative importance of DET and MET have been conducted with pure microbial cultures (Schröder and Harnisch, 2010). However, in the complex ecology of BESs, inter-microbial interactions also influence the efficiency of these electrode respiration mechanisms. Although DET-capable microbes live in syntrophy with fermenters, the electroactive complex in DET is a cellular component - structurally specific and indigenous to the concerned microbes (e.g., OmcZ or OmcB in *G. sulfurreducens*), and therefore fermenters cannot use this complex to respire with the electrode. However, ecological interactions have tremendous implications in MET processes. There have been several studies highlighting the ability of a wide range of fermenters to use exogenous mediators to generate current (Pham et al., 2008; Rabaey et al., 2004b; Rabaey et al., 2007), implying that mediators are electrochemically-compatible with multiple microbes. We have shown previously how the interaction between a fermenter (*E. aerogenes*) and a MET-capable respirer (*P. aeruginosa*) can lead to a 14-fold increase in current production compared to the current production by pure cultures of these organisms (Venkataraman et al., 2011). In that study, *P. aeruginosa* produced the mediators (phenazines) and *E. aerogenes* was able to switch its metabolism from fermentation to electrode-based respiration with these phenazines. The mutualism between these two organisms served to: i) benefit *P. aeruginosa* by stimulating higher phenazine production with the fermentation product of *E. aerogenes* - 2,3-butanediol compared

to glucose; and ii) improve the bioenergetics of *E. aerogenes* by switching its metabolism from fermentation to respiration.

Since we observed that bacterial partnerships greatly improved the efficiency of MET (Venkataraman et al., 2011) compared to pure-culture MET, we postulated that mutualism driven MET by *E. aerogenes* and *P. aeruginosa* would be important for current generation in a defined mixed culture BES alongside DET by *G. sulfurreducens*. Here, our experimental results substantiate this hypothesis and highlight the importance of ecological networks in determining the relative contribution of both mechanisms towards the net current in BESs. Further, on the basis of a mathematical model, we elucidated that the rate-limiting step with respect to current generation by a pure culture of *P. aeruginosa* was the reduction of the oxidized mediator. In the mutualism between *E. aerogenes* and *P. aeruginosa*, *E. aerogenes* overcame this limitation, resulting in improved MET.

6.2 Materials and methods

6.2.1 Bacterial strains and growth media

We obtained *P. aeruginosa* PA14 wildtype from the PA14 Transposon Insertion Mutant Library (Liberati et al., 2006), *G. sulfurreducens* from ATCC (strain 51573), and *E. aerogenes* from NRRL (strain B-115). Experiments were performed in: i) minimal AB medium supplemented with a trace metal and vitamin mix (Clark and Maaløe, 1967); ii) FW medium (Richter et al., 2007); or iii) a 1:1 mixture of AB and FW medium supplemented with the appropriate carbon source as shown in Table 6.2. The mixture of AB and FW medium is referred to as FWAB medium throughout the text. All experiments were conducted at 30^{o}C.

6.2.2 Electrochemical experiments

The electrochemical cells consisted of a glass reactor with a three-electrode setup: working electrode (anode) – 162 cm^2 carbon cloth (PANEX ® 30 - PW06, Zoltek Corp, St Louis, MO) mounted to a graphite rod (Poco graphite, Decatur, TX) with carbon cement (CCC Carbon Adhesive, EMS, Hatfield, PA); counter electrode – graphite rod (Poco graphite); and reference electrode – Ag/AgCl sat. KCl (all potentials given vs. this reference). The vessel was autoclaved and filled with sterile medium (420 mL). For anaerobic experiments, the reactors were continuously sparged with 80%:20% N_2/CO_2 through a 0.22-µm filter. For microaerobic experiments, oxygen was allowed to diffuse through a 0.22-µm filter into the headspace (dissolved oxygen < 0.3 mg/L). The electrochemical measurements with a potentiostat (BioLogic VSP; Bio-Logic USA, Knoxville, TN) were structured in a repetitive loop, starting with cyclic voltammetry from -0.5 V to +0.5 V @ 2 mV/s and followed by chronoamperometry for 24 h at 0.3 V vs. Ag/AgCl sat. KCl for up to 21 days. The inoculum for all experiments consisted of a *P. aeruginosa* and/or *E. aerogenes* grown in Luria-Bertani (LB) broth and/or *G. sulfurreducens* grown in serum bottles with FW medium (fumarate as the electron acceptor).

6.2.3 Continuous flow experiments

The three-electrode BES described above was also operated in continuous-flow mode with recycle for up to 15 days as the operating period. The reactors were initially inoculated with all three microbes in the batch mode to allow growth. Once the current started to increase and reached a stable value after 3 days, media was pumped at a flow rate of 0.25 mL/min (hydraulic retention time equals 28 h) and the recycle was maintained at 0.125 mL/min.

6.2.4 Metabolite and phenazine analysis

The metabolites and phenazines were analyzed as previously described in Venkataraman et al. (2011).

6.2.5 Mathematical model formulation

The objective of the model is to simulate the synergistic mediator-based electron transfer between *E. aerogenes* and *P. aeruginosa*. DET by *G. sulfurreducens* is not considered in this model. *E. aerogenes* and *P. aeruginosa* are present in both the planktonic and biofilm phases, however, we do not simulate the biofilm composition. The cylindrical BES (Venkataraman et al., 2011) was modeled as an axisymmetric 2-D transient diffusion problem in the Chemical Engineering Module of COMSOL Multiphysics™ 3.5a (Figure 6.1). Biofilm thickness is assumed to be 50 μm. We used coupled ordinary differential equations to describe the process and the electric current was calculated using the lumped parameter approach of Zhang and Halme (1995) via Faraday's law. The equations for all the species are listed in Table 6.2. The units and values for all the input parameters are listed in Table 6.3. Due to the lack of published information regarding some parameters and the complexity of experiments required for their determination, their values were adjusted to obtain a better fit between the simulated and experimental results; these have been accordingly listed as fitting parameters in Table 6.3. In addition, some parameters were assumed based on the generic ranges listed in Heijnen et al. (1999). The computational mesh consisted of 21057 triangular elements and 347776 degrees of freedom. The linear system solver using the generalized minimal residual (GMRES) method was used for the computation (time step of 1 day; maximum number of iterations per time step were 1000). Each simulation used 1 CPU hour on a Intel Pentium core (3.6 GHz) with a 2.00 GB RAM workstation. The default boundary conditions of axial symmetry at r = 0, flux continuity at

r = 50 μm, and insulation at r = 20 cm were retained in the simulation. We make the following assumptions:

1. Since *E. aerogenes* grows much faster than *P. aeruginosa*, there is no competition for glucose (the starting substrate). Glucose is consumed by *E. aerogenes* to produce 2, 3-butanediol and ethanol, which act as carbon sources and electron donors for *P. aeruginosa* (Venkataraman et al., 2011).
2. Phenazines are produced by *P. aeruginosa* and the oxidized form of the phenazine is reduced only by *E. aerogenes*. This is based on our previous experimental results (Venkataraman et al., 2011).
3. Monod kinetics is used to describe microbial growth and metabolite consumption.
4. Reduction of the oxidized mediator follows Michaelis-Menten kinetics.
5. Temperature and pH are constant.
6. There is no overpotential for the oxidation of the reduced phenazine.
7. The electrochemical oxidation of the reduced mediator is a first order reaction.
8. The production of the reduced phenazine by *P. aeruginosa* is a second order reaction involving *P. aeruginosa* and the substrate (i.e., 2, 3-butanediol or ethanol). Any biochemical enzymatic limitations in the production are not considered.
9. Current production involves only the reduced form of the mediator.

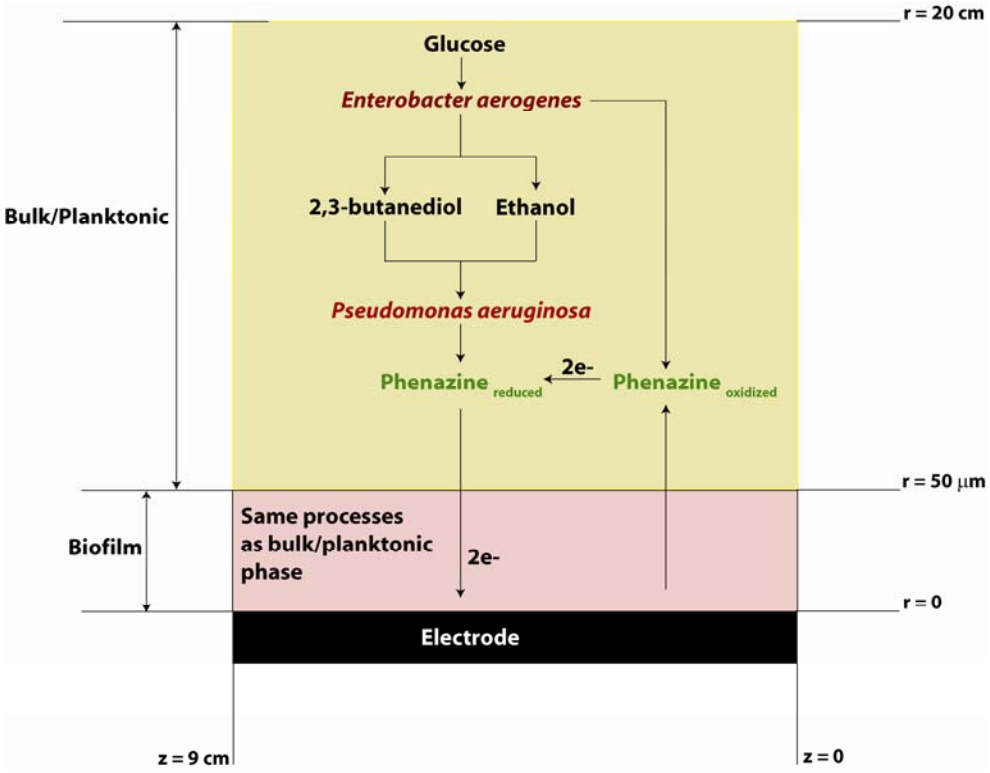

Figure 6.1. Conceptual mathematical model and schematic of computational domain. Note that the depicted processes are happening both in the bulk and biofilm phases.

Table 6-2. Equations used in COMSOL

Species	**Equation**
All	$\frac{\partial c_i}{\partial t} = D_i \frac{1}{r}\frac{\partial}{\partial r}\left(r\frac{\partial c_i}{\partial r}\right) + D\frac{\partial^2 c_i}{\partial z^2} + r_i$,where i= Glucose, *E. aerogenes*, 2,3-butanediol, Ethanol, *P. aeruginosa*, Reduced form of mediator, and Oxidized form of mediator. Symbols D and c represent the diffusivity and concentrations respectively.
Glucose	$r_{Glucose} = -k_1 \times [E.aerogenes] \times \frac{[Glucose]}{[k_2] + [Glucose]}$
E. aerogenes	$r_{E.aerogenes} = k_3 \times [Glucose] - k_4 \times [E.aerogenes]$
2,3-butanediol	$r_{2,3-butanediol} = k_5 \times [E.aerogenes] \times \frac{[Glucose]}{k_6 + [Glucose]} - k_7 \times [P.aeruginosa] \times \frac{[2,3-butanediol]}{k_8 + [2,3-butanediol]}$

Ethanol	$r_{ethanol} = k_9 \times [E.aerogenes] \times \frac{[Glucose]}{k_{10} + [Glucose]} - k_{11} \times [P.aeruginosa] \times \frac{[Ethanol]}{k_{12} + [Ethanol]}$
P. aeruginosa	$r_{P.aeruginosa} = k_{13} \times [2,3 - butanediol] + k_{14} \times [Ethanol] - k_{15} \times [P.aeruginosa]$
Reduced form of mediator	$r_{Mediator_{reduced}} = k_{16} \times [P.aeruginosa] \times [2,3 - butanediol] - k_{17} \times \frac{[P.aeruginosa]}{k_{18} + [2,3 - butanediol]} + k_{19} \times [P.aeruginosa] \times [Ethanol] - k_{20} \times \frac{[P.aeruginosa]}{k + [Ethanol]} - k_{22} \times [Mediator_{reduced}] + k_{23} \times [E.aerogenes] \times \frac{[Mediator_{oxidized}]}{[k_{24}] + [Mediator_{oxidized}]}$
Oxidized form of mediator	$r_{Mediator_{oxidized}} = k_{22} \times [Mediator_{reduced}] - k_{23} \times [E.aerogenes] \times \frac{[Mediator_{oxidized}]}{[k_{24}] + [Mediator_{oxidized}]}$
Current production	$I = n \times F \times k_{25} \times [Mediator_{reduced}] \times V_{reactor}$

Table 6-3. Input parameters to the model.

Constant	Value	Units	Source/Explanation
k_1	60	1/d	(Batstone et al., 2002)
k_2	300	mM	(Batstone et al., 2002)
k_3	0.28	1/d	(Heijnen, 1999)
k_4	0.008	1/d	(Heijnen, 1999)
k_5	0.52	1/d	Fitting parameter based upon experimental data
k_6	1	mM	(Batstone et al., 2002)
k_7	0.14	1/d	Fitting parameter based upon experimental data
k_8	1	mM	(Batstone et al., 2002)
k_9	0.8	1/d	Fitting parameter based upon experimental data
k_{10}	1	mM	(Batstone et al., 2002)
k_{11}	0.2064	1/d	Fitting parameter based upon experimental data
k_{12}	1	mM	(Batstone et al., 2002)
k_{13}	0.1	1/d	(Heijnen, 1999)

k_{14}	0.1	1/d	(Heijnen, 1999)
k_{15}	0.1	1/d	(Heijnen, 1999)
k_{16}	0.053	1/mM d	Fitting parameter based upon experimental data
k_{17}	0.1	mM/d	(Batstone et al., 2002; Heijnen, 1999)
k_{18}	1	mM	(Batstone et al., 2002; Heijnen, 1999)
k_{19}	0.053	1/ mM d	Fitting parameter based upon experimental data
k_{20}	0.1	mM/d	(Batstone et al., 2002; Heijnen, 1999)
k_{21}	1	mM	(Batstone et al., 2002; Heijnen, 1999)
k_{22}	0.06	1/d	(Heijnen, 1999)
k_{23}	0.001	1/d	Fitting parameter based upon experimental data
k_{24}	1	mM	(Batstone et al., 2002; Heijnen, 1999)
k_{25}	0.944	1/d	Fitting parameter based upon experimental data
n	2	none	2 electrons are involved in redox activity of phenazines (Wang and Newman, 2008)
F	96485	C/mol	Faraday's constant
$V_{reactor}$	0.42	Litre	Amount of liquid in reactor
$D_{Glucose}$	$6.1x10^{-5}$	m^2/d	Diffusivity of glucose in water (Batstone et al., 2002)
$D_{E.\ aerogenes}$	$7.8x10^{-5}$	m^2/d	Diffusivity of *E. aerogenes* in water – assumed to be similar to *Klebsiella pneumoniae* (Kim, 1996)
$D_{P.aeruginosa}$	$1.8x10^{-4}$	m^2/d	Diffusivity of *P. aeruginosa* in water (Kim, 1996)
$D_{2,3\text{-butanediol}}$	$6.5x10^{-6}$	m^2/d	Diffusivity of 2,3-butanediol in water – assumed similar to ethylene glycol (Kuhn et al., 2009)
$D_{Ethanol}$	$1.4x10^{-5}$	m^2/d	Diffusivity of ethanol in water (Kuhn et al., 2009)
$D_{Mediator}$	$2x10^{-6}$	m^2/d	Diffusivity of mediator in water (Picioreanu et al. 2007)
Initial conc. of glucose	30	mM	Based upon experiments; Initial concentration of all other species = 0

6.3 Results and discussion

6.3.1 Defined mixed culture composition and growth media

Our defined mixed culture consisted of a fermenter (*E. aerogenes*), an exclusively MET-capable microbe (*P. aeruginosa*), and an exclusively DET-capable microbe (*G. sulfurreducens*). With these three organisms, we can approximate the three dominant metabolic pathways existent in mixed culture BESs. In addition, since: i) *E. aerogenes* and *P. aeruginosa* are ecologically related via metabolite based mutualism (Venkataraman et al., 2011); and ii) *P. aeruginosa* produces extracellular virulence factors capable of inhibiting other microbes (Mashburn et al., 2005), our experimental design also captures some of the probable ecological interactions involved in the biotransformation of a composite substrate (glucose) into electric current.

For defined mixed culture experiments it is pertinent to create optimal growth conditions for all the included microbes to prevent experimental bias. *P. aeruginosa* requires the ions Mg^{2+}, SO_4^{2-}, PO_4^{2-}, and Fe^{3+} for optimal growth and production of the phenazine – pyocyanin (Swan and Felton, 1957). Thus, the optimum minimal medium for the growth of this microbe is the phosphate buffered AB medium (Clark and Maaløe, 1967). However, the minimal medium typically used for *G. sulfurreducens* is FW medium (Bond and Lovley, 2003), which contains low concentrations of the above mentioned ions and uses carbonate buffer. The growth of *E. aerogenes* is similar in both AB and FW media. Therefore, to eliminate the medium dependent growth bias of *P. aeruginosa* and *G. sulfurreducens*, we measured current production by different combinations of the three microbes in three different media: i) AB medium; ii) FW medium; and iii) FWAB medium (Table 6.4). Since we have previously established that microaerobic conditions greatly improve the current production of *E. aerogenes* and *P. aeruginosa* (Venkataraman et al., 2011; Venkataraman et al., 2010), all experiments involving these two microbes were conducted under microaerobic conditions. However, *G. sulfurreducens*

does not grow as a pure culture under microaerobic conditions (Table 6.4), and therefore all experiments involving a pure culture of this microbe were performed under an active over pressure of 80%:20% N_2/CO_2. A discussion of mixed-culture experiments involving *G. sulfurreducens* is provided in section 6.3.2. The current production by a pure culture of *G. sulfurreducens* was not significantly affected between FW and FWAB medium, whereas it was adversely affected in AB medium (82.303 ± 9.249 μA/cm^2 in AB medium vs. 114 ± 41.01 μA/cm^2 in FW medium and 137.85 ± 15.53 μA/cm^2 in FWAB medium). Most importantly, the current production by a pure culture of *P. aeruginosa* improved nearly 5-fold between FW medium and AB or FWAB medium (0.707 ± 0.082 μA/cm^2 in FW medium vs. 3.25 ± 0.14 μA/cm^2 in AB medium and 3.79 ± 0.43 μA/cm^2 in FWAB medium). Further, we also observed the synergism between *E. aerogenes* and *P. aeruginosa* in all the three media, though this effect was 6-fold higher in AB and FWAB media compared to FW medium (Table 6.4). In summary, we determined that FWAB medium was optimum for all three microbes. Further, our findings underscore the importance of an optimal growth medium for experiments involving defined mixed cultures, especially because both MET by the concerted action of *E. aerogenes* and *P. aeruginosa* and DET by *G. sulfurreducens*, are significantly influenced by varying media composition.

Table 6-4. Experimental maximum current densities under three different media conditions with different combinations of the three microbes in batch mode.

	O_2 condition	Initial Substrate	Maximum current density ($\mu A/cm^2$)		
			FW medium	**AB medium**	**FWAB medium**
Pure cultures					
E. aerogenes	Microaerobic	Glucose 30 mM	0.423 ± 0.015	2.53 ± 1.3	0.59 ± 0.15
P. aeruginosa	Microaerobic	Glucose 30 mM	0.707 ± 0.082	3.25 ± 0.14	3.79 ± 0.43
G. sulfurreducens	Microaerobic	Acetate 14 mM	0 ± 0	0 ± 0	0 ± 0
G. sulfurreducens	Anaerobic	Acetate 2 mM	114 ± 41.01	82.303 ± 9.249	137.8593 ± 15.53
G. sulfurreducens	Anaerobic	Acetate 7 mM	372.74 ± 67.7	208.42 ± 15.47	368.3 ± 27.83
G. sulfurreducens	Anaerobic	Acetate 14 mM	462.59 ± 80	372.03 ± 25.64	494.48 ± 45.87
***E. aerogenes* with**					
P. aeruginosa	Microaerobic	Glucose 30 mM	6.39 ± 1.34	43.6 ± 4.02	39.09 ± 4.67
G. sulfurreducens	Microaerobic	Glucose 30 mM	100.3 ± 28	45.77 ± 8.59	212.45 ± 21.569
***P. aeruginosa* with**					
G. sulfurreducens	Microaerobic	2,3-butanediol 15 mM + Ethanol 15 mM	12.34 ± 2.45	23.45 ± 3.7	27.713 ± 4.366
***E. aerogenes* and *P. aeruginosa* with**					
G. sulfurreducens	Microaerobic	Glucose 30 mM	124.65 ± 37.95	47.63 ± 4.028	65.13 ± 13.07
***G. sulfurreducens* in**					
supernatant of *E. aerogenes* and *P. aeruginosa*	Anaerobic	Acetate ~ 4.44 mM	30.42 ± 13.16	27.87 ± 9.257	32 ± 2.7

6.3.2 Microaerobic conditions for *G. sulfurreducens*

All defined mixed culture experiments involving *G. sulfurreducens* were conducted under microaerobic conditions. Typically, *G. sulfurreducens* is an obligate anaerobe requiring an overpressure of N_2/CO_2 for optimal growth as a pure culture (we did not observe any growth of *G. sulfurreducens* as a pure culture under microaerobic conditions; Table 6.4). However, Lin et al. (2004) have demonstrated that *G. sulfurreducens* can tolerate up to 10% oxygen in the headspace for a period of 24 h. This indicates that microaerobic conditions (rather than strict anaerobic conditions) are sufficient for optimum growth of this microbe. In defined mixed culture experiments with *E. aerogenes* and *G. sulfurreducens* (microaerobic conditions with 30 mM glucose), *E. aerogenes* produced ~2 mM acetate as a fermentation product, which was subsequently the carbon source for *G. sulfurreducens*. Under these microaerobic mixed culture conditions, *G. sulfurreducens* was able to produce similar currents than when it was grown as a pure culture under anaerobic conditions with 2 mM acetate (Table 6.4). This is possible because, in our microaerobic BES, *E. aerogenes* efficiently scavenges the oxygen, thus, creating optimal growth conditions for *G. sulfurreducens* without the necessity of an active overpressure of N_2/CO_2.

Recently, the long-standing notion of the necessity of strict anaerobic conditions for BES performance has been questioned by some studies (Biffinger et al., 2008; Rosenbaum et al., 2009). Previously, we have shown that microaerobic conditions increased current production by a pure culture of *P. aeruginosa* and also enhanced the synergism between *E. aerogenes* and *P. aeruginosa* (Venkataraman et al., 2011; Venkataraman et al., 2010). These findings combined with our experimental result that scavenging of O_2 by *E. aerogenes* was sufficient for the growth of *G. sulfurreducens* highlight the benefits of microaerobic conditions on BES performance.

Subsequently, all experiments involving the defined mixed culture of *E. aerogenes*, *P. aeruginosa*, and *G. sulfurreducens* were conducted under microaerobic conditions.

6.3.3 Contribution of DET and synergistic MET towards current generation

In the BES operated with all three microbes under microaerobic conditions, the total current generation (I) was due to: i) DET by *G. sulfurreducens*; and ii) MET by the concerted action of *E. aerogenes* and *P. aeruginosa*. *G. sulfurreducens* does not use the phenazines of *P. aeruginosa* to shuttle electrons to the electrode ($I_{G.sulfurreducens + P.\ aeruginosa} << I_{G.\ sulfurreducens}$; Table 6.4) and *E. aerogenes* cannot use the conductive biofilm of *G. sulfurreducens* to respire with the electrode ($I_{G.sulfurreducens + E.\ aerogenes} \approx I_{G.\ sulfurreducens}$; Table 6.4). Further, we have shown previously that the synergism between *E. aerogenes* and *P. aeruginosa* is only with respect to MET and does not involve any DET (Venkataraman et al., 2011). Therefore, DET and MET in our BES with the three microbes are mutually exclusive. This implies that if we subtract the current produced by the binary culture of *E. aerogenes* and *P. aeruginosa* (MET) from the total current with all the three microbes, the difference would yield the current from DET (Equation 1).

$$I_{\mathrm{Total}} = [I_{E.aerogenes} + I_{P.aeruginosa}]_{\mathrm{MET}} + [I_{G.sulfurreducens}]_{\mathrm{DET}} \quad (1)$$

To draw valid conclusions regarding the relative importance of DET and MET in our BES, we performed this analysis for all the three media described in section 6.3.1 using the experimental data from Table 6.4 (Figures 6.2a-c). MET contributes 59.6 ± 10.67 % of the current production in FWAB medium (optimum for all the microbes) whereas this contribution is only 5.02 ± 0.976 % in FW medium (optimum for *G. sulfurreducens* and suboptimal for *P. aeruginosa*). Further, in AB medium (optimum for *P. aeruginosa* and suboptimal for *G. sulfurreducens*), the current production via DET by *G. sulfurreducens* is only 8.45 ± 4.45 %. This is also confirmed in the cyclic voltammograms (CVs) obtained in the different media (Figures 6.2d-f). In FW medium,

the CV shows only the catalytic wave responsible for extracellular electron transfer via outer membrane cytochromes, indicating that in this medium DET was dominant. In AB medium, the CV shows the characteristic peaks associated with pyocyanin, indicating that MET was dominant. In FWAB medium, the peaks for cytochromes and pyocyanin are observed, indicating the presence of both mechanisms. Next, if we assume that *G. sulfurreducens* is predominantly confined to the biofilm on the electrode and *E. aerogenes* and *P. aeruginosa* to the planktonic phase in our BES, then this means that in a continuous-flow BES with all the three microbes in FW medium (where current is mainly due to DET by *G. sulfurreducens*), the current should not decrease drastically with flow since the biofilm will not be lost from the system, while in FWAB medium (where current is almost equally distributed between DET by *G. sulfurreducens* and MET by *E. aerogenes* and *P. aeruginosa*), the current should decrease with flow because the phenazines would be flushed out. Indeed, we observed that in a continuous-flow BES with all three microbes in FW medium, when the flow was switched on (HRT = 18.6 h), the current decreased by 38.13 % (from 24.39 mA to 15.04 mA; Figure 10.1 in Appendix 3). On the other hand, in a continuous-flow BES with all three microbes in FWAB medium, upon switching the flow on (HRT = 18.6 h), the current decreased by 81.62 % (from 8 mA to 1.47 mA; Figure 10.1 in Appendix 3), indicating that current production in this medium was dependent upon both DET and MET.

In summary, these results confirm our hypothesis that in a growth medium optimum for all the microbes (FWAB medium) irrespective of whether the BES is in batch or continuous-flow mode, synergism between *E. aerogenes* and *P. aeruginosa* leads to MET being a significant contributor to current generation alongside DET by *G.sulfurreducens*. In contrast, *P. aeruginosa* by itself contributes only 5.65 ± 1.67 % of the current in FWAB medium via MET, reinforcing the

importance of ecological interactions when comparing the relative significance of DET and MET in a BES.

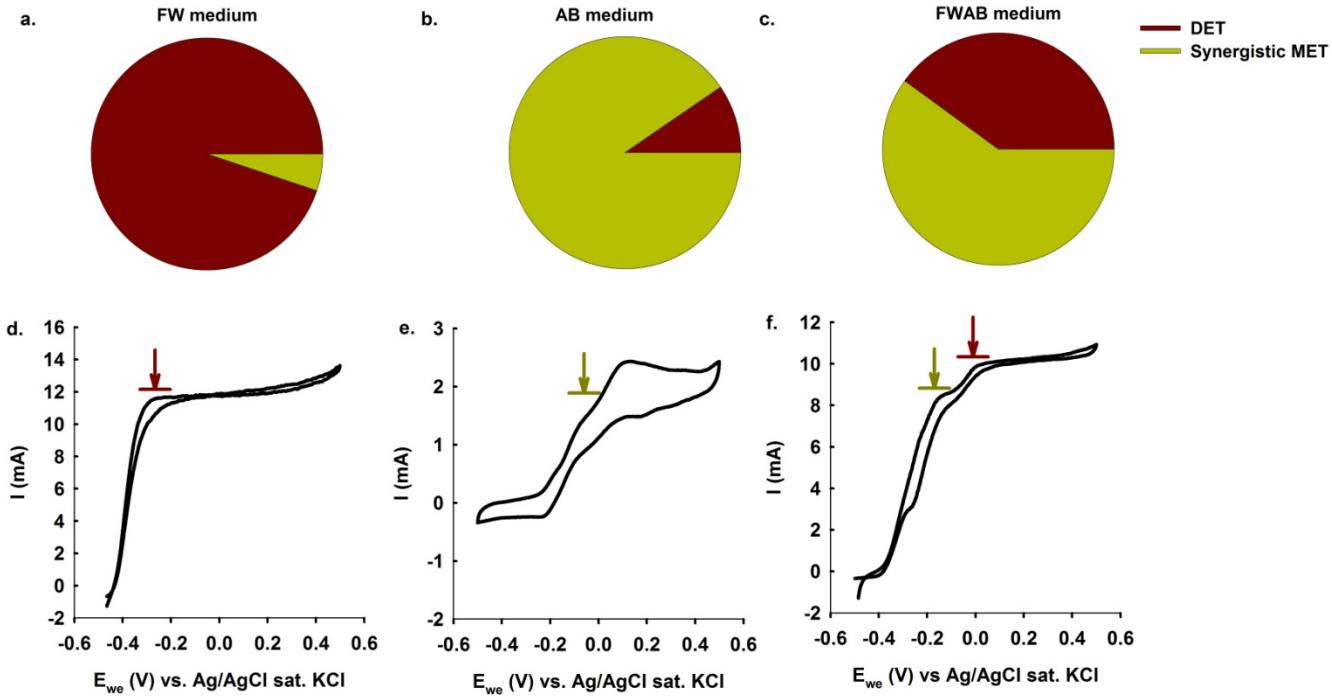

Figure 6.2. Direct electron transfer (DET) vs. synergistic mediated electron transfer (MET) in a defined mixed-culture BES: a-c: contribution of direct electron transfer and mediated electron transfer towards total current generation in a potentiostatically controlled 3-electrode BES with a mixed culture of *E. aerogenes*, *P. aeruginosa*, and *G. sulfurreducens* in 3 different media; and d-f: cyclic voltammograms in the three different media, the arrows indicate the mid peak potential of the electrochemically active component (dark brown – cytochrome; green – pyocyanin).

6.3.4 Mathematical modeling of the synergism between *E. aerogenes* and *P. aeruginosa*

6.3.4.1 Model validation

Thus far, we have demonstrated that the synergism between *E. aerogenes* and *P. aeruginosa* greatly increases the importance of MET towards current production in a defined mixed culture BES even when a DET capable microbe – *G. sulfurreducens* is present in the system. Subsequently, we constructed a mathematical model to describe this synergism. The results of the simulation were correlated with the experimental data involving the defined mixed culture of

E. aerogenes and *P. aeruginosa* in AB medium (Figure 6.3). The simulated and experimental currents agree well (p- value = 0.0425; 95 % confidence limit; Figure 6.3e), thereby, validating our supposition that in the synergism, *P. aeruginosa* only produces the phenazines, while *E. aerogenes* performs the majority of the electrode-based respiration with these compounds.

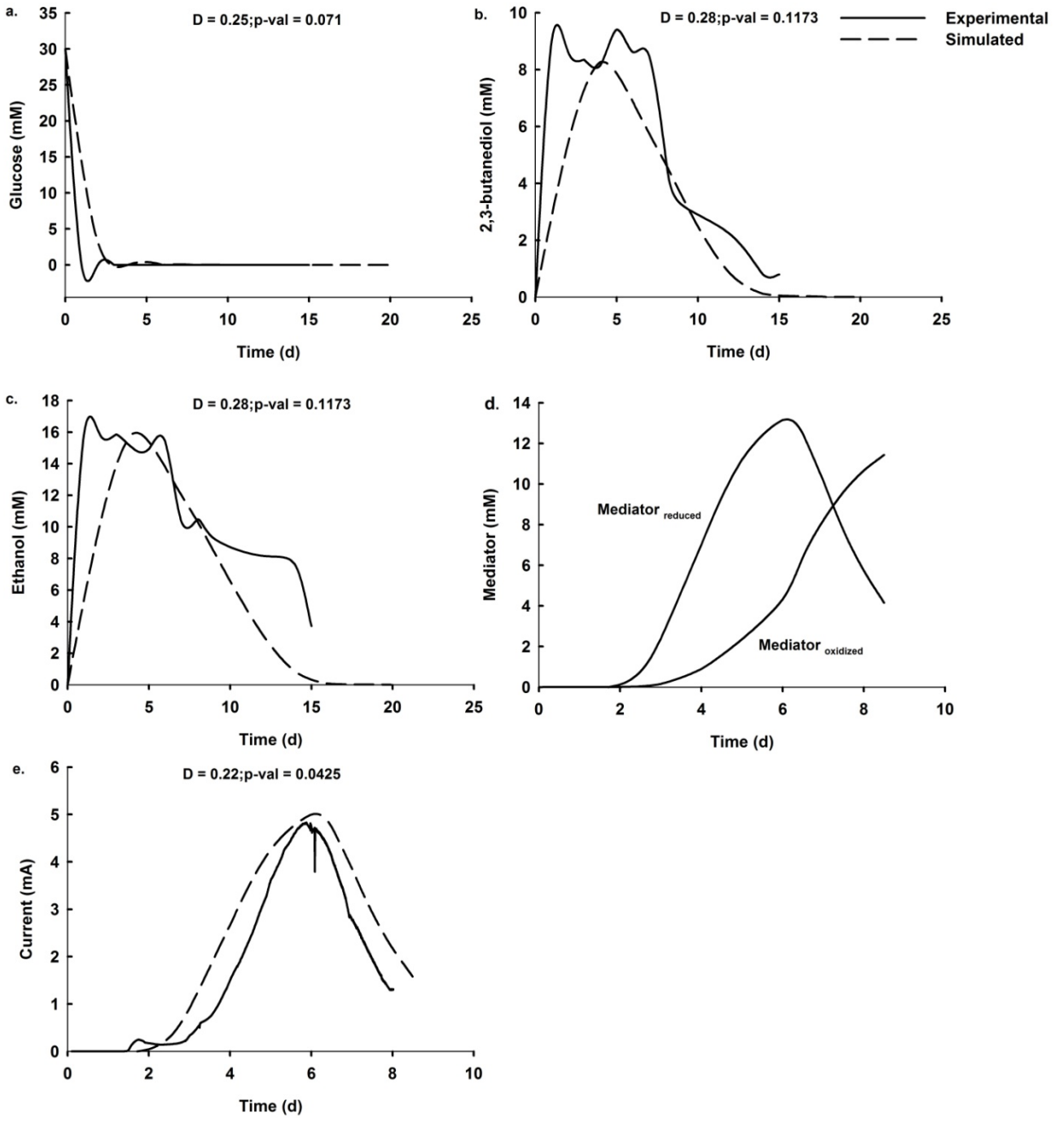

Figure 6.3. Model validation. Comparison of simulated and experimental results. The D-statistic and p-value are obtained from performing a Kolmogorov-Smirnov test on the experimental and simulated results. D ranges from 0 (a perfect fit) to 1 (an imperfect fit). A p-value < 0.1 indicates a 90% confidence limit. Note that the mediator concentration is only the simulated value.

6.3.4.2 Kinetic limitation of *P. aeruginosa* in reducing the oxidized phenazines

Our previous experimental results (Venkataraman et al., 2011), showed that in the synergism between *E. aerogenes* and *P. aeruginosa*, the latter microbe was just supporting phenazine production, while the former microbe was responsible for almost 90 % of the electrode based respiration via these phenazines. MET is as a cyclic two-step process in which: i) the electron-rich reduced mediator (i.e., phenazines produced by *P. aeruginosa* in our case) is electrochemically oxidized at the electrode to the electron-deficient oxidized form; and ii) the electron-deficient oxidized mediator is microbially reduced (mostly by *E. aerogenes* in our case) to replenish the pool of reduced mediator available for electrochemical oxidation. Therefore, maximum current generation via MET should have no limitations in either the electrochemical oxidation or the microbial reduction. In our BES, the working electrode is maintained at a constant potential of +0.3 V vs. Ag/AgCl - well above the required potential for phenazine oxidation ($E_{pyocyanin}$= -0.055 V vs. Ag/AgCl), which implies that electrochemical oxidation is not limiting MET. Since we observed low currents with a pure culture of *P. aeruginosa* despite its ability to produce phenazines, we hypothesized that this microbe must be kinetically limited in its ability to reduce the oxidized phenazines. Furthermore, we postulated that in the synergism, *E. aerogenes* overcame this inadequacy by possessing faster kinetics of phenazine reduction, and thereby improving the overall efficiency of MET.

Since our model described the experimental results with reasonable accuracy, we consider the input parameters from Table 6.3 as baseline values representing the actual experimental conditions. Consequently, we changed the equations and the parameters from their baseline format and values (Table 6.2 and Table 6.3) to answer our hypothesis regarding the kinetic limitation of *P. aeruginosa* in reducing the oxidized phenazine. For this, we consider the

scenario that in our BES, only *P. aeruginosa* is responsible for reducing the oxidized phenazine and *E. aerogenes* solely ferments glucose to 2,3-butanediol and ethanol and has no role in reducing the phenazines. First, *E. aerogenes* was removed from the equations for the reduced and oxidized mediator and only *P. aeruginosa* was retained (equations 2 and 3).

$$r_{Mediator_{reduced}} = k_{16} \times [P.aeruginosa] \times [2,3-butanediol] - k_{17} \times \frac{[P.aeruginosa]}{k_{18}+[2,3-butanediol]} + k_{19} \times [P.aeruginosa] \times [Ethanol] - k_{20} \times \frac{[P.aeruginosa]}{k\ +[Ethanol]} - k_{22} \times [Mediator_{reduced}] + k_{23} \times [P.aeruginosa] \times \frac{[Mediator_{oxidized}]}{[k_{24}]+[Mediator_{oxidized}]} \quad (2)$$

$$r_{Mediator_{oxidized}} = k_{22} \times [Mediator_{reduced}] - k_{23} \times [P.aeruginosa] \times \frac{[Mediator_{oxidized}]}{[k_{24}]+[Mediator_{oxidized}]} \quad (3)$$

Second, since in our experiments, a pure culture of *P. aeruginosa* grown on 2,3-butanediol and ethanol produces nearly 14-fold lower current than the co-culture of *E. aerogenes* and *P. aeruginosa* (Venkataraman et al., 2011) the rate constant of reduction of the oxidized phenazine (k_{23}) in equations 2 and 3 was changed to 7.1428e-5 1/d (14-fold lower than that of *E. aerogenes* in Table 6.3). Indeed, the simulated current production when only *P. aeruginosa* was responsible for reducing the phenazines decreased 4-fold compared to the current production by a co-culture of *E. aerogenes* and *P. aeruginosa* (Figure 6.4). Although this confirms our hypothesis that *P. aeruginosa* is kinetically limited in its ability to reduce the oxidized phenazines, based on our experimental data, the current production should have decreased 14-fold when only *P. aeruginosa* was responsible for reducing the oxidized phenazines. We attribute this discrepancy to the assumption in the model that the entire reduced mediator is oxidized electrochemically. To further confirm that *P. aeruginosa* was limited in its ability to reduce the phenazines, the rate constant of reduction of the oxidized mediator (k_{23}) was restored to its original value from Table

6.3 (0.001 1/d) while still retaining only *P. aeruginosa* in the equation for the reduced and oxidized mediator in the model. As expected, the simulated current production by a pure culture of *P. aeruginosa* came very close to the values obtained with the mixed culture of *E. aerogenes* and *P. aeruginosa* (Figure 6.4). Therefore, in summary, *P. aeruginosa* as a pure culture is, indeed, kinetically limited in its ability to reduce the phenazines and in the synergism *E. aerogenes* is exclusively responsible for reducing the oxidized phenazines. This also describes how in the BES microbiota, the action of one organism compensating for the inadequacies of another organism can lead to improved process functionality.

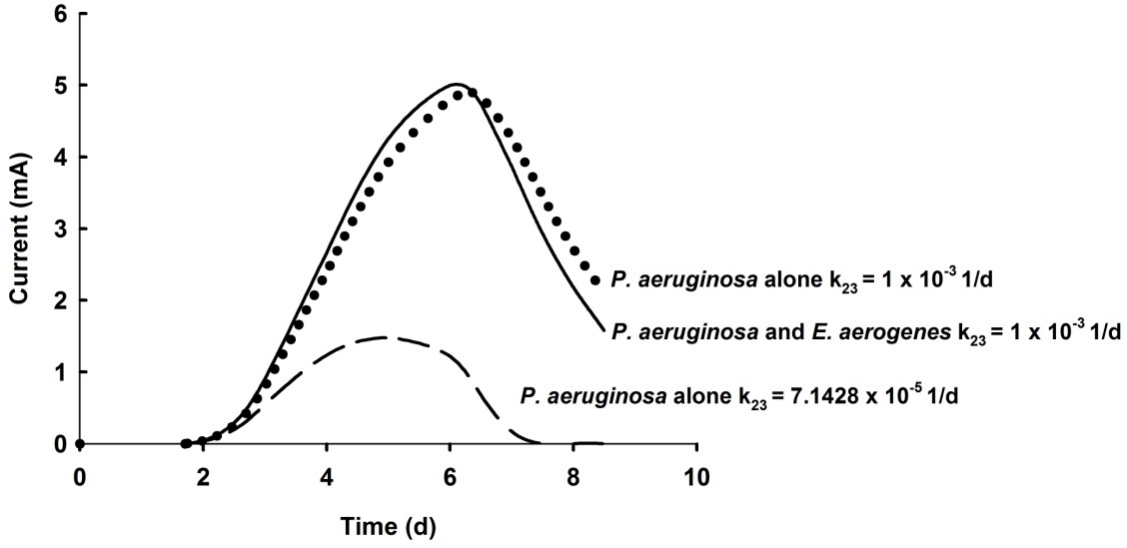

Figure 6.4. Effect of the rate constant of reduction of oxidized phenazine by *P. aeruginosa* on current production. Simulated currents with mixed culture of *E. aerogenes* and *P. aeruginosa* and with pure cultures of *P. aeruginosa* with two different rate constants.

6.3.4.3 Effect of rate constant of reduction of oxidized phenazine by *E. aerogenes* on current production

Our equations for the reduced and oxidized mediator involve enzymatic Michaelis-Menten type kinetics. This implies that similar to enzyme kinetics, after a threshold concentration of

phenazines (dictated by the half-saturation constant k_{24}) has been reached, the reduction rate of the oxidized phenazine by either *E. aerogenes* or *P. aeruginosa* would attain a maximum possible value. In this situation, the maximum current would not be significantly dependent upon the rate constant of reduction of the oxidized phenazine (k_{23}). In section 6.3.4.2 we have demonstrated that *P. aeruginosa* is kinetically limited with respect to phenazine reduction and that in the synergism *E. aerogenes* is responsible for the bulk of phenazine reduction. Consequently, our next hypothesis was that *E. aerogenes* possessed the maximum possible kinetics with respect to reduction of the oxidized phenazine. Therefore, we explored the dependence of maximum current on the rate of reduction of the oxidized phenazine by *E. aerogenes*, by simulating the current production with different rates of reduction of the oxidized phenazine (k_{23}) by *E. aerogenes* (Figure 6.5). As expected, the current improved non-linearly by insignificant amounts with increasing rate constants of reduction of the oxidized phenazine (Figure 6.5a), whereas the current remained unaffected by a decrease in the rate constant of reduction of the oxidized phenazine (Figure 6.5b). The fact that the current increases only by 1.2-fold when the rate constant is increased by 200-fold suggests that the synergistic current production in our BES is close to the maximum possible value. However, as the rate constant is increased by 100-fold or 200-fold (this is hypothetical and cannot be achieved in the real world), the current starts approaching a stable phase instead of a sharp decay as encountered in our experiments (Figure 6.5a). This is because, in this situation, the oxidized mediator is being rapidly reduced by *E. aerogenes*, thereby, constantly replenishing the pool of reduced phenazine available for electrochemical oxidation. In essence, this hypothetical situation captures the equilibrium between electrochemical oxidation and biological phenazine reduction that would result in an indefinitely constant current.

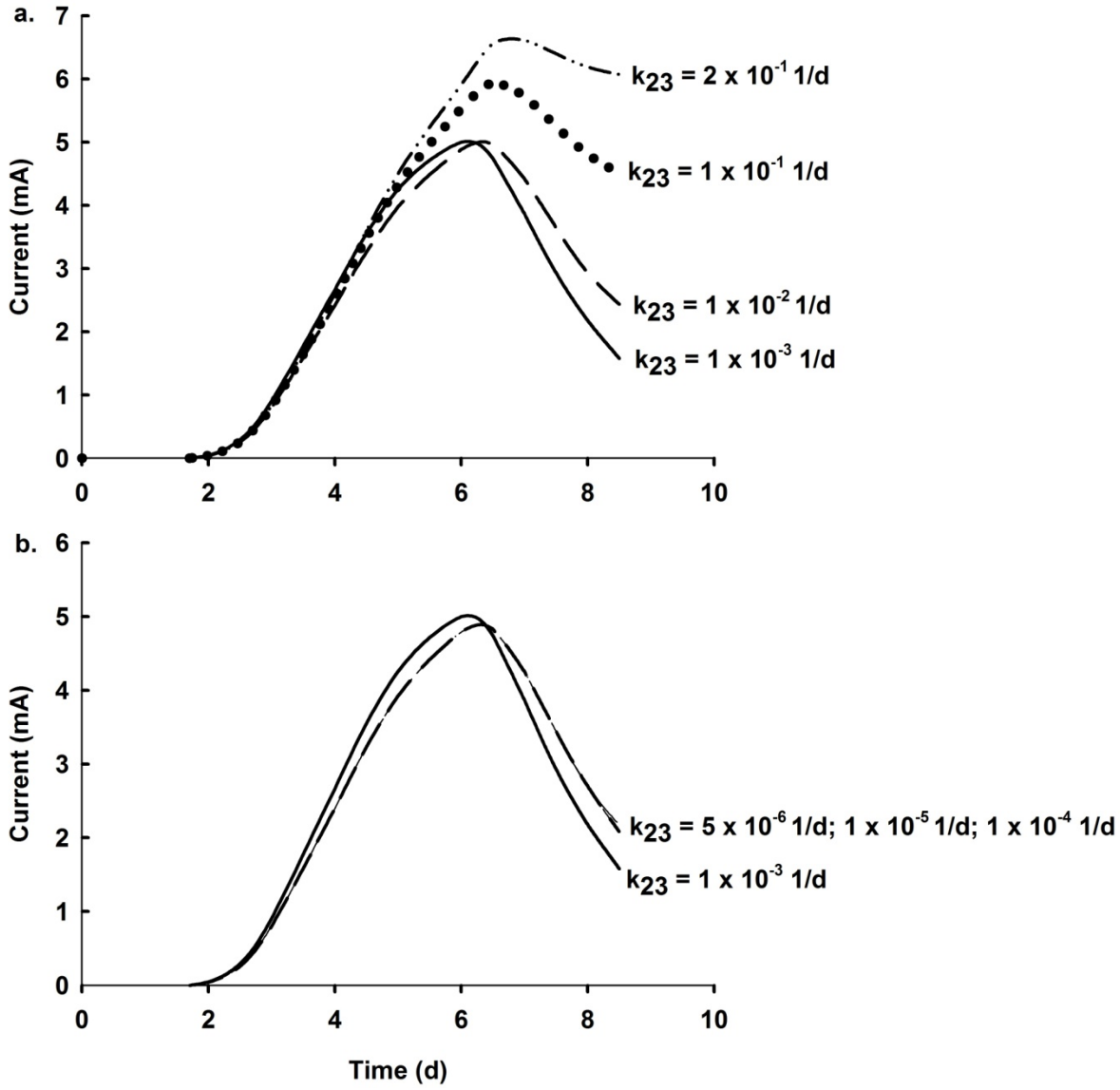

Figure 6.5. Effect of the rate constant of reduction of oxidized phenazine by *E. aerogenes* on current production: a: increasing rate constant; and b: decreasing rate constant. Simulated currents with mixed culture of *E. aerogenes* and *P. aeruginosa* with different rate constants of reduction of the oxidized phenazine by *E. aerogenes* as indicated in the figure. The curve obtained with a value of 0.001 1/d corresponds to the real-life situation. Note that in (b) three of the curves overlap with each other.

6.3.4.4 Effect of growth of *E. aerogenes* on current production

After determining the effect of the rate constant of reduction of the oxidized phenazine by *E. aerogenes* on the current production, we estimated whether the cell density of *E. aerogenes* had a significant effect on the current production since this microbe is exclusively responsible for

biological reduction of the oxidized phenazine. To test this, we varied the growth constant (k_3) of *E. aerogenes* in the mathematical model. Interestingly, we found that increasing the growth 10-fold had little effect on the current production whereas decreasing the growth 10-fold reduced the current by 77% (Figure 6.6). Additionally, the curve exhibits a significantly longer lag phase with respect to current production when the growth of *E. aerogenes* is decreased 10-fold. This indicates that despite the faster kinetics of phenazine reduction possessed by *E. aerogenes*, a threshold concentration of *E. aerogenes* needs to be established in the BES for efficient phenazine reduction, resulting in improved MET. Previously, we have shown that *E. aerogenes* exhibits higher growth in the presence of the phenazines (Venkataraman et al., 2011). Although, we have not included this directly in our model formulation, the results of this *in-silico* experiment indirectly support this experimental observation since the growth is correlated to current production.

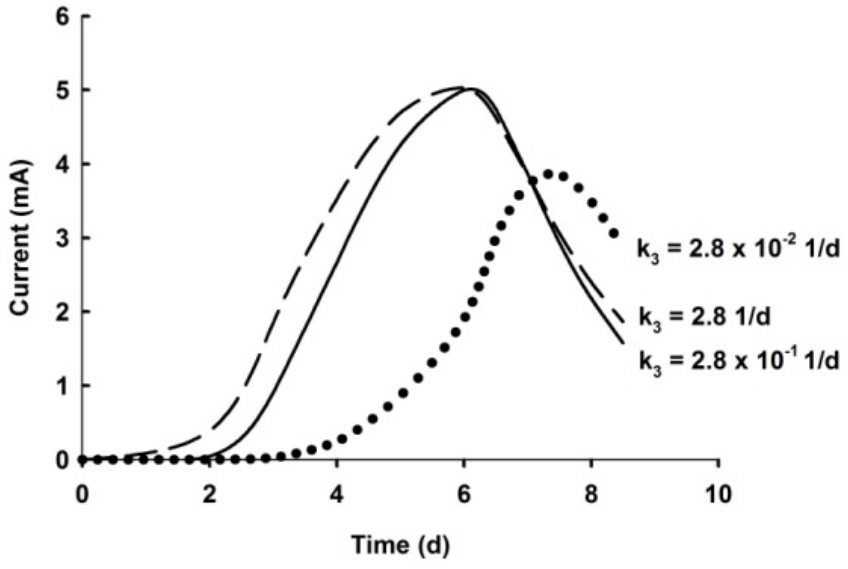

Figure 6.6. Effect of growth of *E. aerogenes* on current production. Simulated currents with mixed culture of *E. aerogenes* and *P. aeruginosa* with different growth constants (k_3) of *E. aerogenes* as indicated in the figure. Note that the curve obtained with a value of 0.28 1/d corresponds to the real-life situation.

In summary, we effectively described the synergism between *E. aerogenes* and *P. aeruginosa* with a simple mathematical model (Figure 6.3) and used it to gain further insight into this process. With the help of *in-silico* experiments, we have shown that *P. aeruginosa* as a pure culture is limited with respect to its kinetics of reduction of the oxidized phenazine (Figure 6.4), restricting the current production by a pure culture of this microbe as observed in our experiments. This limitation is overcome by *E. aerogenes* by possessing faster kinetics of phenazine reduction, which results in the experimentally observed synergism with respect to current production. Further, since we did not observe any significant variability in the simulated current production with changes in the rate constant of reduction of the oxidized phenazine by *E. aerogenes* (Figure 6.5), we suggest that *E. aerogenes* already possesses the maximum possible kinetics with respect to biological phenazine reduction. However, this needs to be experimentally tested by comparing the current production of a co-culture of *P. aeruginosa* with other fermenters (e.g., *Brevibacillus* sp., and *Enterococcous faecium*) to the currents with a co-culture of *P. aeruginosa* and *E. aerogenes*. Lastly, we show *in silico* that the synergistic current production is also dependent upon the cell density of *E. aerogenes* (Figure 6.6), indicating that synergism between *E. aerogenes* and *P. aeruginosa* is reliant on both the growth of *E. aerogenes* and its superior ability to reduce the phenazines compared to *P. aeruginosa*.

6.3.5 Inhibition of *G. sulfurreducens* by *P.aeruginosa*

Thus far, we have demonstrated *in vitro* and *in silico* that MET via bacterial synergism is an important aspect of current production in a BES and that *E. aerogenes* is responsible for ~90 % of this MET-based current. However, the other microbe in the synergism - *P. aeruginosa* - is known to produce several extracellular virulence factors, such as elastase, chitinase, exotoxin A, hydrogen cyanide, superoxide radicals, which can inhibit some bacteria (Mashburn et al., 2005).

Although, *E. aerogenes* is not inhibited by these compounds (Angell et al., 2006; Venkataraman et al., 2011), we observed that DET by *G. sulfurreducens* was significantly inhibited in a co-culture with *P. aeruginosa*. *P. aeruginosa* generates ~4.4 mM acetate as a byproduct from the consumption of 15 mM 2,3-butanediol and 15 mM ethanol. Consequently, we expect that in a BES with a defined mixed culture of *P. aeruginosa* and *G. sulfurreducens* (with 2,3-butanediol and ethanol as the starting substrate), DET by *G. sulfurreducens* should yield an electric current of at least 23.48 mA (corresponding to pure culture experiments with *G. sulfurreducens* with ~4.4. mM acetate). However, with a mixed culture of *P. aeruginosa* and *G. sulfurreducens*, irrespective of the growth medium, we obtained significantly lower currents (~4.4 mA) than the expected value (~23.48 mA). Therefore, we conducted experiments to determine the cause of this inhibition. We took the cell-free supernatant of a culture of *E. aerogenes* and *P. aeruginosa* in a BES, removed oxygen by bubbling 80%:20% N_2/CO_2 overnight and adding cysteine sulfide, followed by inoculation with *G. sulfurreducens*. Since all traces of oxygen are removed in this case, it eliminates the possibility of O_2 based inhibition of *G. sulfurreducens*. Therefore, the reduction in the electrochemical activity of *G. sulfurreducens* can be exclusively attributed to the virulence factors of *P. aeruginosa*. Indeed, we observed that the electrochemical activity of a pure culture of *G. sulfurreducens* was inhibited at least 5.2-fold (Figure 6.7a) in the cell-free supernatant compared to anoxic fresh medium (control). This was further confirmed by growing a pure culture of *G. sulfurreducens* in FW medium (optimum for *G. sulfurreducens*) with 4 mM acetate and when the current had reached a stable value, we gradually exchanged the medium with an anaerobic cell-free supernatant of *P. aeruginosa* grown in FW medium (containing ~4 mM acetate) (Figure 6.7b). Following the exchange, the current decreased by ~80% of the original value and did not recover, thereby, implying an irreversible inhibition of the

electrochemical activity of *G. sulfurreducens* by the virulence factors of *P. aeruginosa*. Although we determined that pyocyanin was not causing any oxidative stress on *G. sulfurreducens* (data not shown), further work must be performed to determine the inhibitory compound(s) responsible for this phenomenon.

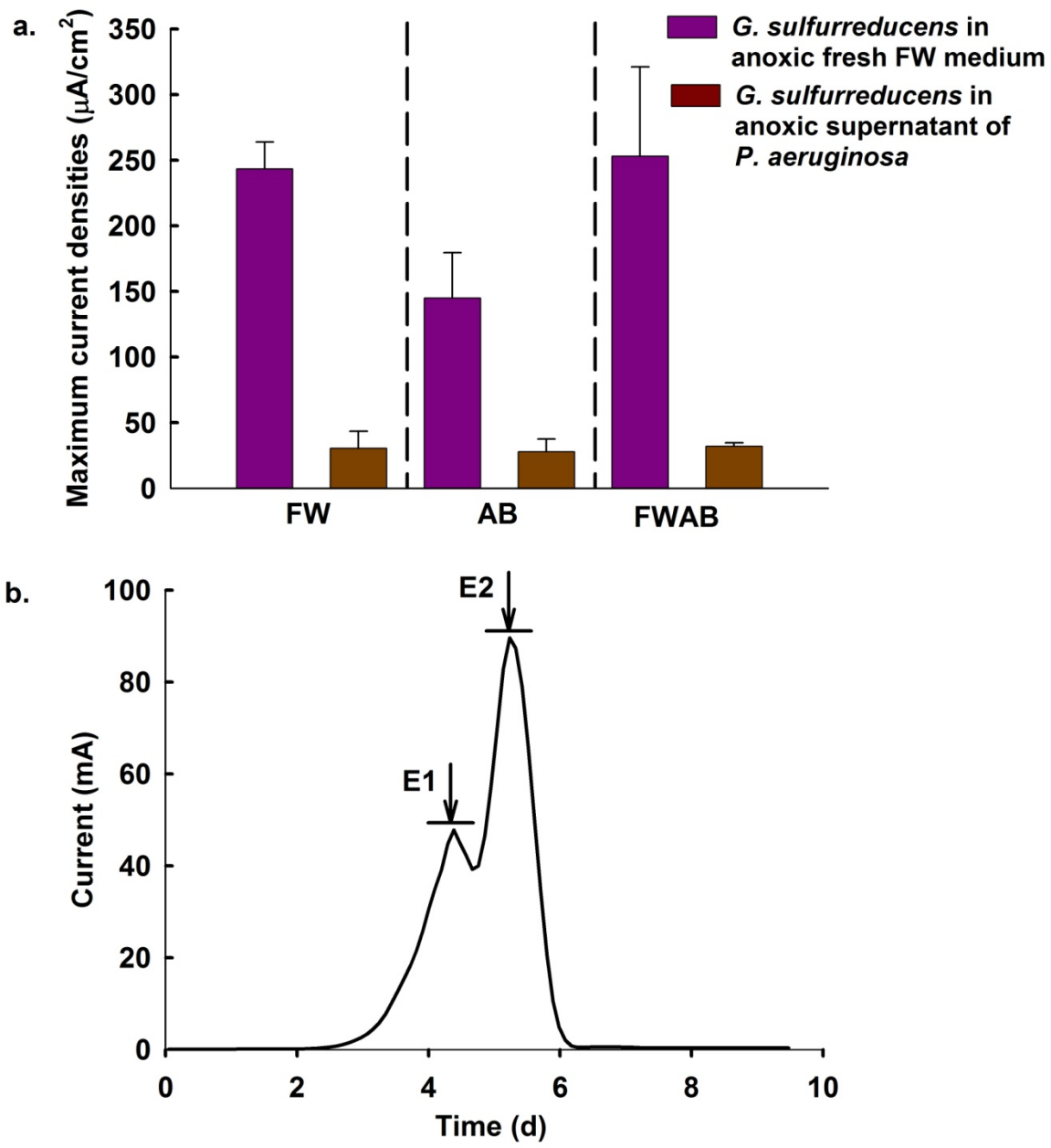

Figure 6.7. Inhibition of *G. sulfurreducens* by *P. aeruginosa*: a: maximum current densities (μA/cm^2) obtained with a pure culture of *G. sulfurreducens* grown anaerobically in FW medium (purple) and in supernatant of *E. aerogenes* and *P. aeruginosa* (brown), both conditions had similar concentrations of acetate; and b: current (mA) vs. time (days) for a pure culture of *G. sulfurreducens*, at time point E1 the medium was exchanged with fresh FW medium containing 4.4 mM acetate, and at point E2 the medium was exchanged with a supernatant of *P. aeruginosa* containing 4.4 mM acetate. Time point E1 serves as a control to show that oxygen was not introduced at inhibitory concentrations during the medium exchange and therefore, the inhibition of *G. sulfurreducens* was due to the extracellular virulence factors of *P. aeruginosa*.

6.3.6 Implications for BES research

Studies discussing the relative merits of DET and MET have been principally concerned with pure microbial cultures. However, the experimental designs, thus far, have not accounted for the impact of microbial interactions on process functionality in BES. This study, in conjunction with previous experimental work (Venkataraman et al., 2011) shows that: i) *E. aerogenes* and *P. aeruginosa* exhibit synergism with respect to current production; ii) this synergism (wherein *E. aerogenes* compensates for the inadequacies of *P. aeruginosa*) leads to MET being equal to DET in BESs; and iii) DET by *G. sulfurreducens* is inhibited by *P. aeruginosa*. Multiple studies (Bond and Lovley, 2005; Lovley, 2006; Schröder, 2007) have suggested that in continuous-flow BESs, which are a more realistic representation of pilot scale applications of these devices, the mediators would be removed from the system with flow and this would reduce the efficacy of MET compared to biofilm-based DET. However, in our continuous flow experiments we still showed that MET is equally important to DET. Based on these findings, we suggest that co-operative (i.e., *E. aerogenes* and *P. aeruginosa* in our case) and conflictive (i.e., *P. aeruginosa* and *G. sulfurreducens* in our case) interspecies relationships will greatly dictate the efficiency of the two well established mechanisms of extracellular electron transfer with profound implications on the overall BES performance.

6.4 Conclusions

Here, we showed that synergistic MET by *E. aerogenes* and *P. aeruginosa* can be equally important to DET by *G. sulfurreducens* in both batch and continuous-flow BESs. With a mathematical model, we demonstrate that *P. aeruginosa* as a pure culture is limited with respect to its kinetics of reduction of the oxidized phenazine, restricting the current production by this microbe alone. This limitation is overcome by *E. aerogenes*, which results in the observed

synergism with respect to current production. In addition, *G. sulfurreducens* was inhibited by the virulence factors of *P. aeruginosa*, which also reduces the efficacy of DET in a BES. In summary, inter-bacterial synergism compensates for the constraints of pure culture MET, resulting in MET becoming an important electron transfer mechanism to the electrode.

6.5 Acknowledgement

This research was supported through NSF CAREER grant # 0939883 to L.T.A..

7 CHAPTER 7. Summary and recommendations for future work.

This chapter is not published.

7.1 Summary

P. aeruginosa is a model organism for studying quorum sensing and biofilm formation. The remarkably high resilience exhibited by this organism in infections (e.g., burn wounds, cystic fibrosis etc.) has stimulated widespread research focused on the mechanism(s) of its pathogenicity and development of novel treatment techniques. Apart from human infections, this organism is ubiquitous in several natural and artificial environments. One such surrounding is a bioelectrochemical system (BES) wherein *P. aeruginosa* respires with the electrode as the terminal electron acceptor via endogenously produced electrochemically active compounds called phenazines. However, production of phenazines by *P. aeruginosa* in BESs is not unique and is omnipresent in ecosystems characterized by the presence of redox gradients (e.g., soil, marine sediments, pipeline corrosion, biofilms etc.). Further, it is very well established that phenazine production by *P. aeruginosa* is strongly influenced by multiple stimuli, including quorum sensing. Therefore, in BESs, the three seemingly different but intertwined phenotypes of *P. aeruginosa* - quorum sensing, phenazine production, and bacterial respiration may be collectively represented by the single phenotype - real-time and *in situ* current production. Indeed, with the help of mutants in the quorum-sensing pathway(s), we showed that quorum sensing controls current production by this microbe by modulating phenazine production (Chapter 3). In addition, since we correctly predicted the effect of well known exogenous quorum-sensing inhibitors (e.g., Fe(III)) or upregulators (e.g., Homoserine lactones) on current production by *P. aeruginosa* (Chapter 3), we propose that BESs are attractive tools for real-time monitoring of the status of quorum sensing under various environmental conditions in this

microbe. Given the wide biodiversity of BESs, it is expected that the phenazine production by *P. aeruginosa* would also be significantly influenced by the actions of other community members. We showed that one such interspecies communication between *P. aeruginosa* and *Enterobacter aerogenes* involved metabolite-based mutualism (Chapter 4). The fermentation production of *E. aerogenes* - 2,3-butanediol - concomitantly stimulated *P. aeruginosa* to produce more phenazines compared to the starting substrate – glucose, and steered the composition of these phenazines towards 92 % pyocyanin. In return, under these conditions, *E. aerogenes*, which is a conventional fermenter, was able to use the pyocyanin produced by *P. aeruginosa* to respire with the electrode, resulting in higher bioenergetics for *E. aerogenes*. The net effect of this synergism was a 14-fold higher current generation by the co-culture of these two microbes compared to a pure culture of either organism. *P. aeruginosa* is frequently found in association with fermenters, such as *E. aerogenes* in other oxygen limited ecosystems, especially in cystic fibrosis. Therefore, based on our understanding from Chapter 4 that a fermentation product benefited *P. aeruginosa*, we showed that the presence of fermenters in certain oxygen limited ecosystems causes *P. aeruginosa* to exhibit increased virulence via positive regulation of quorum sensing by the fermentation products (Chapter 5). Next, we demonstrated that the synergism between *P. aeruginosa* and *E. aerogenes* greatly increased the importance of phenazine-based electrode respiration in BESs (Chapter 6). Finally, the well known electrode-respirer *Geobacter sulfurreducens* was inhibited by the extracellular virulence factors of *P. aeruginosa*. In summary, our findings demonstrate the relevance of community dynamics of *P. aeruginosa* in: i) process functionality of BESs by affecting phenazine production; and ii) on the pathogenicity by affecting the production of extracellular virulence factors. Based on this, the following recommendations for future work are proposed:

7.2 Recommendations for future work

7.2.1 Determining the pathway for reduction of phenazines in *P. aeruginosa*, *E. aerogenes*, *Enterococcus faecium*, and *Brevibacillus* sp.

Phenazines by *P. aeruginosa* are widespread in several ecosystems and there are multiple studies characterizing their importance for *P. aeruginosa*. Although the pathway (*phzA1-G1* and *phzA2-G2*) for their production has been well established, there have been no studies highlighting the pathway responsible for their reduction. One thing that is clear from the fact that multiple members from other genera or phyla, such as *Enterobacter aerogenes* and *Brevibacillus* sp., can also reduce the oxidized form of the phenazines is that the pathway for reduction is not indigenous or specific to *P. aeruginosa*. The ecological and evolutionary role of phenazines is unclear, though there is strong evidence supporting the hypotheses that these compounds play an important role as alternative electron acceptors for microbes and may also be involved in mineral cycling in soil ecosystems. Additionally, it is puzzling as to why an organism should devote such a dedicated part of its energetic process in producing these secondary metabolites?. Characterizing the pathway(s) used by the microbes listed above for reduction of these phenazines, looking at if these pathways are conserved among different genera/phyla, and if possible understanding the structure of the protein responsible for this action (using a two pronged approach of experimental and molecular modeling) will definitely answer some of these questions and perhaps provide an insight into the role of these phenazines in a diverse microbiota. This aim would require studies with the *P. aeruginosa* Δ*phz* mutant (Dietrich et al., 2006) using radioactively labeled pyocyanin (tritium instead of hydrogen). Based on the radioactivity, one could screen for certain candidates for reduction in the cytoplasm, inner membrane and outer membrane, such as NADH, glutathione, quinones, and cytochromes.

Difference spectra measurements can also be performed to determine the supposed role of cytochromes in the reduction of the phenazines.

7.2.2 Determining the biochemical mechanism of increase in virulence of *P. aeruginosa* due to fermentation products

The findings from Chapter 5 are a good foundation for more *in vitro* studies regarding the behavior of *P. aeruginosa* in polymicrobial infections. For these findings to effectively translate into a novel treatment strategy, it is necessary to understand the exact biochemical mechanism underlying this phenomenon. Although, our proteomics experiments confirmed our hypothesis regarding the increase in virulence of *P. aeruginosa* with the fermentation products and we, indeed, found that quorum sensing was upregulated with 2,3-butanediol compared to glucose, they did not provide clues regarding the mechanisms. To answer this question multiple approaches need to be taken:

1. Proteomics with glucose and all the fermentation products (lactate, acetate, ethanol, and 2,3-butanediol) in synthetic CF medium (Palmer et al., 2007) need to be performed at different time points of growth of *P. aeruginosa* under micro-oxic conditions. This needs to be followed up with data mining and compiling a common set of pathways that are affected in all the fermentation products compared to glucose. Subsequently, these selected pathways can be screened by creating mutants and analyzing their behavior when grown on fermentation products compared to glucose. These experimental studies can be effectively complemented by performing *in-silico* molecular dynamics studies which might help us predict the kind of molecular mechanism underpinning this phenomenon of increase in virulence. Eventually, this could result in creating a novel drug target based on the ecological interactions. We do not believe that simply

eliminating all fermenters is the right strategy because this would only promote the growth of *P. aeruginosa*, which is well known for its remarkable antibiotic resistance.

2. *Pseudomonas aeruginosa* PA14 has two well established pathogenicity islands, though, their exact composition still needs to be fully characterized. qRT-PCR studies of the expression of these islands with all the fermentation products in synthetic CF medium (Palmer et al., 2007) will be another step towards understanding this phenomenon at a deeper biochemical level.
3. One of the key components of the success of *P. aeruginosa* in cystic fibrosis is its ability to undergo rapid genotypic changes *in vivo* (Oliver et al., 2000). Since we have shown that fermentation products contribute greatly to the prevalence of *P. aeruginosa*, it would be in line to observe whether these fermentation products also cause *P. aeruginosa* to exhibit mutations in certain key pathways, such as GacS/GacA, RpoS, ClpA, MvaT. Another interesting addition to this approach would be to also determine if growth on fermentation products actually increases the mutation frequency thereby introducing a selective pressure for survival of the fittest member.

7.2.3 Performing mock-community experiments *in vitro* as a follow up to the above recommendation

The microbial community in cystic fibrosis is being well characterized due to increasing access and confidence in culture independent sequencing approaches such as 454 or Illumina. A mock community needs to be created based on findings from these studies and community dynamics over time in synthetic CF medium can be studied in bioreactors, followed by lung-on-a-chip devices (Graham-Rowe, 2009; Huh et al., 2010) and finally a mouse model (Gabriel et al., 1994). A critical component to this is performing these experiments in micro-oxic conditions that are

prevalent in cystic fibrosis conditions. The biggest challenge in this endeavor is to be able to follow the growth of the microbes very accurately over time.

NOTE: For recommendations in sections 7.2.2 and 7.2.3, it is paramount that all experiments be conducted under tightly controlled oxygen conditions because oxygen has a significant influence on the behavior of *P. aeruginosa*. Canfield et al. (2007) provides a nice starting point for experimental design.

7.2.4 Stability, robustness, redundancy, and resilience in BES microbiota

Our findings from Chapter 4 and Chapter 6 clearly demonstrate that BES performance is significantly impacted by community interactions. The impact of community dynamics on process functionality in engineered systems is very well known. Although, such studies have been performed in well characterized systems such as anaerobic digesters (Werner et al., 2011), we believe that for BESs to achieve maximum performance, community dynamics in these systems needs to be better understood. The mock community in this thesis (Chapter 6) consisted of a fermenter, a direct electron transfer (DET) capable microbe, and a mediated electron transfer (MET) capable microbe. We observed the highest current densities with all three microbes in FW medium, where DET by *G. sulfurreducens* was the most important mechanism of electrode respiration and where the growth of *P. aeruginosa* was inhibited. This has implications with respect to selective enrichment of microbiota in a full-scale BES for maximizing electric current generation. On the other hand, with respect to maximizing coulombic efficiency, there are two perspectives since the degradation of complex carbon sources in wastewater will result in multiple by-products (e.g., glucose to principally 2,3-butanediol and ethanol with minor concentrations of acetate). First, the presence of phenazines can switch the metabolism of a conventional fermenter from fermentation to electrode based respiration, resulting in fewer

fermentation products translating into higher coulombic efficiency. Second, given the limited substrate diversity of the DET capable *G. sulfurreducens* (i.e., this microbe only consumes acetate), for maximum biotransformation of a complex starting substrate into electric current, MET via bacterial partnership is necessary (i.e., *P. aeruginosa* uses 2,3-butanediol and ethanol to respire with the electrode).

Therefore, understanding the effect of community composition on the performance parameters is necessary. An approach similar to Wittebolle et al. (2009) needs to be undertaken for BESs as well. Given the multitude of studies characterizing the BES microbiota, it would be possible to create a more complex mock community than the one we have used for our experiments (Chapter 6) for example by including *Lactobacillus* sp., *Brevibacillus* sp., *Rhodopseudomonas palustris*, *Shewanella oneidensis* MR-1 etc.. A challenge in this endeavor would be to assign a particular function to the ecosystem, especially because as discussed above, current and coulombic efficiency are negatively correlated with the microbial players. One way to circumvent this would be to use both parameters as functional indices and then determine the necessary community composition for optimum performance.

8 APPENDIX 1. Supplemental information for Metabolite-based mutualism between *Pseudomonas aeruginosa* PA14 and *Enterobacter aerogenes* enhances current generation in bioelectrochemical systems.

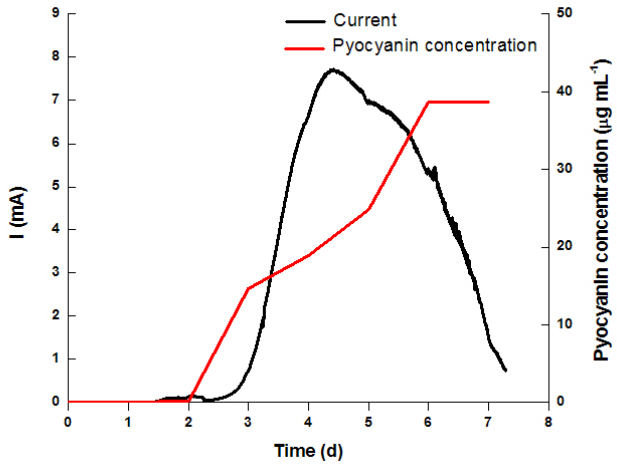

Figure 8.1. Current vs. time and pyocyanin vs. time for one trial of the co-culture experiment (*E. aerogenes* in association with *P. aeruginosa*).

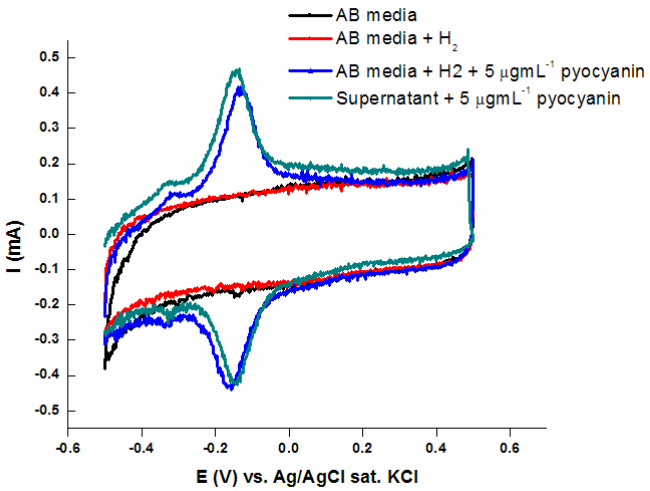

Figure 8.2. Cyclic voltammograms of carbon cloth electrode in AB media sparged with hydrogen and addition of 5 µg mL^{-1} pyocyanin.

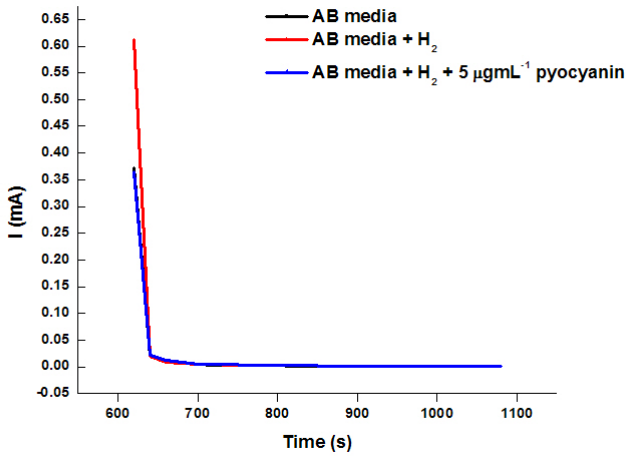

Figure 8.3. Chronoamperometry with carbon cloth electrode in AB media sparged with hydrogen and addition of 5 µg mL^{-1} pyocyanin at 0.3 V vs. Ag/AgCl sat. KCl.

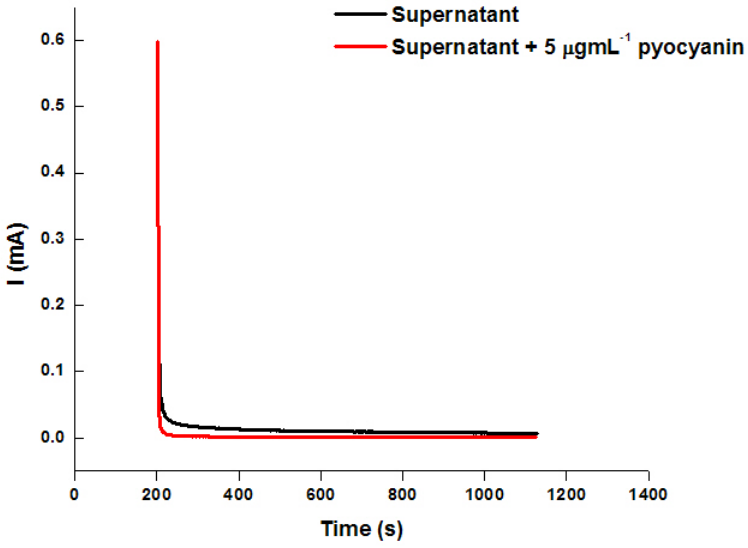

Figure 8.4. Chronoamperometry with carbon cloth electrode of *E. aerogenes* with 0 µg mL^{-1} pyocyanin and 5 µg mL^{-1} pyocyanin at 0.3 V vs. Ag/AgCl sat. KCl.

9 APPENDIX 2. Supplemental information for Common fermentation products increase virulence of *Pseudomonas aeruginosa*.

Table 9-1. Dry cell weights in g L^{-1} of *P. aeruginosa* PA14 grown on different carbon sources

Substrate	Aeration condition	Dry cell weight (g L^{-1})
Lactate	Microaerobic	0.094 ± 0.007
Acetate	Microaerobic	0.086 ± 0.008
Ethanol	Microaerobic	0.074 ± 0.01
2,3-butanediol	Microaerobic	0.077 ± 0.008
	Aerobic	0.159 ± 0.01
Glucose	Microaerobic	0.113 ± 0.008
	Aerobic	0.782 ± 0.074

Table 9-2. List of all statistically significantly changed proteins in a comparative proteomics analysis of *P. aeruginosa* PA14 cells grown aerobically in AB medium with 2,3-butanediol or glucose as carbon source, respectively.

Functional category	Label	log (B/G) down	log (B/G) up
Quorum sensing/Virulence factors/Biofilm formation	PA14_30800 Putative nitroreductase	-0.854	
	PA14_18180 Putative antibiotic biosynthesis monooxygenase	-0.750	
	PA14_61390 Putative lipoprotein	-0.658	
	PA14_27460 Thiopurine methyl transferase	-0.398	
	PA14_28450 Ecotin precursor		0.336
	PA14_7650 Putative sporulation protein		0.406

	PA14_65000 Azurin precursor		0.444
	PA14_62420 Zinc metallo peptidase		0.484
	PA14_1490 Putative hemolysin		0.486
	PA14_69370 Alginate regulatory protein		0.496
	PA14_36980 Putative outer membrane protein		0.568
	PA14_56070 Transcriptional regulator MvaT P-16 subunit		0.582
Transporter	PA14_3930 Putrescine ABC transporter putrescine-binding protein potF	-0.575	
	PA14_62650 TolA protein	-0.399	
	PA14_16510 Peptide chain release factor 2	-0.368	
	PA14_68260 TRAP-type C4-dicarboxylate transport system, periplasmic component		0.328
	PA14_51810 FIG000859 (not subsystem-based): hypothetical protein		0.372
	PA14_21175 Phosphonate ABC transporter phosphate-binding periplasmic component		0.399
	PA14_46910 Glutamate Aspartate periplasmic binding protein precursor gltI		0.407
	PA14_50520 High-affinity leucine-specific transport system, periplasmic binding protein livK		0.415
Transporter	PA14_52790 Arginine/ornithine ABC transporter, periplasmic arginine/ornithine binding protein		0.448
	PA14_45930 GGDEF and EAL domain proteins		0.454

	PA14_24020 General secretion pathway protein G		0.501
	PA14_67840 Glutamate ABC transporter, periplasmic glutamine-binding protein		0.579
	PA14_57840 Uncharacterized ABC transporter, auxiliary component YrbC		0.613
	PA14_64900 Branched-chain amino acid ABC transporter, amino acid-binding protein		0.646
	PA14_7870 ABC transporter, periplasmic spermidine putrescine-binding protein potD		0.656
	PA14_46220 Putrescine ABC transporter putrescine-binding protein potF		1.113
	PA14_54540 Putative tricarboxylic transport TctC		1.122
	PA14_68070 Arginine/ornithine ABC transporter, periplasmic arginine/ornithine binding protein		1.210
	PA14_39350 Ribose ABC transport system, periplasmic ribose-binding protein RbsB		1.367
	PA14_14390 Putative ABC-type transport protein periplasmic c		1.399
	PA14_73120 Putative periplasmic transport protein		1.501
	PA14_33530 Putative ABC transporter periplasmic substrate binding protein		1.501
	PA14_67850 ABC type amino acid transport protein periplasmic component		1.656
Structure	PA14_14910 Outer membrane protein YfgL,	-0.832	

	PA14_68200 Glucose-1-phosphate thymidylyltransferase	-0.758	
	PA14_68210 dTDP-4-dehydrorhamnose 3,5-epimerase	-0.548	
	PA14_50930 type IV pilus biogenesis protein PilE		0.307
	PA14_63030 Outer membrane lipoprotein SmpA,		0.447
Structure	PA14_30310 Outer membrane lipoprotein carrier protein LolA		0.561
Stress Response	PA14_34460 Alkylhydroperoxidase	-1.775	
	PA14_67090 Glucans biosynthesis protein G precursor	-0.775	
	PA14_56590 Universal stress protein family 4	-0.647	
	PA14_68380 ADP compounds hydrolase NudE	-0.565	
	PA14_56940 Copper sensory histidine kinase CusS	-0.503	
	PA14_4730 Gamma-glutamyltranspeptidase	-0.409	
	PA14_21220 Universal stress protein family	-0.332	
	PA14_48590 Trans-aconitate 2-methyltransferase	-0.304	
	PA14_62970 Chaperone protein DnaK		0.339
	PA14_24770 Probable transmembrane protein		0.368
	PA14_70740 Probable transmembrane protein		0.577
	PA14_49410 Cold shock protein		1.368
	PA14_21760 Cold acclimation protein B		1.577
Regulation	PA14_73020 C4-type zinc finger protein, DksA/TraR family	-1.099	

	PA14_23720 Putative translation initiation inhibitor, yjgF family	-0.440	
	PA14_64930 Nudix-related transcriptional regulator NrtR	-0.390	
	PA14_25800 Transcriptional regulator, TetR family	-0.390	
	PA14_65280 HflK protein	-0.306	
	PA14_52570 Carbon storage regulator		0.376
	PA14_41250 Cell division trigger factor		0.397
Redox	PA14_22710 Coenzyme F420-1:L-glutamate ligase	-0.759	
	PA14_14680 Myo-inositol-1(or 4)-monophosphatase	-0.576	
	PA14_69420 Homolog of E. coli HemY protein	-0.545	
	PA14_23380 UDP-N-acetyl-D-mannosaminuronate dehydrogenase	-0.503	
Redox	PA14_46980 Signal transduction histidine kinase HoxJ	-0.463	
	PA14_15120 Copper metallochaperone, bacterial analog of Cox17 protein	-0.374	
	PA14_20140 Ferredoxin--NADP(+) reductase	-0.334	
	PA14_69970 membrane c-type cytochrome cy		0.305
	PA14_31810 Thiol peroxidase, Tpx-type		0.337
	PA14_69200 Thioredoxin		0.424
	PA14_14750 Iron binding protein IscA for iron-sulfur cluster assembly		0.557
	PA14_51980 Arsenate reductase		0.692

	PA14_29020 Biotin synthesis protein bioH		0.778
Phosphorous metabolism	PA14_28960 PhnB protein	-0.305	
	PA14_46830 PhnB protein		0.341
	PA14_2450 NAD(P) transhydrogenase alpha subunit		0.493
	PA14_11690 Inorganic pyrophosphatase		0.537
	PA14_64460 Phosphate starvation inducible protein		1.537
Phenazines	PA14_39960 Phenazine biosynthesis protein PhzB		0.487
	PA14_9420 Phenazine biosynthesis protein PhzF		0.550
Chemotaxis/ Motility	PA14_30700 Chemotaxis protein methyltransferase CheR	-1.413	
	PA14_68400 Flagellar hook-length control protein fliK	-0.343	
	PA14_67010 Aerotaxis sensor receptor protein	-0.338	
	PA14_58390 Dipeptide-binding ABC transporter, periplasmic substrate-binding component		0.366
	PA14_61200 Flagellar hook-length control protein fliK		0.482
	PA14_58350 Dipeptide-binding ABC transporter, periplasmic substrate-binding component		0.589
	PA14_45810 Flagellar biosynthesis protein fliL		0.808
Chemotaxis/ Motility	PA14_69100 Flagellar biosynthesis protein fliL		0.822
Metabolism	PA14_53250 Chitin binding protein	-1.080	
	PA14_71720 Pyruvate carboxyl transferase subunit B	-0.956	

	PA14_67500 Lactoylglutathione lyase	-0.907	
	PA14_22910 Phosphogluconate dehydratase	-0.777	
	PA14_49660 Beta-galactosidase	-0.691	
	PA14_15340 GMP synthase	-0.587	
	PA14_37570 Benzoate 1,2-dioxygenase (EC 1.14.12.10)	-0.578	
	PA14_27960 Transaldolase (EC 2.2.1.2)	-0.472	
	PA14_25080 Enoyl-CoA hydratase (EC 4.2.1.17)	-0.471	
	PA14_53220 Fumarate hydratase class II (EC 4.2.1.2)	-0.449	
	PA14_54470 YgfY COG2938	-0.434	
	PA14_25660 3-oxoacyl-[acyl-carrier protein] reductase (EC 1.1.1.100)	-0.431	
	PA14_41670 Phosphoenolpyruvate synthase (EC 2.7.9.2)	-0.399	
	PA14_8460 Enoyl-[acyl-carrier-protein] reductase [FMN] (EC 1.3.1.9)	-0.398	
	PA14_56240 Pyruvate kinase (EC 2.7.1.40)	-0.383	
	PA14_57890 Arabinose 5-phosphate isomerase (EC 5.3.1.13)	-0.370	
	PA14_66290 Pyruvate dehydrogenase E1 component (EC 1.2.4.1)	-0.367	
	PA14_10290 Transcriptional activator of acetoin dehydrogenase operon acoR	-0.366	
	PA14_40830 Alcohol dehydrogenase (EC 1.1.1.1)	-0.356	
	PA14_27730 Acyl-CoA dehydrogenase, short-chain specific (EC 1.3.99.2)	-0.355	

	PA14_70370 Orotate phosphoribosyltransferase (EC 2.4.2.10)	-0.354	
	PA14_71850 diguanylate cyclase/phosphodiesterase (GGDEF & EAL domains) with PAS/PAC sensor(s)	-0.353	
Metabolism	PA14_57600 Putative oxido-reductase aldo-keto reductase family	-0.351	
	PA14_21540 3-oxoacyl-[acyl-carrier-protein] synthase, KASIII (EC 2.3.1.41)	-0.335	
	PA14_25090 Acetyl-CoA acetyltransferase (EC 2.3.1.9)	-0.331	
	PA14_25650 Malonyl CoA-acyl carrier protein transacylase (EC 2.3.1.39)	-0.323	
	PA14_4150 Fumarylacetoacetate hydrolase family protein	-0.315	
	PA14_10250 Acetoin dehydrogenase E1 component beta-subunit (EC 1.2.4.-)		0.316
	PA14_9550 6-phosphogluconolactonase (EC 3.1.1.31)		0.329
	PA14_49330 Candidate 1: dienelactone hydrolase		0.347
	PA14_11810 Aldehyde dehydrogenase (EC 1.2.1.3)		0.398
	PA14_10230 2,3-butanediol dehydrogenase, R-alcohol forming, (R)- and (S)-acetoin-specific (EC 1.1.1.4)		0.401
	PA14_73280 ATP synthase delta chain (EC 3.6.3.14)		0.435
	PA14_73230 ATP synthase epsilon chain (EC 3.6.3.14)		0.459
	PA14_10260 Acetoin dehydrogenase E1 component alpha-subunit (EC 1.2.4.-)		0.485

	PA14_64110 Biotin carboxylase of acetyl-CoA carboxylase (EC 6.3.4.14)		0.486
	PA14_10280 Short-chain alcohol dehydrogenase associated with acetoin utilization		0.615
	PA14_10240 Dihydrolipoamide acetyltransferase component (E2) of acetoin dehydrogenase complex (EC 2.3.1.-)		0.683
	PA14_51170 Acetyl-CoA synthetase (ADP-forming) alpha and beta chains, putative		0.736
	PA14_24790 hydroxycinnamate specific porine		0.785
	PA14_25670 Acyl carrier protein		0.797
	PA14_38860 Quino(hemo)protein alcohol dehydrogenase, PQQ-dependent (EC 1.1.99.8)		1.077
Metabolism	PA14_66875 Polyhydroxyalkanoate synthesis protein PhaF		1.486
	PA14_25900 Putative short chain alcohol-dehydrogenase		
Iron accquisition	PA14_3800 Outer membrane porin, coexpressed with pyoverdine biosynthesis regulon	-0.967	
	PA14_9220 Pyochelin biosynthetic protein PchB	-0.589	
	PA14_42820 Isochorismatase (EC 3.3.2.1)	-0.429	
	PA14_62300 Periplasmic hemin-binding protein	-0.356	
	PA14_33710 PvdO, pyoverdine responsive serine/threonine kinase		0.380
	PA14_56830 Iron-regulated protein A precursor		0.397
DNA/RNA/protein	PA14_70190 LSU ribosomal protein L28p	-0.950	

	PA14_41380 Glutaminyl-tRNA synthetase (EC 6.1.1.18)	-0.749	
	PA14_19870 Leucine dehydrogenase (EC 1.4.1.9)	-0.742	
	PA14_70270 Phosphomannomutase (EC 5.4.2.8)	-0.646	
	PA14_58630 ArPA14nine decarboxylase (EC 4.1.1.19)	-0.580	
	PA14_72520 Ribonucleotide reductase of class II (coenzyme B12-dependent) (EC 1.17.4.1)	-0.560	
	PA14_12400 Thiamin-phosphate pyrophosphorylase (EC 2.5.1.3)	-0.545	
	PA14_49870 Peptide deformylase (EC 3.5.1.88)	-0.505	
	PA14_5230 Cystathionine gamma-lyase (EC 4.4.1.1)	-0.475	
	PA14_54640 Enoyl-CoA hydratase [valine degradation] (EC 4.2.1.17)	-0.459	
	PA14_23320 Cytidylate kinase (EC 2.7.4.14)	-0.449	
	PA14_54480 COG0354: Predicted aminomethyltransferase related to GcvT	-0.440	
	PA14_28650 Threonyl-tRNA synthetase (EC 6.1.1.3)	-0.407	
	PA14_3450 5-aminovalerate aminotransferase (EC 2.6.1.48)	-0.403	
	PA14_70440 Guanylate kinase (EC 2.7.4.8)	-0.403	
DNA/RNA/protein	PA14_23110 Pseudouridine synthase family protein	-0.392	
	PA14_12080 Membrane-bound lytic murein transglycosylase B (EC 3.2.1.-)	-0.390	
	PA14_25560 Ribonuclease E (EC 3.1.4.-)	-0.389	

	PA14_51310 tRNA 5-methylaminomethyl-2-thiouridine synthase TusA	-0.362	
	PA14_8760 DNA-directed RNA polymerase beta subunit (EC 2.7.7.6)	-0.361	
	PA14_67810 Carboxyl-terminal protease (EC 3.4.21.102)	-0.356	
	PA14_8790 SSU ribosomal protein S12p (S23e)	-0.351	
	PA14_24445 NADP-specific glutamate dehydrogenase (EC 1.4.1.4)	-0.347	
	PA14_24270 Membrane alanine aminopeptidase N (EC 3.4.11.2)	-0.341	
	PA14_64490 LSU ribosomal protein L21p	-0.332	
	PA14_67110 Proline iminopeptidase (EC 3.4.11.5)	-0.326	
	PA14_12230 Leucyl-tRNA synthetase (EC 6.1.1.4)	-0.316	
	PA14_57580 SSU ribosomal protein S9p (S16e)	-0.311	
	PA14_66790 ATP-dependent hsl protease ATP-binding subunit hslU	-0.303	
	PA14_20 DNA polymerase III beta subunit (EC 2.7.7.7)	-0.303	
	PA14_57010 Heat shock protein 60 family chaperone GroEL		0.323
	PA14_60460 LSU ribosomal protein L21p		0.326
	PA14_8990 SSU ribosomal protein S8p (S15Ae)		0.339
	PA14_9000 LSU ribosomal protein L6p (L9e)		0.351
	PA14_8940 SSU ribosomal protein S17p (S11e)		0.353
	PA14_45110 Sulfate and thiosulfate binding protein cysP		0.353
	PA14_30330 Seryl-tRNA synthetase (EC 6.1.1.11)		0.366

	PA14_21030 ATP-dependent Clp protease proteolytic subunit (EC 3.4.21.92)		0.375
	PA14_62900 Transcription elongation factor GreA		0.405
DNA/RNA/protein	PA14_17050 Methionine aminopeptidase (EC 3.4.11.18)		0.406
	PA14_22450 Peptidyl-prolyl cis-trans isomerase ppiA precursor (EC 5.2.1.8)		0.423
	PA14_17060 SSU ribosomal protein S2p (SAe)		0.440
	PA14_23330 SSU ribosomal protein S1p		0.444
	PA14_21880 Tail-specific protease precursor (EC 3.4.21.102)		0.449
	PA14_9010 LSU ribosomal protein L18p (L5e)		0.450
	PA14_46970 L-asparaginase (EC 3.5.1.1)		0.452
	PA14_62720 SSU ribosomal protein S15p (S13e)		0.499
	PA14_8720 LSU ribosomal protein L11p (L12e)		0.584
	PA14_41390 Peptidyl-prolyl cis-trans isomerase ppiB (EC 5.2.1.8)		0.658
	PA14_70600 DNA-binding protein HU-alpha		0.682
	PA14_68860 Glycine cleavage system H protein		0.841
	PA14_44620 conserved protein of unknown function likely to be involved in DNA repair		0.892
	PA14_8750 LSU ribosomal protein L7/L12 (L23e)		0.921
	PA14_9890 Peptidyl-prolyl cis-trans isomerase ppiC (EC 5.2.1.8)		0.979

	PA14_65310 RNA-binding protein Hfq		1.039
	PA14_27210 Translation elongation factor P		1.080
	PA14_8930 LSU ribosomal protein L29p (L35e)		1.110
	PA14_68710 TRANSCRIPTION ACCESSORY PROTEIN (S1 RNA binding domain)		1.225
	PA14_ Putative ribosomal protein L25		2.225
Miscellaneous	PA14_30800 Putative nitroreductase	-0.854	
	PA14_18180 Putative antibiotic biosynthesis monooxygenase	-0.750	
Miscellaneous	PA14_61390 Putative lipoprotein	-0.658	
	PA14_27460 Thiopurine methyl transferase	-0.398	
	PA14_28450 Ecotin precursor		0.336
	PA14_7650 Putative sporulation protein		0.406
	PA14_65000 Azurin precursor		0.444
	PA14_62420 Zinc metallo peptidase		0.484
	PA14_1490 Putative hemolysin		0.486
	PA14_69370 AlPA14nate regulatory protein		0.496
	PA14_36980 Putative outer membrane protein		0.568
	PA14_56070 Transcriptional regulator MvaT P-16 subunit		0.582

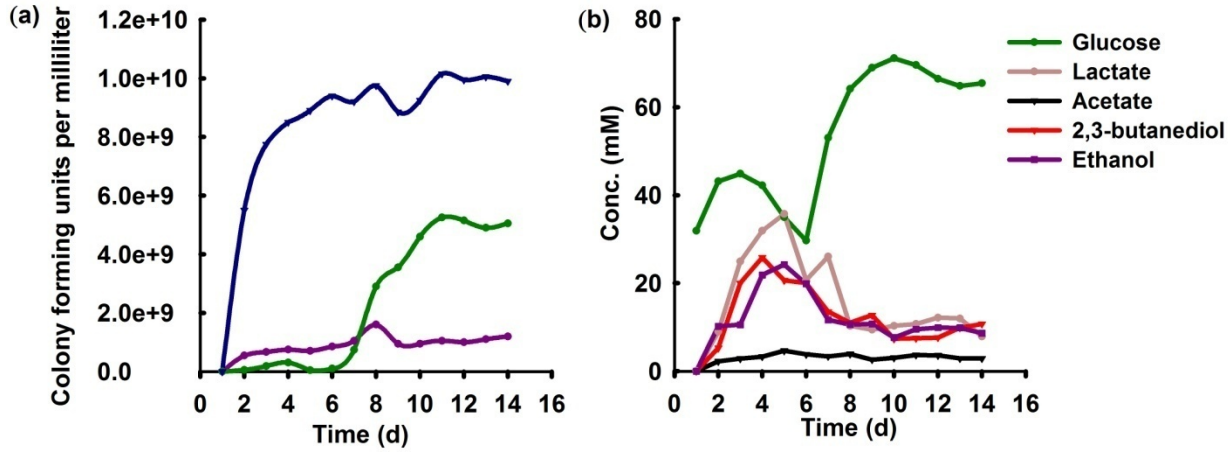

Figure 9.1. Biological replicate of Figure 5.3: (a) tracking the population of *S. marcescens* (dark pink) in a co-culture with *P. aeruginosa* (dark green) over time, and the population of a pure culture of *S. marcescens* (deep blue) under similar operating conditions; and (b) metabolite profile in the bioreactor operated with a co-culture of *S. marcescens* and *P. aeruginosa*.

10 APPENDIX 3. Supplemental information for Mediator-based and direct contact-based exocellular electron transfer are equally important within synergistic bacterial communities in bioelectrochemical systems.

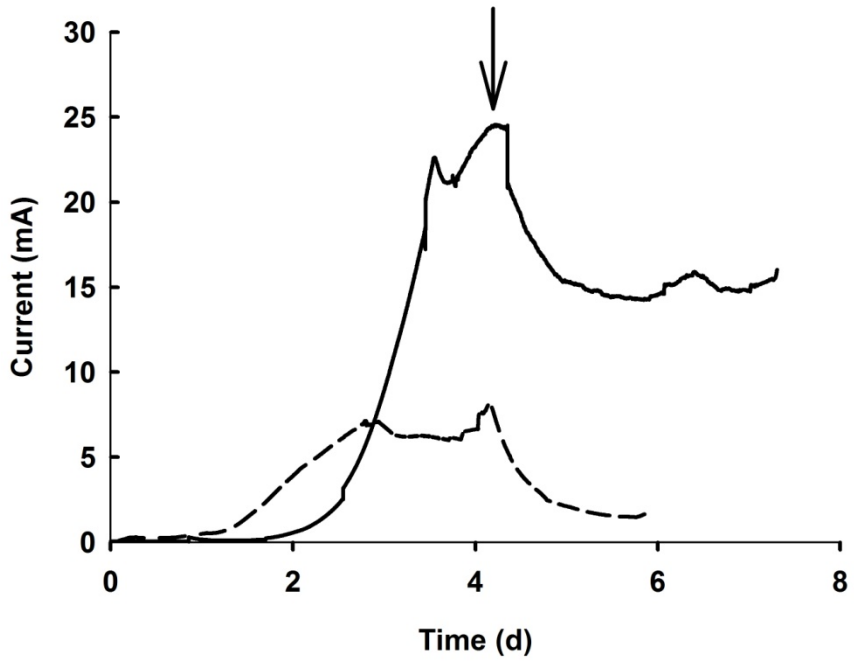

Figure 10.1. Current vs. time for the defined mixed culture of *E. aerogenes*, *P. aeruginosa*, and *G. sulfurreducens* in FW medium (solid line) and FWAB medium (dashed line). The arrow indicates the time at which flow was switched on.

11 APPENDIX 4. Protocols

Luria-Bertani broth

Materials:
Luria-Bertani (LB) powder: 20 g/L
Distilled water
I liter glass bottle
Stir bar
Stir and heat plate

Procedure:
1. Add 20 g of LB powder to one liter of distilled water in glass bottle with stir bar.
2. Stir vigorously on the stir plate with heating till dissolved completely.
3. Autoclave at 121 C for 20 minutes with the lid of the bottle slightly open to allow expansion in the autoclave.
4. Once taken out of the autoclave, close tightly.
5. Allow to cool to room temperature prior to using.

AB medium

Materials:
One 100 mL glass bottle
One 1 liter glass bottle
Graduated cylinder
Glucose
Component A contains (g/L):
$(NH_4)_2SO_4$: 10;Na_2HPO_4: 30; KH_2PO_4: 15; NaCl: 15; Na_2SO_4: 0.55
Component B contains (g/L):
$MgCl_2$: 0.2; $CaCl_2$: 0.01; $FeCl_3.7H_2O$: 0.0005

Procedure:

1. Dissolve all constituents of component A in 100 mL distilled water in the 100 mL glass bottle.
2. Dissolve all constituents of component B in 850 mL distilled water in the 1000 mL glass bottle. Use the same weight of chemicals as if preparing 1 L of component B, because the final volume of this bottle will be 1L.
3. Autoclave both bottles separately at 121 C for 20 minutes with lid of the bottle slightly open to allow expansion during autoclaving.
4. Close lid tightly once out of the autoclave.
5. Allow bottles to cool down to room temperature.
6. Mix the contents of both bottles to a final volume of 950 mL.
7. Dissolve 27 g of glucose in 250 mL distilled water for stock solution.
8. Filter sterilize glucose stock solution in 250 mL sterile filter units.
9. Add 50 mL of glucose stock solution to the 950 mL from step 6.

Note that any carbon source can be substituted for glucose at a concentration of 600 mM, i.e., 50 mL of 600 mM carbon source needs to be added to 950 mL of the medium prior to use.

FW medium

Materials:
One 1 liter glass bottle
Graduated cylinder
$NaHCO_3$: 2.5 g/L; NaH_2PO_4: 0.52 g/L; KCl: 0.1 g/L
Vitamin mix: 10 mL (see procedure below)
Mineral mix: 10 mL (see procedure below)
Sodium acetate
Sodium fumarate
Water

Procedure for preparing vitamin mix:

Dissolve 2 mg biotin, 2 mg folic acid, 10 mg pyridoxine-HCl, 5 mg Thiamine-HCl·$2H_2O$, 5 mg Riboflavin, 5 mg Nicotinic acid, 5 mg D-Ca-pantothenate, 0.1 mg vitamin B_{12}, 5 mg p-aminobenzoic acid, 5 mg lipoic acid in one liter of distilled water.

Procedure for preparing mineral mix:

Dissolve 1.5 g nitrilotriacetic acid, 3.0 g $MgSO_4 \cdot 7H_2O$, 0.5 g $MnSO_4 \cdot H_2O$, 1 g NaCl, 0.1 g $FeSO_4 \cdot 7H_2O$, 0.18 g $CoSO_4 \cdot 7H_2O$, 0.1 g $CaCl_2 \cdot 2H_2O$, 0.18 g $ZnSO_4 \cdot 7H_2O$, 0.01 g $CuSO_4 \cdot 5H_2O$, 0.02 g $KAl(SO_4)_2 \cdot 12H_2O$, 0.01 g H_3BO_3, 0.01 g $Na_2MoO_4 \cdot 2H_2O$, 0.025 g $NiCl \cdot 6H_2O$, 0.3 mg $Na_2SeO_3 \cdot 5H_2O$ in one liter of distilled water.

Procedure for FW medium:

1. Dissolve salts mentioned above in 930 mL distilled water in a one liter glass bottle.
2. Autoclave at 121 C for 20 minutes with the lid of the bottle slightly open to allow expansion in the autoclave.
3. Once taken out of the autoclave, close tightly.
4. Allow to cool to room temperature.
5. Add 10 mL of vitamin mix and 10 mL of mineral mix in the biosafety cabinet bringing the total volume to 950 mL.
6. Dissolve 4.1 g of sodium acetate in 250 mL distilled water.
7. Filter sterilize acetate stock solution in 250 mL sterile filter units.
8. Add 50 mL of the above acetate stock solution to 950 mL of the medium
9. Leave bottle in anaerobic hood overnight to remove oxygen, alternatively the medium can be vigorously sparged with 80%:20% N_2:CO_2 for one hour.

In this case sodium acetate is added at a concentration of 10 mM, for other concentrations adjust volume of water accordingly so that final volume of the medium is 1 L. If sodium fumarate is needed it should be added at a concentration of 40 mM for growing *G. sulfurreducens* in serum bottles, for electrochemical experiments sodium fumarate and acetate are added at a molar ratio of 1:1. Additionally, if needed cysteine sulfide can be added anaerobically and aseptically at a final concentration of 25g /L: volume of water should be adjusted accordingly.

FWAB medium

Materials:
Salts of AB medium
Salts of FW medium.
Vitamin mix
Mineral mix
1L glass bottle.
100 mL glass bottle.
Graduated cylinder

Procedure:

1. Prepare component B of AB medium along with the salts of FW medium in 830 mL of distilled water using one 1L glass bottle.
2. Prepare component A of AB medium separately in 100 mL using one 100 mL glass bottle.
3. After autoclaving, mix the two solutions from step 1 and step 2.
4. Add 10 mL of vitamin mix and 10 mL of mineral mix to solution from step 3 bringing it up to a volume of 950 mL.
5. Add 50 mL of carbon source stock solution as needed. (Molarity needs to be calculated depending upon final molarity needed).
6. If needed, add sodium fumarate and cysteine sulfide (read section below the procedure for preparing FW medium) and accordingly adjust the amount of water in step 1.

Growth curves

Materials:
96-well sterile plate
Sterile plate cover
Growth medium
200 μL pipette
30 μL pipette

Procedure:

1. Grow bacterial culture in a 15 or 50 mL sterile vial overnight.
2. Measure OD_{600} in triplicate on the BioTek plate reader.
3. Dilute culture from step 1 to an OD_{600} of 0.1 in the same growth medium being used for the growth curve.
4. Pipette 197 μL of cell free fresh culture medium into wells of 96-well plate.
5. Pipette 3 μL of bacterial culture from step 3 into the wells containing fresh culture medium from step 4.
6. Cover the plate with a sterile plate cover; make sure that the cover fits closely on the plate.
7. Setup a kinetic experiment with hourly reading for 16 h and continuous shaking at chosen temperature in the BioTek plate reader.

Note that all experiments must be done in triplicate and appropriate positive or negative controls must be performed in triplicate on the same plate as well.

LB agar plates

Materials:
LB powder
Agar powder
Sterile petri plates
Water
Glass bottle

Procedure:
1. Dissolve 20 g of LB powder and 15 g of agar in 1 L of distilled water.
2. Autoclave at 121 C for 20 minutes with the lid of the bottle slightly open to allow expansion in the autoclave.
3. Cool to 55 C.
4. Pour equal volumes (15/20 mL) of solution in petri plates in the biosafety cabinet.
5. Allow to solidify.
6. Put agar plates in bag and seal to prevent dehydration and store at 4 C.

Motility assay

Materials:
DIFCO nutrient broth
Agar
Petri plate
Carbon source

Procedure:

1. Dissolve 8g/L of nutrient broth in appropriate volume (20 mL of final solution is required for every plate).
2. Add appropriate concentration of agar (0.3% for swimming motility, 0.5% for swarming motility, and 1.0% for twitching motility) to solution in step 1.
3. Autoclave at 121 C for 20 minutes with the lid of the bottle slightly open to allow expansion in the autoclave.
4. Add carbon source at needed concentration (usually 30 mM is enough) to solution in step 3.
5. Make sure to pour 20 mL in each petri plate.
6. Cool and allow to solidify.
7. Once solidified, add 3 μL of bacterial culture exactly at centre of the plate.
8. Allow the droplet to dry in the biosafety cabinet.
9. Cover the plate and incubate at 37 C.
10. Take photographs as needed.

Note that the 0.3% agar plate will have very low viscosity. Make sure to cool it completely before inoculating and be very careful when transporting it to the incubator.

Reference electrodes

Materials:
Agar
KCl
Distilled water
Graduated cylinder
Beaker
Stir bar
Heat plate
Stainless steel needle

Procedure:
1. Dissolve agar to a final concentration of 1.5 % in appropriate volume (each reference electrode requires ~ 10 mL).
2. Once agar is completely dissolved, keep adding KCl till saturation is reached.
3. Suck air or remaining liquid out from the reference electrode using a needle.
4. Pour solution from step 2 into reference electrode. Make sure to suck air out completely from reference electrode at this stage with the needle so that the solution occupies the entire reference electrode. Any air gap will increase the resistance and not allow proper measurement of current.
5. Fill the remaining of the reference electrode.
6. Insert an oxidized silver wire into the reference electrode when the solution is still liquid.

Phosphate buffered saline

Materials:
NaCl: 8g/L
KCl: 0.2g/L
Na_2HPO_4: 1.44 g/L
KH_2PO_4: 0.24 g/L
HCl/NaOH 1M
Distilled water

Procedure:
1. Dissolve the chemicals in 800 mL distilled water. Use the same weight of chemicals as if preparing 1 L of solution, because the final volume of this bottle will be 1L.
2. Adjust pH to 7.4 using 1M HCl/NaOH.
3. Bring volume up to 1L.

Elastase

Materials:
Porcine pancreas elastase.
Elastin congo red.
200 mM Tris HCl, pH 8.8
0.5 M EDTA pH 8
2 mL centrifuge tubes.

Procedure:
1. Measure 10 mg Elastin congo red into 2 mL centrifuge tubes.
2. Add 750 μL of Tris HCl to the tube.
3. Add 100 μL of the cell free supernatant.
4. Incubate at 37 C for 24 h.
5. Quench on ice and add 20 μL EDTA to stop reaction.
6. Centrifuge at 10,000 RPM for 10 minutes.
7. Measure absorbance at 495 nm in triplicate.
8. Normalize the absorbance at 495 nm to the optical density at 600 nm or another measure of cell growth.
9. Alternatively, generate a standard curve using porcine pancreas elastase and convert the absorbance at 495 nm to units enzyme/mL.

Note that appropriate control must be added (i.e., three tubes with 850 μL of Tris HCl and three tubes with 750 μL Tris HCl and 100 μL sterile water).

Dry cell weight

Materials:
Sterile tube
Oven at 105 C
Weighing balance

Procedure:

1. Grow bacterial cultures in as many flasks as needed for the standard curve of optical density vs. dry cell weight (100 mL of culture in a 500 mL flask).
2. Sacrifice one flask every 3 h.
3. Measure the weight of the sterile tubes to be used in step 4. Before this, the sterile tube should be kept in an oven at 105 C for 24 h so that the dry weight is being recorded in this step.
4. Centrifuge contents of flask at 8000 RPM for 10 minutes.
5. Discard supernatant.
6. Place tubes in oven at 105 C for 24 h.
7. Measure weight of the sterile tube.
8. Calculate dry cell weight as: [Weight of tube in step 7-Weight of tube in step 3]/Volume of liquid centrifuged in step 4.

Note that the standard curve should be generated in triplicate.

Pyoverdine assay

Materials:
Fluorescence plate
Plate reader
Tris EDTA (TE) buffer 10 mM, pH 7.4

Procedure:
1. Add 100 μL of cell free supernatant to a 96-well plate.
2. Add 100 μL of TE buffer to the wells in step 1.
3. Record the fluorescence (excitation 400 nm and emission 460 nm).
4. Normalize the fluorescence to the dry cell weight.

Note that depending upon the fluorescence the volume of supernatant and TE buffer will have to be adjusted to get the reading within the detection limits. All measurements must be performed in triplicate. Make sure to include control (i.e. TE buffer and distilled water).

Protein extraction for proteomics and data analysis

Materials:
Centrifuge tubes
French press
Sodium dodecyl sulfate (SDS)
Urea
Speed Vac
BCA protein assay

Procedure:
1. Grow bacterial cells (100 mL in 500 mL flask) with vigorous shaking.
2. Centrifuge the contents at 10,000 RPM for 10 minutes.
3. Discard supernatant.
4. Wash cells in Phosphate Buffered Saline (PBS; see recipe above) by resuspending the pellet and centrifuging at 10,000 RPM for 10 minutes.
5. Discard supernatant and freeze pellet till ready for extraction (from step 6) at -20 C.
6. Thaw pellet and resuspend in 4 mL milliQ water. Keep centrifuge tubes on ice throughout the extraction process.
7. Lyse cells by passing through the French press at 8000 lb/in^2.
8. Centrifuge to remove unlysed cells and debris at 10000 RPM for 10 minutes at 4 C.
9. Add 5 µL of 1% w/v SDS and 50 µL of 4 M urea to the supernatant from step 8.
10. Vortex solution from step 9 for 10 minutes.
11. Speed vac the solution down to 50 µL.
12. Measure protein concentration using the BCA protein assay (http://www.piercenet.com/browse.cfm?fldID=02020101). Make sure that the standards also contain the same concentration of SDS and urea as the analyte.
13. Once raw data is obtained from proteomics core facility the next step is to classify the proteins into functional categories. This can be done by checking each of the annotations (i.e., PA14_68670 etc.) with the functional categories listed on the web page www. pseudomonas.com (for example http://www.pseudomonas.com/getAnnotation.do?locusID=PA14_68670).
14. Once each protein has been categorized, group all the proteins from one function manually in Excel.
15. Calculate the log ratio of the protein signal from the two experimental conditions for each replicate.
16. To obtain a list of statistically significant proteins, perform a two-way ANOVA between the actual protein signals from step 15 and the value 0 (because log 1 = 0, which basically means that the protein signal between the two conditions is the same).
17. Screen all proteins with a p-value < 0.05
18. Calculate the average log ratio of the protein signal for each protein in step 17.
19. From the list in step 18, all proteins with an average log ratio > 2 are upregulated in one condition and < 0.5 are downregulated.
20. This will give a list of all statistically significant proteins (both upregulated and downregulated) in their respective functional category that can be used for hypothesis building.

Biofilm protein density measurement

Materials:
Glass coverslip
0.1 N NaOH
Thermoscientific BCA protein measurement
(http://www.piercenet.com/browse.cfm?fldID=02020101)

Procedure:

1. Suspend glass coverslips in the bioreactor. Make sure that there is enough distance between the stirbar and the lower end of the coverslip (~6-8 cm).
2. Once experiment is over, remove coverslip gently using sterile forceps in biosafety cabinet and place it in a known volume of 0.1 N NaOH. The coverslip should be completely immersed in the solution.
3. Place the beaker containing the glass coverslip and solution at 96 C for 40 minutes.
4. Measure protein concentration using the BCA assay in triplicate. Make sure that the standards for generating a standard curve also contain 0.1 N NaOH.
5. Calculate total mass of protein by multiplying the protein concentration with the volume of NaOH in step 2.
6. Divide the mass from step 5 by the total area of the coverslip to obtain the protein density. Make sure to include both sides in the calculations.

Biofilm gram staining

Materials:
Glass coverslip
Gram staining reagents

Procedure:
1. Suspend glass coverslips in the bioreactor. Make sure that there is enough distance between the stir bar and the lower end of the coverslip (~6-8 cm).
2. Once experiment is over, remove coverslip gently using sterile forceps in biosafety cabinet and wash in sterile phosphate buffered saline (PBS; see recipe above).
3. Immerse the coverslip in crystal violet for 1 minute.
4. Wash with PBS.
5. Gently remove and place it in Gram's Iodine for 30 seconds.
6. Wash twice with PBS.
7. Wash with decolorizer (ethanol) for 5 seconds.
8. Wash with water.
9. Counter stain with safranin for 1 minute.
10. Wash with water till stain stops bleeding from coverslip.
11. Let slide dry in dessicator overnight before imaging.

Calculating coulombs

1. For metabolites calculate the total number of moles as
$$Conc.(mM) \times 1e-3 \times Volume\ (liters)$$
   a. Calculate the total number of electrons in the compound (for most compounds the values per carbon can be found in Table 3 of Heijnen et al. (1999)).
   b. Calculate the coulombs as

$$Total\ number\ of\ moles\ \times Total\ number\ of\ electrons\ \times 96485\ \ (Faraday's\ constant)$$

2. For biomass determine the dry cell weight per liter (see procedure above).
   a. Convert weight per liter to moles per liter by assuming a molecular weight of 24.6 (from the formula $CH_{1.8}O_{0.8}N_{0.2}$; Heijnen et al. (1999)).
   b. Calculate the total number of moles as
$$Conc.(M) \times 1e-3 \times Volume\ (liters)$$
   c. Calculate the coulombs as
$$Total\ number\ of\ moles\ \times Total\ number\ of\ electrons$$
$$(=4.8) \times 96485\ \ (Faraday's\ constant)$$

Autoplating

Materials:
One syringe for each reactor
5 LB agar (1.5%) plates for each reactor – Allow to dry for 1 hour prior to plating
1.5 mL centrifuge tubes (2 per reactor)

Procedure:
1. Flame luer lock of needle in the reactor. Do not use ethanol.
2. Withdraw 3 mL using syringe from each reactor.
3. Dispense 1.5 mL into a sterile centrifuge tube.
4. From step 4, all actions must be performed in the biosafety cabinet.
5. Take nine empty 1.5 mL sterile centrifuge tubes.
6. Add 900 µL of sterile phosphate buffered saline (PBS; see recipe above) into each tube from step 5.
7. Place these tubes in one row of tube rack.
8. Take twelve 500 µL sterile tubes and place them in the next row of the tube rack.
9. Make a serial dilution by dispensing 100 µL of cell culture from reactor (from step 3) into the first tube with 900 µL PBS, vortexing it for 15 seconds, taking 100 µL from this tube and adding it to the next one and so on till the last tube.
10. Switch autoplater and vacuum on (let a vacuum corresponding to 15/20 in Hg be created).
11. Pour sterile water in container marked water on left side of the autoplater.
12. Pour 70 % ethanol in container marked disinfectant on left side of the autoplater.
13. Press CLEAN button.
14. Use dilutions number 5,6,7,8, and 9 for plating.
15. Since the autoplater only holds 500 µL tubes, pipette 500 µL from each dilution into a 500 µL sterile centrifuge tube (step 7).
16. Label each plate with reactor no., day no. and dilution.
17. Press MIN and [-] on the autoplater.
18. Place appropriate 500 µL tube and plate on the holder and plate holder respectively. The 500 µL tube has to be well settled into the slot (top left hole on the transparent perspex holder on right side of the autoplater).
19. Make sure that tube and plate are nicely situated in their respective compartments.
20. Press FILL and wait for the syringe on right side of the autoplater to fill with liquid.
21. Press PLATE.
22. Once plating is complete, replace plate and tube with the next in line dilution.
23. Press CLEAN before plating.
24. Keep repeating steps 12-22 for all dilutions.
25. Press CLEAN after the last plate two times.
26. Incubate plates at 32-33 C.
27. Count colonies from appropriate plate the following day (depending upon the plate, it might be necessary to count plates from two or three different dilutions and take the average value).

Note that the autoplater offers several different options for plating. For every microorganism, a serial dilution of the pure culture must be plated with all the different options prior to choosing an appropriate method.

Calculate colony forming units/ mL as $Number\ of\ colonies \times Volume\ used\ for\ plating \times 10^{number\ of\ dilution}$

Sampling for metabolite and phenazine analysis

Materials:
2 mL centrifuge tubes (two for each reactor)
3 mL syringe (one for each reactor)

Procedure:
1. Flame luer lock of needle in the reactor. Do not use ethanol.
2. Withdraw 3 mL using syringe from each reactor.
3. Dispense 1.5 mL into two sterile centrifuge tubes.
4. Centrifuge tube at 10,000 RPM for 10 minutes.
5. Remove supernatant gently from one centrifuge tube without disturbing pellet and dispense 1 mL into a HPLC vial. Store at 4 C.
6. Remove supernatant gently from the other centrifuge tube without disturbing pellet and dispense 1.5 mL into a LC/MS vial. Store at -20 C.

HPLC analysis

Running samples:
All components of the HPLC are controlled through the System Controller- adjustment to the detector and autosampler are not necessary

1. Open up PeakSimple on the computer and turn to channel 4
2. Load samples to be used into 96 well carousel.
3. Using the Direct control setting, slowly ramp the pump speed to 0.6 mL/min and ensure that the system pressure is stable (about 600 PSI)
4. If system pressure is erratic, open the reference valve on the front of the pump and sparge the pumps with eluent at a rate of 5 mL/min for 10 minutes.
5. The reference valve bypasses the column and waste is drained from black hose in front of pump.
6. If system pressure is high, ensure that the column oven is 60 °C
7. Using the System Controller, pull up the Program Method
8. Each method line must be manually input
9. If you want a wash step between each sample, you must specify the wash vial and insert a line command for this vial in between each of your samples.
10. Sample run time for each step must be less than or equal to corresponding sample measurement time on PeakSimple Details tab.
11. After method matrix has been programmed, push the Save function key
12. Previous tables can be cleared by pressing the More function key then Clear Table function key
13. Press the Program Table function key and set flow and gradient to your desired parameters for the method.
14. Press the Operate Method function button and ensure that "new" flow condition and gradient conditions match with your program.
15. Press the Operate Method function button again and the summary of conditions screen will appear and the Controller will take control of the autosampler and detector and prepare for the method.
16. After initializing, the Controller will replace the Abort button with a Start Run button on a function key. Press Start Run and the method will begin.
17. The controller will automatically start PeakSimple recording for each sample and autozero the detector.
18. Peak Simple can be programmed to save files in a consecutive order if an original file name and directory are designated in the Postrun Tab in PeakSimple

Start-Up:
1. Turn on Detector and Autosampler and allow them to initialize before turning on the System Controller.
2. After Controller run the startup configuration, press OK
3. Under Direct Control on the System Controller set the sparge rate to 100 mL/min and degas reservoirs to be used for 30 minutes

4. After degassing, turn He flow rate to 15 ml/min and flow pump eluent through the system for 15 minutes at a rate of 0.2 mL/min to equilibrate the system and remove methanol from the lines.
5. Purge the reference cell in the detector by pressing the 2nd function key and then purge.
6. Purge the Autosampler by pressing Purge Page and then Start Purge

Shutting Down:

1. To prevent microbial growth, do not leave water or buffer in the fluidic lines while the system is not in use
2. Flush the lines with HPLC grade water, followed by an aqueous 10% methanol solution
3. Turn of the controller, detector and autosampler.

Data Analysis:

1. Open ."Instrument 1 (offline)." on the computer
2. Go to ."File." and ."Load Signal.", and load your first standard vial
3. Go to"Calibration." and click ."Add Peaks." and put in the calibration level
4. (concentration) when prompted.
5. Remove (delete) unwanted peaks from the calibration table.
6. Use manual integration to ensure the baseline is proper for each peak.
7. Put in the names of the peaks
8. Load a new standard vial and under ."Calibration." click on "Add Level.". The
9. program should automatically recognize the proper peaks.
10. Once you have filled your calibration table, you can load your data signals, one at a time.
11. Click on the magnifying glass at the top right, which should bring up the report for your vial, with concentrations of the analytes.

Miller Units Assay

Materials:

E. coli strain pkDT17
LB broth
Arabinose
Ortho-nitrophenyl-β-galactoside (ONPG)
Z-buffer containing (g/L): 16 g $Na_2HPO_4.7H_2O$; 5.6 g $NaH_2PO_4.H_2O$; 0.7 g KCl; 2 mL of $MgSO_4$ (0.5 M)
β-mercaptoethanol
1M Na_2CO_3
0.1 M Phosphate buffer (0.06 M Na_2HPO_4 and 0.04 M NaH_2PO_4) pH = 7.0
Sodium dodecyl sulfate (0.1 %)

Procedure:

1. Grow *E. coli* strain pkDT17 in LB overnight.
2. Dilute overnight culture to OD_{600} 0.1 in LB with arabinose (Final concentration of arabinose: 1 mM; Arabinose is the inducer)
3. Add supernatant from a *P. aeruginosa* culture (the analyte in which the homoserine lactone concentration is going to be measured).
4. Leave culture from step 2 for 5 hours in incubator at 37 C
5. Add 2.7 µL of β-mercaptoethanol per mL of Z-buffer
6. Dissolve ONPG in 0.1 M phosphate buffer to a final concentration of 4 mg/mL
7. Incubate cell culture on ice for 20 minutes, chill Z-buffer also.
8. Pellet 2 mL of cell culture at 4 C by centrifuging at 10000 RPM for 10 minutes
9. Remove supernatant
10. Resuspend pellet in 2 mL of chilled Z-buffer
11. Measure OD_{600} by blanking against Z-buffer
12. Dilute the cells down to OD_{600} in the range 0.1 to 0.3.
13. Permeabilize 50 µL of diluted cells with 100 µL chloroform and 50 µL 0.1 % SDS
14. Vortex
15. Leave at room temperature for 5 minutes
16. Add 200 µL ONPG in phosphate buffer (step 6) to each sample.
17. Mix well and incubate at room temperature.
18. Record starting time.
19. Stop the reaction by adding 500 µL of 1M Na_2CO_3
20. Spin cells for 5 minutes to remove debris and chloroform
21. Record absorbance at 420 nm and 550 nm.
22. Calculate Miller Units as:

$$Miller\ Units = 1000 \times \left[\frac{OD_{420} - (1.75 \times OD_{550})}{time(minutes) \times volume\ of\ supernatant\ added\ (mL) \times OD_{600}}\right]$$

Cyclic voltammetry and chronoamperometry

1. Click “new experiment” in EC-Lab
2. Click on “Experimental techniques”-“Voltamperometric techniques”
3. Choose Cyclic voltammetry
4. Once window opens, input values as follows:
   tR (h:m:s) 0:00:0.0000
   dER/dt (mV/h) 0.0
   dER (mV) 0.00
   dtR (s) 0.1000
   Ei (V) -0.500
   vs. Ref
   dE/dt (mV/s) 2.000
   E1 (V) 0.500
   vs. Ref
   Step percent 50
   N 5
   I Range Auto
   Bandwidth 5
   E2 (V) -0.500
   vs. Ref
   nc cycles 1
   Reverse Scan 0
   Ef (V) 0.000
   vs. Eoc
5. Click on “Edit –Insert new technique-Experimental techniques-Voltamperometric techniques – Chronoamperometry/Chronocoulometry”.
6. Once window opens, input values as follows:
   tR (h:m:s) 0:00:0.0000
   dER/dt (mV/h) 0.0
   dER (mV) 0.00
   dtR (s) 1.0000
   Ei (V) 0.300
   vs. Ref
   ti (h:m:s) 23:00:10.0000
   Imax pass
   unit Imax mA
   Imin pass
   unit Imin mA
   dQM 0.000
   unit dQM mA.h
   record <I>
   dI 5.000
   unit dI uA
   dQ 0.000
   unit dQ mA.h

dt (s) 0.1000
dta (s) 20.00
I Range Auto
Bandwidth 5
goto Ns' 0
nc cycles 0

7. Click on “Edit –Insert new technique-Experimental techniques-Technique builder-loop”.
8. Once window opens, input values as follows:
   goto Ne 1
   nt times 42
9. This set of steps will result in cyclic voltammetry being performed every day for one hour during the course of the experiment with chronoamperometry for the remaining 23 hours. This will be repeated for 42 days. The experiment can be terminated at any time by clicking on the stop button in EC-Lab.
10. Load the CV file from Load data file in EC-Lab. This contains all the CVs that were obtained during the course of the experiment.
11. Then extract each cycle from the file using Tools-extract cycles.
12. Each CV can be analyzed for peaks using the Analysis-general math-min/max or peak analysis function in EC-Lab.
13. For CVs with indistinguishable peaks, export the file (Experiment-export as text in EC-Lab) as a .txt file, copy and paste the values into SigmaPlot, and use the derivative function in SigmaPlot by clicking on Toolbox-compute 1^{st} derivative. Maximas and minimas will have a derivative value of 0. The data can also be smoothed using a fourier transform via Transform-smooth 2D data for easier analysis.
14. The mid-peak potential for each redox couple is the average of the minimum potential (on the reduction wave) and the maximum potential (on the oxidation wave).

LC/MS analysis parameters

Depending upon the instrument, the protocol will vary, however, all the parameters for a successful replication of the method are listed below.

LC/MS system: ThermoFisher

Accela HPLC

Quantum Access triple quadrupole MS:

HPLC column: C18 phase, Gemini-NX, 3µm, 150x2.00mm (Phenomenex, Torrance, CA)

HPLC solvents: A: 0.1% formic acid in acetonitrile

B: 0.1% formic acid in water

solvents are LC/MS grade (Fisher Scientific)

flow rate 300µL min^{-1}

HPLC gradient:

time [min]	%A	%B
0	10	90
4	10	90
15	30	70
17	80	20
20	80	20

MS ion source: positive Electrospray Ionization (ESI)

tune parameters: spray voltage: 4kV

capillary temp.: 390°C

SRM conditions:

compound	parent ion $[M+H]^+$	product ion
1-OH-PHZ	197	168
Pyo	211	168
PCN	224	179
PCA	225	179

collision-induced dissociation (CID) energy: 35V

collision gas (argon) pressure: 1.5 mTorr

12 References

Angell, S., Bench, B.J., Williams, H., and Watanabe, C.M.H. (2006). Pyocyanin isolated from a marine microbial population: Synergistic production between two distinct bacterial species and mode of action. Chem. Biol. *13*, 1349-1359.

Aulenta, F., Canosa, A., Majone, M., Panero, S., Reale, P., and Rossetti, S. (2008). Trichloroethene dechlorination and H_2 evolution are alternative biological pathways of electric charge utilization by a dechlorinating culture in a bioelectrochemical system. Environ. Sci. Technol. *42*, 6185-6190.

Back, J.H., Kim, M.S., Cho, H., Chang, I.S., Lee, J.Y., Kim, K.S., Kim, B.H., Park, Y.I., and Han, Y.S. (2004). Construction of bacterial artificial chromosome library from electrochemical microorganisms. FEMS Microbiol. Lett. *238*, 65-70.

Batstone, D., Keller, J., Angelidaki, L., Kalyuzhnyi, S.V., Pavlostathis, S.G., Rozzi, A., Sanders, W.T.M., Sidgrist, H., and Vavilin, V., A, (2002). Anaerobic digestion model No. 1 (ADM1), IWA Task Group for Mathematical Modeling of Anaerobic Digestion Processes (London: IWA Publishing).

Bensel, T., Stotz, M., Borneff-Lipp, M., Wollschläger, B., Wienke, A., Taccetti, G., Campana, S., Meyer, K.C., Jensen, P.Ø., Lechner, U*., et al.* (2010). Lactate in cystic fibrosis sputum. J. Cyst. Fibros. *10*, 37-44.

Biffinger, J.C., Byrd, J.N., Dudley, B.L., and Ringeisen, B.R. (2008). Oxygen exposure promotes fuel diversity for *Shewanella oneidensis* microbial fuel cells. Biosens. Bioelectron. *23*, 820-826.

Bond, D.R., and Lovley, D.R. (2003). Electricity production by *Geobacter sulfurreducens* attached to electrodes. Appl. Environ. Microbiol. *69*, 1548-1555.

Bond, D.R., and Lovley, D.R. (2005). Evidence for Involvement of an Electron Shuttle in Electricity Generation by *Geothrix fermentans*. Appl. Environ. Microbiol. *71*, 2186-2189.

Bretschger, O., Gorby, Y.A., and Nealson, K.H. (2010). A survey of direct electron transfer from microbes to electronically active surfaces. In Bioelectrochemical Systems: from extracellular electron transfer to biotechnological application, L.T. Angenent, K. Rabaey, U. Schröder, and J. Keller, eds. (London, U.K.: International Water Association), pp. 81-95.

Burns, J.L., Emerson, J., Stapp, J.R., Yim, D.L., Krzewinski, J., Louden, L., Ramsey, B.W., and Clausen, C.R. (1998). Microbiology of sputum from patients at cystic fibrosis centers in the United States. Clin. Infect. Dis. *27*, 158-163.

Byun, T., Zeng, A., and Deckwer, W. (1994). Reactor comparison and scale-up for the microaerobic production of 2,3-butanediol by *Enterobacter aerogenes* at constant oxygen transfer rate. Bioprocess. Biosyst. Eng. *11*, 167-175.

Cao, X., Huang, X., Liang, P., Xiao, K., Zhou, Y., Zhang, X., and Logan, B.E. (2009a). A new method for water desalination using microbial desalination cells. Environ. Sci. Technol. *43*, 7148-7152.

Cao, X.X., Huang, X., Liang, P., Boon, N., Fan, M.Z., Zhang, L., and Zhang, X.Y. (2009b). A completely anoxic microbial fuel cell using a photo-biocathode for cathodic carbon dioxide reduction. Energy Environ. Sci. *2*, 498-501.

Caporaso, J.G., Bittinger, K., Bushman, F.D., DeSantis, T.Z., Andersen, G.L., and Knight, R. (2010). PyNAST: a flexible tool for aligning sequences to a template alignment. Bioinformatics *26*, 266-267.

Chang, I.S., Moon, H., Jang, J.K., and Kim, B.H. (2005). Improvement of a microbial fuel cell performance as a BOD sensor using respiratory inhibitors. Biosens. Bioelectron. *20*, 1856-1859.

Cheng, S.A., Xing, D.F., Call, D.F., and Logan, B.E. (2009). Direct biological conversion of electrical current into methane by electromethanogenesis. Environ. Sci. Technol. *43*, 3953-3958.

Clark, D.J., and Maaløe, O. (1967). DNA replication and divison cycle in *Escherichia coli*. J. Mol. Biol. *23*, 99-103.

Clauwaert, P., Rabaey, K., Aelterman, P., De Schamphelaire, L., Ham, T.H., Boeckx, P., Boon, N., and Verstraete, W. (2007). Biological denitrification in microbial fuel cells. Environ. Sci. Technol. *41*, 3354-3360.

Clauwaert, P., and Verstraete, W. (2009). Methanogenesis in membraneless microbial electrolysis cells. Appl. Microbiol. Biotechnol. *82*, 829-836.

Converti, A., Perego, P., and Del Borghi, M. (2003). Effect of specific oxygen uptake rate on *Enterobacter aerogenes* energetics: Carbon and reduction degree balances in batch cultivations. Biotechnol. Bioeng. *82*, 370-377.

De Schamphelaire, L., Cabezas, A., Marzorati, M., Friedrich, M.W., Boon, N., and Verstraete, W. (2010). Microbial community analysis of anodes from sediment microbial fuel cells powered by rhizodeposits of living rice plants. Appl. Environ. Microbiol. *76*, 2002-2008.

DeSantis, T.Z., Hugenholtz, P., Larsen, N., Rojas, M., Brodie, E.L., Keller, K., Huber, T., Dalevi, D., Hu, P., and Andersen, G.L. (2006). Greengenes, a chimera-checked 16S rRNA gene database and workbench compatible with ARB. Appl. Environ. Microbiol. *72*, 5069-5072.

Dethlefsen, L., McFall-Ngai, M., and Relman, D.A. (2007). An ecological and evolutionary perspective on human-microbe mutualism and disease. Nature *449*, 811-818.

Dietrich, L.E.P., Price-Whelan, A., Petersen, A., Whiteley, M., and Newman, D.K. (2006). The phenazine pyocyanin is a terminal signalling factor in the quorum sensing network of *Pseudomonas aeruginosa*. Mol. Microbiol. *61*, 1308-1321.

Diggle, S.P., Winzer, K., Lazdunski, A., Williams, P., and Camara, M. (2002). Advancing the quorum in *Pseudomonas aeruginosa*: MvaT and the regulation of n-acylhomoserine lactone production and virulence gene expression. J. Bacteriol. *184*, 2576-2586.

Emde, K.M., Smith, D.W., and Facey, R. (1992). Initial Investigation of Microbially Influenced Corrosion (MIC) in a Low Temperature Water Distribution System. Water Res. *26*, 169-175.

FitzSimmons, S.C. (1993). The changing epidemiology of cystic fibrosis. J. Pediatrics *122*, 1-9.

Fornero, J.J., Rosenbaum, M., Cotta, M.A., and Angenent, L.T. (2008). Microbial fuel cell performance with a pressurized cathode chamber. Environ. Sci. Technol. *42*, 8578-8584.

Fornero, J.J., Rosenbaum, M., Cotta, M.A., and Angenent, L.T. (2010). Carbon Dioxide Addition to Microbial Fuel Cell Cathodes Maintains Sustainable Catholyte pH and Improves Anolyte pH, Alkalinity, and Conductivity. Environmental Science & Technology *44*, 2728-2734.

Frank, D. (2008). XplorSeq: A software environment for integrated management and phylogenetic analysis of metagenomic sequence data. BMC Bioinformatics *9*, 420.

Freguia, S., Rabaey, K., Yuan, Z.G., and Keller, J. (2008). Syntrophic processes drive the conversion of glucose in microbial fuel cell anodes. Environ. Sci. Technol. *42*, 7937-7943.

Fuqua, W.C., Winans, S.C., and Greenberg, E.P. (1994). Quorum sensing in bacteria - The LuxR-LuxI family of cell density-responsive transcriptional regulators. J. Bacteriol. *176*, 269-275.

Gabriel, S.E., Brigman, K.N., Koller, B.H., Boucher, R.C., and Stutts, M.J. (1994). Cystic fibrosis heterozygote resistance to cholera toxin in the cystic fibrosis mouse model. Science *266*, 107-109.

Girguis, P.R., Nielsen, M.E., and Reimers, C.E. (2010). Fundamentals of benthic microbial fuel cells: theory, development and application. In Bioelectrochemical Systems: from extracellular electron transfer to biotechnological application, L.T. Angenent, K. Rabaey, U. Schröder, and J. Keller, eds. (London, U.K.: International Water Association), pp. 327-346.

Gooderham, W.J., and Hancock, R.E.W. (2009). Regulation of virulence and antibiotic resistance by two-component regulatory systems in *Pseudomonas aeruginosa*. FEMS Microbiol. Rev. *33*, 279-294.

Goodman, A.L., Merighi, M., Hyodo, M., Ventre, I., Filloux, A., and Lory, S. (2009). Direct interaction between sensor kinase proteins mediates acute and chronic disease phenotypes in a bacterial pathogen. Genes Dev. *23*, 249-259.

Graham-Rowe, D. (2009). Could a 'lung-on-a-chip' replace countless lab rats? New Scientist *202*, 20-20.

Gregory, K.B., and Lovley, D.R. (2005). Remediation and recovery of uranium from contaminated subsurface environments with electrodes. Environ. Sci. Technol. *39*, 8943-8947.

Guss, A.M., Roeselers, G., Newton, I.L.G., Young, C.R., Klepac-Ceraj, V., Lory, S., and Cavanaugh, C.M. (2011). Phylogenetic and metabolic diversity of bacteria associated with cystic fibrosis. ISME J. *5*, 20-29

Hassan, H.M., and Fridovich, I. (1980). Mechanism of the Antibiotic Action of Pyocyanine. J. Bacteriol. *141*, 156-163.

Hassett, D.J., Charniga, L., Bean, K., Ohman, D.E., and Cohen, M.S. (1992). Response of *Pseudomonas aeruginosa* to pyocyanin - mechanisms of resistance, antioxidant defenses, and demonstration of a manganese-cofactored superoxide-dismutase. Infect. Immun. *60*, 328-336.

Hassett, D.J., Ma, J.F., Elkins, J.G., McDermott, T.R., Ochsner, U.A., West, S.E.H., Huang, C.T., Fredericks, J., Burnett, S., Stewart, P.S*., et al.* (1999). Quorum sensing in *Pseudomonas aeruginosa* controls expression of catalase and superoxide dismutase genes and mediates biofilm susceptibility to hydrogen peroxide. Mol. Microbiol. *34*, 1082-1093.

He, Z., Wagner, N., Minteer, S.D., and Angenent, L.T. (2006). An upflow microbial fuel cell with an interior cathode: Assessment of the internal resistance by impedance Spectroscopy. Environ. Sci. Technol. *40*, 5212-5217.

Heijnen, J.J. (1999). Bioenergetics of microbial growth. In Encylopedia of Bioprocess Technology: Fermentation, Biocatalysis, and Bioseparation., M.C. Flickinger, and S.W. Drew, eds. (New York: Wiley-Interscience), pp. 267-291.

Hoffman, L.R., Richardson, A.R., Houston, L.S., Kulasekara, H.D., Martens-Habbena, W., Klausen, M., Burns, J.L., Stahl, D.A., Hassett, D.J., Fang, F.C., and Miller, S.I. (2010). Nutrient availability as a mechanism for selection of antibiotic tolerant *Pseudomonas aeruginosa* within the CF airway. PLoS. Pathog. *6*, e1000712.

Hsieh, S.C., Lu, C.C., Horng, Y.T., Soo, P.C., Chang, Y.L., Tsai, Y.H., Lin, C.S., and Lai, H.C. (2007). The bacterial metabolite 2,3-butanediol ameliorates endotoxin-induced acute lung injury in rats. Microb. Infect. *9*, 1402-1409.

Huh, D., Matthews, B.D., Mammoto, A., Montoya-Zavala, M., Hsin, H.Y., and Ingber, D.E. (2010). Reconstituting Organ-Level Lung Functions on a Chip. Science *328*, 1662-1668.

Ishii, S., Hotta, Y., and Watanabe, K. (2008a). Methanogenesis versus electrogenesis: Morphological and phylogenetic comparisons of microbial communities. Biosci. Biotechnol. Biochem. *72*, 286-294.

Ishii, S., Shimoyama, T., Hotta, Y., and Watanabe, K. (2008b). Characterization of a filamentous biofilm community established in a cellulose-fed microbial fuel cell. BMC Microbiol. *8*.

Jeong, C.M., Choi, J.D.R., Ahn, Y.H., and Chang, H.N. (2008). Removal of volatile fatty acids (VFA) by microbial fuel cell with aluminum electrode and microbial community identification with 16S rRNA sequence. Korean J. Chem. Eng. *25*, 535-541.

Ji, X.-J., Huang, H., and Ouyang, P.-K. (2011). Microbial 2,3-butanediol production: a state-of-the-art review. Biotechnol. Adv. *29*, 351-364.

Johansen, L., Bryn, K., and Stormer, F.C. (1975). Physiological and biochemical role of butanediol pathway in *Aerobacter* (*Enterobacter*) aerogenes. J. Bacteriol. *123*, 1124-1130.

Jong, B.C., Kim, B.H., Chang, I.S., Liew, P.W.Y., Choo, Y.F., and Kang, G.S. (2006). Enrichment, performance, and microbial diversity of a thermophilic mediatorless microbial fuel cell. Environ. Sci. Technol. *40*, 6449-6454.

Katayama, S., Kubo, Y., and Yamada, N. (2002). Characterization and mechanical properties of flexible dimethylsiloxane-based inorganic/organic hybrid sheets. J. Am. Ceram. Soc. *85*, 1157-1163.

Kessler, E., Safrin, M., Gustin, J.K., and Ohman, D.E. (1998). Elastase and the LasA protease of *Pseudomonas aeruginosa* are secreted with their propeptides. J. Biol. Chem. *273*, 30225-30231.

Kim, E.J., Sabra, W., and Zeng, A.P. (2003). Iron deficiency leads to inhibition of oxygen transfer and enhanced formation of virulence factors in cultures of *Pseudomonas aeruginosa* PAO1. Microbiol.-SGM *149*, 2627-2634.

Kim, E.J., Wang, W., Deckwer, W.D., and Zeng, A.P. (2005). Expression of the quorum-sensing regulatory protein LasR is strongly affected by iron and oxygen concentrations in cultures of *Pseudomonas aeruginosa* irrespective of cell density. Microbiol.-SGM *151*, 1127-1138.

Kim, G.T., Webster, G., Wimpenny, J.W.T., Kim, B.H., Kim, H.J., and Weightman, A.J. (2006). Bacterial community structure, compartmentalization and activity in a microbial fuel cell. J. Appl. Microbiol. *101*, 698-710.

Kim, Y.-C. (1996). Diffusivity of bacteria. Korean J. Chem. Eng. *13*, 282-287.

Kim, Y., and Logan, B.E. (2011). Hydrogen production from inexhaustible supplies of fresh and salt water using microbial reverse-electrodialysis electrolysis cells. Proc. Natl. Acad. Sci. USA, doi: 10.1073/pnas.1106335108

Kuhn, J., Castillo-Sanchez, J.M., Gascon, J., Calero, S., Dubbeldam, D., Vlugt, T.J.H., Kapteijn, F., and Gross, J. (2009). Adsorption and Diffusion of Water, Methanol, and Ethanol in All-Silica DD3R: Experiments and Simulation. J. Phys. Chem C *113*, 14290-14301.

Lee, J.Y., Phung, N.T., Chang, I.S., Kim, B.H., and Sung, H.C. (2003). Use of acetate for enrichment of electrochemically active microorganisms and their 16S rDNA analyses. FEMS Microbiol. Lett. *223*, 185-191.

Ley, R.E., Turnbaugh, P.J., Klein, S., and Gordon, J.I. (2006). Microbial ecology: human gut microbes associated with obesity. Nature *444*, 1022-1023.

Li, J., Liu, G., Zhang, R., Luo, Y., Zhang, C., and Li, M. (2010). Electricity generation by two types of microbial fuel cells using nitrobenzene as the anodic or cathodic reactants. Bioresour. Technol. *101*, 4013-4020.

Li, Z., Rosenbaum, M.A., Venkataraman, A., Tam, T.K., Katz, E., and Angenent, L.T. (2011). Bacteria-based AND logic gate: a decision-making and self-powered biosensor. Chem. Commun. *47*, 3060-3062.

Liang, P., Wu, W., Wei, J., Yuan, L., Xia, X., and Huang, X. (2011). Alternate charging and discharging of capacitor to enhance the electron production of bioelectrochemical systems. Environ. Sci. Technol. *45*, 6647-6653.

Liberati, N.T., Urbach, J.M., Miyata, S., Lee, D.G., Drenkard, E., Wu, G., Villanueva, J., Wei, T., and Ausubel, F.M. (2006). An ordered, nonredundant library of *Pseudomonas aeruginosa* strain PA14 transposon insertion mutants. Proc. Natl. Acad. Sci. USA *103*, 19931-19931.

Logan, B.E., Call, D., Cheng, S., Hamelers, H.V.M., Sleutels, T.H.J.A., Jeremiasse, A.W., and Rozendal, R.A. (2008). Microbial electrolysis cells for high yield hydrogen gas production from organic matter. Environ. Sci. Technol. *42*, 8630-8640.

Lopes, S., Machado, I., and Pereira, M. (2010). Role of planktonic and sessile extracellular metabolic byproducts of *Pseudomonas aeruginosa* on *Escherichia coli*. J. Ind. Microbiol. Biotechnol., 1-8.

Lovley, D.R. (2006). Bug juice: harvesting electricity with microorganisms. Nat. Rev. Micro. *4*, 497-508.

Madigan, T.M., Martinko, M.J., and Parker, J. (2002). Brock Biology of Microorganisms, 10 edn (New Jersey: Pearson Education Inc.).

Malvankar, N.S., Vargas, M., Nevin, K.P., Franks, A.E., Leang, C., Kim, B.-C., Inoue, K., Mester, T., Covalla, S.F., Johnson, J.P.*, et al.* (2011). Tunable metallic-like conductivity in microbial nanowire networks. Nat. Nano. *advance online publication*.

Marcus, A.K., Torres, C.I., and Rittmann, B.E. (2007). Conduction-based modeling of the biofilm anode of a microbial fuel cell. Biotechnol. Bioeng. *98*, 1171-1182.

Marshall, C.W., and May, H.D. (2009). Electrochemical evidence of direct electrode reduction by a thermophilic Gram-positive bacterium, *Thermincola ferriacetica*. Energy Environ. Sci. *2*, 699-705.

Marsili, E., Baron, D.B., Shikhare, I.D., Coursolle, D., Gralnick, J.A., and Bond, D.R. (2008a). *Shewanella* secretes flavins that mediate extracellular electron transfer. Proc. Natl. Acad. Sci. USA *105*, 3968-3973.

Marsili, E., Rollefson, J.B., Baron, D.B., Hozalski, R.M., and Bond, D.R. (2008b). Microbial Biofilm Voltammetry: Direct Electrochemical Characterization of Catalytic Electrode-Attached Biofilms. Applied and Environmental Microbiology *74*, 7329-7337.

Mashburn, L.M., Jett, A.M., Akins, D.R., and Whiteley, M. (2005). *Staphylococcus aureus* serves as an iron source for *Pseudomonas aeruginosa* during *in vivo* coculture. J. Bacteriol. *187*, 554-566.

Nakashimada, Y., Rachman, M.A., Kakizono, T., and Nishio, N. (2002). Hydrogen production of *Enterobacter aerogenes* altered by extracellular and intracellular redox states. Int. J. Hydrogen Energy *27*, 1399-1405.

Nevin, K.P., Hensley, S.A., Franks, A.E., Summers, Z.M., Ou, J., Woodard, T.L., Snoeyenbos-West, O.L., and Lovley, D.R. (2011). Electrosynthesis of organic compounds from carbon dioxide is catalyzed by a diversity of acetogenic microorganisms. Appl. Environ. Microbiol. *77*, 2882-2886.

Nevin, K.P., and Lovley, D.R. (2002). Mechanisms for Fe(III) oxide reduction in sedimentary environments. Geomicrobiol. J. *19*, 141-159.

Nguyet Thu, P., Lee, J., Kang, K., Chang, I., Gadd, G.M., and Kim, B. (2004). Analysis of microbial diversity in oligotrophic microbial fuel cells using 16S rDNA sequences. FEMS Microbiol. Lett. *233*, 77-82.

Nivens, D.E., Ohman, D.E., Williams, J., and Franklin, M.J. (2001). Role of alginate and its o-acetylation in formation of *Pseudomonas aeruginosa* microcolonies and biofilms. J. Bacteriol. *183*, 1047-1057.

O'Malley, Y.Q., Reszka, K.J., Spitz, D.R., Denning, G.M., and Britigan, B.E. (2004). *Pseudomonas aeruginosa* pyocyanin directly oxidizes glutathione and decreases its levels in airway epithelial cells. Am J Physiol Lung Cell Mol Physiol *287*, L94-103.

O'Neill, B., Grossman, J., Tsai, M., Gomes, J., Lehmann, J., Peterson, J., Neves, E., and Thies, J. (2009). Bacterial community composition in brazilian anthrosols and adjacent soils characterized using culturing and molecular identification. Microb. Ecol. *58*, 23-35.

Oliver, A., Cantan, R., Campo, P., Baquero, F., and Blajzquez, J. (2000). High frequency of hypermutable *Pseudomonas aeruginosa* in cystic fibrosis lung infection. Science *288*, 1251-1253.

Pal'chykovs'ka, L.H., Aleksieieva, I.V., Kostina, V.H., Platonov, M.O., Nehruts'ka, V.V., Deriabin, O.M., Tarasov, O.A., and Shved, A.D. (2008). New amides of phenazine-1-carboxylic acid: antimicrobial activity and structure-activity relationship. Ukr. Biokhim. Zh. *80*, 140-147.

Palmer, K.L., Aye, L.M., and Whiteley, M. (2007). Nutritional cues control *Pseudomonas aeruginosa* multicellular behavior in cystic fibrosis sputum. J. Bacteriol. *189*, 8079-8087.

Palmer, K.L., Mashburn, L.M., Singh, P.K., and Whiteley, M. (2005). Cystic fibrosis sputum supports growth and cues key aspects of *Pseudomonas aeruginosa* physiology. J. Bacteriol. *187*, 5267-5277.

Parameswaran, P., Zhang, H.S., Torres, C.I., Rittmann, B.E., and Krajmalnik-Brown, R. (2010). Microbial community structure in a biofilm anode fed with a fermentable substrate: the significance of hydrogen scavengers. Biotechnol. Bioeng. *105*, 69-78.

Patil, S.A., Surakasi, V.P., Koul, S., Ijmulwar, S., Vivek, A., Shouche, Y.S., and Kapadnis, B.P. (2009). Electricity generation using chocolate industry wastewater and its treatment in activated sludge based microbial fuel cell and analysis of developed microbial community in the anode chamber. Bioresour. Technol. *100*, 5132-5139.

Pearson, J.P., Gray, K.M., Passador, L., Tucker, K.D., Eberhard, A., Iglewski, B.H., and Greenberg, E.P. (1994). Structure of the autoinducer required for expression of *Pseudomonas aeruginosa* virulence genes. Proc. Natl. Acad. Sci. USA *91*, 197-201.

Perego, P., Converti, A., Del Borghi, A., and Canepa, P. (2000). 2,3-Butanediol production by *Enterobacter aerogenes*: selection of the optimal conditions and application to food industry residues. Bioprocess. Biosyst. Eng. *23*, 613-620.

Perkins, S.D., Woeltje, K.F., and Angenent, L.T. (2010). Endotracheal tube biofilm inoculation of oral flora and subsequent colonization of opportunistic pathogens. Int. J. Med. Microbiol. *300*, 503-511.

Pham, T.H., Boon, N., De Maeyer, K., Hofte, M., Rabaey, K., and Verstraete, W. (2008). Use of *Pseudomonas* species producing phenazine-based metabolites in the anodes of microbial fuel cells to improve electricity generation. Appl. Microbiol. Biotechnol. *80*, 985-993.

Phung, N.T., Lee, J., Kang, K.H., Chang, I.S., Gadd, G.M., and Kim, B.H. (2004). Analysis of microbial diversity in oligotrophic microbial fuel cells using 16S rDNA sequences. FEMS Microbiol. Lett. *233*, 77-82.

Picioreanu, C., Head, I.M., Katuri, K.P., van Loosdrecht, M.C.M., and Scott, K. (2007). A computational model for biofilm-based microbial fuel cells. Water Res. *41*, 2921-2940.

Picioreanu, C., Katuri, K.P., Head, I.M., van Loosdrecht, M.C.M., and Scott, K. (2008). Mathematical model for microbial fuel cells with anodic biofilms and anaerobic digestion. Water Sci. Technol. *57*, 965-971.

Picioreanu, C., Katuri, K.P., van Loosdrecht, M.C.M., Head, I.M., and Scott, K. (2010). Modelling microbial fuel cells with suspended cells and added electron transfer mediator. J. Appl. Electrochem. *40*, 151-162.

Potter, M.C. (1915). Electrical Effects Accompanying the Decomposition of Organic Compounds. II. Ionisation of the Gases Produced during Fermentation. Proceedings of the Royal Society of London. Series A, Containing Papers of a Mathematical and Physical Character *91*, 465-480.

Price, M.N., Dehal, P.S., and Arkin, A.P. (2010). FastTree 2-Approximately Maximum-Likelihood Trees for Large Alignments. Plos One *5*, e9490.

Rabaey, K., Boon, N., Hofte, M., and Verstraete, W. (2005). Microbial phenazine production enhances electron transfer in biofuel cells. Environ. Sci.Technol. *39*, 3401-3408.

Rabaey, K., Boon, N., Siciliano, S.D., Verhaege, M., and Verstraete, W. (2004a). Biofuel cells select for microbial consortia that self-mediate electron transfer. Appl. Environ. Microbiol. *70*, 5373-5382.

Rabaey, K., Boon, N., Siciliano, S.D., Verhaege, M., and Verstraete, W. (2004b). Biofuel cells select for microbial consortia that self-mediate electron transfer. Appl Environ Microbiol *70*, 5373 - 5382.

Rabaey, K., Boon, N., Siciliano, S.D., Verhaege, M., and Verstraete, W. (2004c). Biofuel cells select for microbial consortia that self-mediate electron transfer. Appl. Environ. Microbiol. *70*, 5373-5382.

Rabaey, K., Rodriguez, J., Blackall, L.L., Keller, J., Gross, P., Batstone, D., Verstraete, W., and Nealson, K.H. (2007). Microbial ecology meets electrochemistry: electricity-driven and driving communities. ISME J. *1*, 9-18.

Rabaey, K., and Rozendal, R.A. (2010). Microbial electrosynthesis - revisiting the electrical route for microbial production. Nature Reviews Microbiology *8*, 706-716.

Ramsey, M.M., Rumbaugh, K.P., and Whiteley, M. (2011). Metabolite cross-feeding enhances virulence in a model polymicrobial infection. PLoS. Pathog. *7*, e1002012.

Rashid, M.H., and Kornberg, A. (2000). Inorganic polyphosphate is needed for swimming, swarming, and twitching motilities of *Pseudomonas aeruginosa*. Proc. Natl. Acad. Sci. USA *97*, 4885-4890.

Ratcliff, W.C., and Denison, R.F. (2011). Alternative Actions for Antibiotics. Science *332*, 547-548.

Read, S.T., Dutta, P., Bond, P.L., Keller, J., and Rabaey, K. (2010). Initial development and structure of biofilms on microbial fuel cell anodes. BMC Microbiol. *10*.

Ren, Y.L., Wang, J.J., Liu, Z., Ren, Y.L., and Li, G.Z. (2009). Hydrogen production from the monomeric sugars hydrolyzed from hemicellulose by *Enterobacter aerogenes*. Renewable Energy *34*, 2774-2779.

Rezaei, F., Xing, D., Wagner, R., Regan, J.M., Richard, T.L., and Logan, B.E. (2009). Simultaneous Cellulose Degradation and Electricity Production by Enterobacter cloacae in a Microbial Fuel Cell. Appl. Environ. Microbiol. *75*, 3673-3678.

Richter, H., Lanthier, M., Nevin, K.P., and Lovley, D.R. (2007). Lack of electricity production by *Pelobacter carbinolicus* indicates that the capacity for Fe(III) oxide reduction does not necessarily confer electron transfer ability to fuel cell anodes. Appl. Environ. Microbiol. *73*, 5347-5353.

Ringeisen, B.R., Ray, R., and Little, B. (2007). A miniature microbial fuel cell operating with an aerobic anode chamber. J. Power Sources *165*, 591-597.

Rodriguez, J., and Premier, G.C. (2010). Towards a mathematical description of bioelectrochemical systems. In Bioelectrochemical Systems: from extracellular electron transfer to biotechnological application, L.T. Angenent, K. Rabaey, U. Schröder, and J. Keller, eds. (London, U.K.: International Water Association), pp. 423-448.

Rosenbaum, M., Cotta, A.M., and Angenent, L.T. (2009). Aerated *Shewanella oneidensis* in a continuously-fed bioelectrochemical system for power and hydrogen production. Biotechnol. Bioeng. *105*, 880-888.

Rosenbaum, M.A., Bar, H.Y., Beg, Q.K., Segrè, D., Booth, J., Cotta, M.A., and Angenent, L.T. (2010). *Shewanella oneidensis* in a lactate-fed pure-culture and a glucose-fed co-culture with *Lactococcus lactis* with an electrode as electron acceptor. Bioresour. Technol. *102*, 2623-2628.

Rozendal, R.A., Hamelers, H.V.M., Rabaey, K., Keller, J., and Buisman, C.J.N. (2008). Towards practical implementation of bioelectrochemical wastewater treatment. Trends in Biotechnology *26*, 450-459.

Rozendal, R.A., Leone, E., Keller, J., and Rabaey, K. (2009). Efficient hydrogen peroxide generation from organic matter in a bioelectrochemical system. Electrochem . Commun . *11*, 1752-1755.

Sabra, W., Kim, E.J., and Zeng, A.P. (2002). Physiological responses of *Pseudomonas aeruginosa* PAO1 to oxidative stress in controlled microaerobic and aerobic cultures. Microbiol.-SGM *148*, 3195-3202.

Schloss, P.D., and Handelsman, J. (2005). Introducing DOTUR, a Computer Program for Defining Operational Taxonomic Units and Estimating Species Richness. Appl. Environ. Microbiol. *71*, 1501-1506.

Schloss, P.D., Westcott, S.L., Ryabin, T., Hall, J.R., Hartmann, M., Hollister, E.B., Lesniewski, R.A., Oakley, B.B., Parks, D.H., Robinson, C.J.*, et al.* (2009). Introducing mothur: Open-Source, Platform-Independent, Community-Supported Software for Describing and Comparing Microbial Communities. Appl. Environ. Microbiol. *75*, 7537-7541.

Schröder, U. (2007). Anodic electron transfer mechanisms in microbial fuel cells and their energy efficiency. Phys. Chem. Chem. Phys. *9*, 2619-2629.

Schröder, U., and Harnisch, F. (2010). Electrochemical Losses. In Bioelectrochemical Systems: from extracellular electron transfer to biotechnological application, L.T. Angenent, K. Rabaey, U. Schroder, and J. Keller, eds. (London, U.K.: International Water Association), pp. 119-133.

Schuster, M., and Greenberg, E.P., eds. (2008). LuxR-type proteins in *Pseudomonas aeruginosa* quorum sensing: distinct mechanisms with global implications (Washington DC: ASM press).

Shimoyama, T., Yamazawa, A., Ueno, Y., and Watanabe, K. (2009). Phylogenetic Analyses of Bacterial Communities Developed in a Cassette-Electrode Microbial Fuel Cell. Microbes Environ. *24*, 188-192.

Singh, P.K., Parsek, M.R., Greenberg, E.P., and Welsh, M.J. (2002). A component of innate immunity prevents bacterial biofilm development. Nature *417*, 552-555.

Stewart, P.S., Camper, A.K., Handran, S.D., Huang, C.T., and Warnecke, M. (1997). Spatial distribution and coexistence of *Klebsiella pneumoniae* and *Pseudomonas aeruginosa* in biofilms. Microbial Ecol. *33*, 2-10.

Suh, S.J., Silo-Suh, L., Woods, D.E., Hassett, D.J., West, S.E.H., and Ohman, D.E. (1999). Effect of *rpoS* mutation on the stress response and expression of virulence factors in *Pseudomonas aeruginosa*. J. Bacteriol. *181*, 3890-3897.

Swan, D.G., and Felton, D.G.I. (1957). Phenazines (London: Interscience Publishers).

Tanisho, S., Kamiya, N., and Wakao, N. (1989). Microbial fuel cell using *Enterobacter aerogenes*. Bioelectrochem. Bioenerg. *21*, 25-32.

Thrash, J.C., and Coates, J.D. (2008). Review: Direct and indirect electrical stimulation of microbial metabolism. Environ. Sci. Technol. *42*, 3921-3931.

Vandecandelaere, I., Nercessian, O., Faimali, M., Segaert, E., Mollica, A., Achouak, W., De Vos, P., and Vandamme, P. (2008). Bacterial diversity of the cultivable fraction of a marine electroactive biofilm. Bioelectrochemistry *78*, 62-66.

Venkataraman, A., Rosenbaum, A.M., Perkins, S.D., Werner, J.J., and Angenent, L.T. (2011). Metabolite-based mutualism between *Pseudomonas aeruginosa* PA14 and *Enterobacter aerogenes* enhances current generation in bioelectrochemical systems. Energy Environ. Sci. *4*, 4550-4559.

Venkataraman, A., Rosenbaum, M., Arends, J.B.A., Halitschke, R., and Angenent, L.T. (2010). Quorum sensing regulates electric current generation of *Pseudomonas aeruginosa* PA14 in bioelectrochemical systems. Electrochemistry Communications *12*, 459-462.

Venturi, V. (2003). Control of *rpoS* transcription in *Escherichia coli* and *Pseudomonas*: why so different? Mol.Microbiol. *49*, 1-9.

Wagner, V.E., Bushnell, D., Passador, L., Brooks, A.I., and Iglewski, B.H. (2003). Microarray analysis of *Pseudomonas aeruginosa* quorum-sensing regulons: effects of growth phase and environment. J. Bacteriol. *185*, 2080-2095.

Wang, X., Feng, Y., Liu, J., Lee, H., Li, C., Li, N., and Ren, N. (2010a). Sequestration of CO2 discharged from anode by algal cathode in microbial carbon capture cells (MCCs). Biosens. Bioelectron. *25*, 2639-2643.

Wang, Y., Kern, S.E., and Newman, D.K. (2010b). Endogenous phenazine antibiotics promote anaerobic survival of *Pseudomonas aeruginosa* via extracellular electron transfer. J. Bacteriol. *192*, 365-369.

Wang, Y., and Newman, D.K. (2008). Redox reactions of phenazine antibiotics with ferric (hydr)oxides and molecular oxygen. Environ. Sci. Technol. *42*, 2380-2386.

Wang, Y.F., Masuda, M., Tsujimura, S., and Kano, K. (2008). Electrochemical regulation of the end-product profile in *Propionibacterium freudenreichii* ET-3 with an endogenous mediator. Biotechnol. Bioeng. *101*, 579-586.

Werner, J.J., Knights, D., Garcia, M.L., Scalfone, N.B., Smith, S., Yarasheski, K., Cummings, T.A., Beers, A.R., Knight, R., and Angenent, L.T. (2011). Bacterial community structures are unique and resilient in full-scale bioenergy systems. Proc. Natl. Acad. Sci. USA.

Werner, J.J., Ptak, A.C., Rahm, B.G., Zhang, S., and Richardson, R.E. (2009). Absolute quantification of *Dehalococcoides* proteins: enzyme bioindicators of chlorinated ethene dehalorespiration. Environ. Microbiol. *11*, 2687-2697.

Westfall, L.W., Luna, A.M., Francisco, M.S., Diggle, S.P., Worrall, K.E., Williams, P., Camara, M., and Hamood, A.N. (2004). The *Pseudomonas aeruginosa* global regulator MvaT specifically binds to the *ptxS* upstream region and enhances *ptxS* expression. Microbiol. *150*, 3797-3806.

White, H.K., Reimers, C.E., Cordes, E.E., Dilly, G.F., and Girguis, P.R. (2009). Quantitative population dynamics of microbial communities in plankton-fed microbial fuel cells. ISME J. *3*, 635-646.

Whiteley, M., Lee, K.M., and Greenberg, E.P. (1999). Identification of genes controlled by quorum sensing in *Pseudomonas aeruginosa*. Proc. Natl. Acad. Sci. USA *96*, 13904-13909.

Xavier, J.B., Picioreanu, C., and van Loosdrecht, M.C.M. (2005). A framework for multidimensional modelling of activity and structure of multispecies biofilms. Environ. Microbiol. *7*, 1085-1103.

Xing, D.F., Cheng, S.A., Regan, J.M., and Logan, B.E. (2009). Change in microbial communities in acetate- and glucose-fed microbial fuel cells in the presence of light. Biosens. Bioelectron. *25*, 105-111.

Zhuang, L., Zhou, S., Yuan, Y., Liu, T., Wu, Z., and Cheng, J. (2010). Development of *Enterobacter aerogenes* fuel cells: From in situ biohydrogen oxidization to direct electroactive biofilm. Bioresour. Technol. *102*, 284-289.